



This is a repository copy of *Measurement of W^\pm -boson and Z-boson production cross-sections in pp collisions at $s\sqrt{=2.76}$ TeV with the ATLAS detector.*

White Rose Research Online URL for this paper:
<http://eprints.whiterose.ac.uk/153716/>

Version: Published Version

Article:

Aaboud, M, Aad, G, Abbott, B et al. (2916 more authors) (2019) Measurement of W^\pm -boson and Z-boson production cross-sections in pp collisions at $s\sqrt{=2.76}$ TeV with the ATLAS detector. The European Physical Journal C, 79 (11). ISSN 1434-6044

<https://doi.org/10.1140/epjc/s10052-019-7399-7>

Reuse

This article is distributed under the terms of the Creative Commons Attribution (CC BY) licence. This licence allows you to distribute, remix, tweak, and build upon the work, even commercially, as long as you credit the authors for the original work. More information and the full terms of the licence here:
<https://creativecommons.org/licenses/>

Takedown

If you consider content in White Rose Research Online to be in breach of UK law, please notify us by emailing eprints@whiterose.ac.uk including the URL of the record and the reason for the withdrawal request.



eprints@whiterose.ac.uk
<https://eprints.whiterose.ac.uk/>



Measurement of W^\pm -boson and Z -boson production cross-sections in pp collisions at $\sqrt{s} = 2.76$ TeV with the ATLAS detector

ATLAS Collaboration*

CERN, 1211 Geneva 23, Switzerland

Received: 9 July 2019 / Accepted: 16 October 2019
© CERN for the benefit of the ATLAS collaboration 2019

Abstract The production cross-sections for W^\pm and Z bosons are measured using ATLAS data corresponding to an integrated luminosity of 4.0 pb^{-1} collected at a centre-of-mass energy $\sqrt{s} = 2.76$ TeV. The decay channels $W \rightarrow \ell\nu$ and $Z \rightarrow \ell\ell$ are used, where ℓ can be an electron or a muon. The cross-sections are presented for a fiducial region defined by the detector acceptance and are also extrapolated to the full phase space for the total inclusive production cross-section. The combined (average) total inclusive cross-sections for the electron and muon channels are:

$$\begin{aligned}\sigma_{W^+ \rightarrow \ell\nu}^{\text{tot}} &= 2312 \pm 26 \text{ (stat.)} \\ &\quad \pm 27 \text{ (syst.)} \pm 72 \text{ (lumi.)} \pm 30 \text{ (extr.) pb,} \\ \sigma_{W^- \rightarrow \ell\nu}^{\text{tot}} &= 1399 \pm 21 \text{ (stat.)} \pm 17 \text{ (syst.)} \\ &\quad \pm 43 \text{ (lumi.)} \pm 21 \text{ (extr.) pb,} \\ \sigma_{Z \rightarrow \ell\ell}^{\text{tot}} &= 323.4 \pm 9.8 \text{ (stat.)} \pm 5.0 \text{ (syst.)} \\ &\quad \pm 10.0 \text{ (lumi.)} \pm 5.5 \text{ (extr.) pb.}\end{aligned}$$

Measured ratios and asymmetries constructed using these cross-sections are also presented. These observables benefit from full or partial cancellation of many systematic uncertainties that are correlated between the different measurements.

Contents

1	Introduction
2	ATLAS detector
3	Data and simulation samples
4	Event selection
5	Background estimation
6	Correction for detector effects
7	Systematic uncertainties
8	Results
9	Conclusion
	Appendix
	A Theoretical predictions
	References

* e-mail: atlas.publications@cern.ch

1 Introduction

The processes that produce W and Z bosons¹ in pp collisions via Drell–Yan annihilation are two of the simplest at hadron colliders to describe theoretically. At lowest order in quantum chromodynamics (QCD), W -boson production proceeds via $q\bar{q}' \rightarrow W$ and Z -boson production via $q\bar{q} \rightarrow Z$. Therefore, precision measurements of these production cross-sections yield important information about the parton distribution functions (PDFs) for quarks inside the proton. Factorisation theory allows PDFs to be treated separately from the perturbative QCD high-scale collision calculation as functions of the event energy scale, Q , and the momentum fraction of the parton, x , for each parton flavour. Usually PDFs are defined for a particular starting scale Q_0 and can be evolved to other scales via the DGLAP equations [1–7]. Measurements of on-shell W/Z -boson production probe the PDFs in a range of Q^2 that lies close to $m_{W/Z}^2$. The range of x that is probed depends on the centre-of-mass energy, \sqrt{s} , of the protons and the rapidity coverage of the detector. Each measurement of these production cross-sections at a new value of \sqrt{s} thus provides information complementary to previous measurements. The combinations of initial partons participating in the production processes of W^+ , W^- , and Z bosons are different, so each process provides complementary information about the products of different quark PDFs.

This paper presents the first measurements of the production cross-sections for W^+ , W^- and Z bosons in pp collisions at $\sqrt{s} = 2.76$ TeV. The data were collected by the ATLAS detector at the Large Hadron Collider (LHC) [8] in 2013 and correspond to an integrated luminosity of 4.0 pb^{-1} . To provide further sensitivity to PDFs, and to reduce the systematic uncertainty in the predictions, ratios of these cross-sections and the charge asymmetry for W -boson production are also presented. The measurements are performed for leptonic (electron or muon) decays of the W and Z bosons, in

¹ In this paper it is implicit that Z boson refers to Z/γ^* bosons.

a defined fiducial region, and also extrapolated to the total cross-section.

Previous measurements of the W -boson and Z -boson production cross-sections in pp collisions at the LHC were performed by the ATLAS, CMS and LHCb Collaborations at $\sqrt{s} = 5.02$ TeV [9], 7 TeV [10–14], 8 TeV [15–19] and 13 TeV [20–22], and by the PHENIX and STAR Collaborations at the RHIC at $\sqrt{s} = 500$ GeV [23,24] and 510 GeV [25]. This is the first measurement at 2.76 TeV. Other measurements of these processes were performed in $p\bar{p}$ collisions at $\sqrt{s} = 1.8$ TeV and 1.96 TeV by the CDF [26–30] and D0 [31] Collaborations, and at $\sqrt{s} = 546$ GeV and 630 GeV by the UA1 [32] and UA2 [33] Collaborations.

2 ATLAS detector

The ATLAS detector [34] at the LHC covers nearly the entire solid angle around the collision point. It consists of an inner tracking detector surrounded by a thin superconducting solenoid, electromagnetic (EM) and hadronic calorimeters, and a muon spectrometer (MS) incorporating three large superconducting toroid magnets. The inner-detector system (ID) is immersed in a 2 T axial magnetic field and provides charged-particle tracking in the pseudorapidity range $|\eta| < 2.5$.²

The high-granularity silicon pixel detector covers the vertex region and typically provides three measurements per track. It is followed by the silicon microstrip tracker, which usually provides eight measurements from eight strip layers. These silicon detectors are complemented by the transition radiation tracker (TRT), which enables radially extended track reconstruction up to $|\eta| = 2.0$. The TRT also provides electron identification information based on the fraction of hits (typically 30 in total) above a higher energy-deposit threshold associated with the presence of transition radiation.

The calorimeter system covers the pseudorapidity range $|\eta| < 4.9$. Within the region $|\eta| < 3.2$, EM calorimetry is provided by barrel and endcap high-granularity lead/liquid-argon (LAr) sampling calorimeters, with an additional thin LAr presampler covering $|\eta| < 1.8$ that is used to correct for energy loss in material upstream of the calorimeters. Hadronic calorimetry in this region is provided by the steel/scintillator-tile calorimeter, segmented into three barrel

structures with $|\eta| < 1.7$, and two copper/LAr hadronic endcap calorimeters. The solid angle coverage is completed with forward copper/LAr and tungsten/LAr calorimeter modules optimised for EM and hadronic measurements, respectively.

The muon spectrometer comprises separate trigger and high-precision tracking chambers measuring the deflection of muons in a magnetic field generated by superconducting air-core toroids. The precision chamber system covers the region $|\eta| < 2.7$ with three layers of monitored drift tubes, complemented by cathode strip chambers in the forward region, where the backgrounds are highest. The muon trigger system covers the range $|\eta| < 2.4$ with resistive plate chambers in the barrel and thin gap chambers in the endcap regions.

The ATLAS detector selected events using a three-level trigger system [35]. The first-level trigger is implemented in hardware and used a subset of detector information to reduce the event rate to a design value of at most 75 kHz. This was followed by two software-based triggers that together reduced the event rate to about 200 Hz.

3 Data and simulation samples

The data used in this measurement were collected in February 2013 during a period when proton beams at the LHC were collided at a centre-of-mass energy of 2.76 TeV. During this running period a typical value of the instantaneous luminosity was $1 \times 10^{32} \text{ cm}^{-2} \text{ s}^{-1}$, significantly lower than in 7, 8 and 13 TeV data-taking conditions. The typical value of the mean number of collisions per proton bunch crossing (pile-up) $\langle \mu \rangle$ was 0.3. Only data from stable collisions when the ATLAS detector was fully operational are used, yielding a data sample corresponding to an integrated luminosity of 4.0 pb^{-1} .

Samples of Monte Carlo (MC) simulated events are used to estimate the signals from W -boson and Z -boson production, and the backgrounds containing prompt leptons: electroweak-diboson production and top-quark pair ($t\bar{t}$) production. Background contributions arising from multijet events that do not contain prompt leptons are estimated directly from data, with simulated events used to cross-check these estimations in the muon channel.

Production of single W and Z bosons was simulated using POWHEG-BOX v1 r1556 [36–39]. The parton showering was performed using PYTHIA 8.17 [40]. The PDF set used for the simulation was CT10 [41], and the parton shower parameter values were those of the AU2 tune [42]. Additional quantum electrodynamics (QED) emissions from electroweak (EW) vertices and charged leptons were simulated using PHOTOS++ v3.52 [43]. Additional samples of simulated W -boson events generated with SHERPA 2.1 [44] are used to estimate uncertainties arising from the choice of event generator

² ATLAS uses a right-handed coordinate system with its origin at the nominal interaction point (IP) in the centre of the detector and the z -axis along the beam pipe. The x -axis points from the IP to the centre of the LHC ring, and the y -axis points upwards. Cylindrical coordinates (r, ϕ) are used in the transverse plane, ϕ being the azimuthal angle around the z -axis. The pseudorapidity is defined in terms of the polar angle θ as $\eta = -\ln \tan(\theta/2)$. Angular distance is measured in units of $\Delta R \equiv \sqrt{(\Delta\eta)^2 + (\Delta\phi)^2}$.

model. In these SHERPA samples, simulation of W -boson production in association with up to two additional partons was performed at next-to-leading order (NLO) in QCD while production of W bosons in association with three or four additional partons was performed at leading order (LO) in QCD. The sample cross-sections were normalised to next-to-next-to-leading-order (NNLO) QCD predictions for the total cross-sections described in Sect. 8.

POWHEG-BOX v1 r2330 was used to generate $t\bar{t}$ samples [45]. These samples had parton showering performed using PYTHIA 6.428 [46] with parameters corresponding to the Perugia2011C tune [47]. The CT10 PDF set was used. Additional QED final-state radiative corrections were applied using PHOTOS++ v3.52 and τ -lepton decays were performed using TAUOLA v25feb06 [48]. Single production of top quarks is a negligible contribution to this analysis, compared with $t\bar{t}$ production, so no such samples were generated.

Production of two massive electroweak bosons (WW , ZZ , WZ) was simulated using HERWIG 6.5 [49], with multiparton interactions modelled using JIMMY 4.13 [50]. The CTEQ6L1 PDF set [51] and AUET2 tune [52] were used for these samples.

Multijet production containing heavy-flavour final states, arising from the production of $b\bar{b}$ or $c\bar{c}$ pairs, were simulated using PYTHIA 8.186. The CTEQ6L1 PDF set and AU2 tune were used. Events were required to contain an electron or muon with transverse momentum $p_T > 10$ GeV and $|\eta| < 2.8$.

The detector response to generated events was simulated by passing the events through a model of the ATLAS detector [53] based on GEANT4 [54]. Additional minimum-bias events generated using PYTHIA 8.17 and the A2 set of tuned parameters, were overlaid in such a way that the distribution of $\langle\mu\rangle$ for simulated events reproduced that in the real data. The resulting events were then passed through the same reconstruction software as the real data.

The simulated samples used for the baseline analysis are summarised in Table 1, which shows the generator used for each process together with the order in QCD at which they were generated.

4 Event selection

This section describes the selection of events consistent with the production of W bosons or Z bosons. The W -boson selection requires events to contain a single charged lepton and large missing transverse momentum. The Z -boson selection requires events to contain two charged leptons with opposite charge and the same flavour.

Events were selected by triggers that required at least one charged electron (muon) with $p_T > 15$ GeV (10 GeV). These thresholds yield an event sample with a uniform efficiency

as a function of the E_T and p_T requirements used subsequently to select the final event sample. The hard-scatter vertex, defined as the vertex with highest sum of squared track transverse momenta (for tracks with $p_T > 400$ MeV), is required to have at least three associated tracks.

Electrons are reconstructed from clusters of energy in the EM calorimeter that are matched to a track reconstructed in the ID. The electron is required to have $p_T > 20$ GeV and $|\eta| < 2.4$ (excluding the transition region between barrel and endcap calorimeters of $1.37 < |\eta| < 1.52$). Each electron must satisfy a set of identification criteria designed to suppress misidentified photons or jets. Electrons are required to satisfy the *medium* selection, following the definition provided in Ref. [55]. This includes requirements on the shower shape in the EM calorimeter, the leakage of the shower into the hadronic calorimeter, the number of hits measured along the track in the ID, and the quality of the cluster-track matching. A Gaussian sum filter [56] algorithm is used to re-fit the tracks and improve the estimated electron track parameters. To suppress background from misidentified objects such as jets, the electron is required to be isolated using calorimeter-based criteria. The sum of the transverse energies of clusters lying within a cone of size $\Delta R = 0.2$ around the centroid of the electron cluster and excluding the core³ must be less than 10% of the electron p_T .

Muon candidates are reconstructed by combining tracks reconstructed in the ID with tracks reconstructed in the MS [57]. They are required to have $p_T > 20$ GeV and $|\eta| < 2.4$. The muon candidates are also required to be isolated, by requiring that the scalar sum of the p_T of additional tracks within a cone of size $\Delta R = 0.4$ around the muon is less than 80% of the muon p_T .

The missing transverse momentum vector [58] (E_T^{miss}) is calculated as the negative vector sum of the transverse momenta of electrons and muons, and of the transverse momentum of the recoil. The magnitude of this vector is denoted by E_T^{miss} . The recoil vector is obtained by summing the transverse momenta of all clusters of energy measured in the calorimeter, excluding those within $\Delta R = 0.2$ of the lepton candidate. The momentum vector of each cluster is determined by the magnitude and coordinates of the energy deposits; the cluster is assumed to be massless. Cluster energies are initially measured assuming that the energy deposition occurs only through EM interactions, and are then corrected for the different calorimeter responses to hadrons and electromagnetically interacting particles, for losses due to dead material, and for energy that is not captured by the clustering process [59]. The definition of the recoil does not make use of reconstructed jets, to avoid threshold effects. The procedure used to calibrate the recoil closely follows

³ The core of the shower is the contribution within $\Delta\eta \times \Delta\phi = 0.125 \times 0.175$ around the cluster barycentre.

Table 1 Summary of the baseline simulated samples used

Process	Generator	Generator QCD precision
Signal samples		
$W \rightarrow \ell\nu$	POWHEG-BOX +PYTHIA 8	NLO
$Z \rightarrow \ell^+\ell^-$	POWHEG-BOX +PYTHIA 8	NLO
Background samples		
$W \rightarrow \tau\nu$	POWHEG-BOX +PYTHIA 8	NLO
$Z \rightarrow \tau^+\tau^-$	POWHEG-BOX +PYTHIA 8	NLO
$t\bar{t}$	POWHEG-BOX +PYTHIA 6	NLO
WW	HERWIG	LO
ZZ	HERWIG	LO
WZ	HERWIG	LO
$b\bar{b}$	PYTHIA 8	LO
$c\bar{c}$	PYTHIA 8	LO

that used in the recent ATLAS measurement of the W -boson mass [60], first correcting the modelling of the overall recoil in simulation and then applying corrections for residual differences in the recoil response and resolution that are derived from Z -boson data and transferred to the W -boson sample.

The W -boson selection requires events to contain exactly one lepton (electron or muon) candidate and have $E_T^{\text{miss}} > 25$ GeV. The lepton must match a lepton candidate that met the trigger criteria. The transverse mass, m_T , of the W -boson candidate in the event is calculated using the lepton candidate and E_T^{miss} according to $m_T = \sqrt{2p_T^\ell E_T^{\text{miss}}(1 - \cos(\phi_\ell - \phi_{E_T^{\text{miss}}}))}$. The transverse mass in W -boson production events is expected to exhibit a Jacobian peak around the W -boson mass. Thus, requiring that $m_T > 40$ GeV suppresses background processes. After these requirements there are 3914 events in the $W \rightarrow e^+\nu$ channel, 2209 events in the $W \rightarrow e^-\bar{\nu}$ channel, 4365 events in the $W \rightarrow \mu^+\nu$ channel, and 2460 events in the $W \rightarrow \mu^-\bar{\nu}$ channel.

The Z -boson selection requires events to contain exactly two lepton candidates with the same flavour and opposite charge. At least one lepton must match a lepton candidate that met the trigger criteria. Background processes are suppressed by requiring that the invariant mass of the lepton pair satisfies $66 < m_{\ell\ell} < 116$ GeV. After these requirements there are 430 events in the $Z \rightarrow e^+e^-$ channel, and 646 events in the $Z \rightarrow \mu^+\mu^-$ channel.

5 Background estimation

The background processes that contribute to the sample of events passing the W -boson and Z -boson selections can be separated into two categories: those estimated from MC simulation and theoretical calculations, and those estimated directly from data. The main backgrounds that contribute

to the event sample passing the W -boson selection are processes with a τ -lepton decaying into an electron or muon plus neutrinos, leptonic Z -boson decays where only one lepton is reconstructed, and multijet processes. The main background contribution to the event sample passing the Z -boson selection is production of two massive electroweak bosons.

The backgrounds arising from $W \rightarrow \tau\nu$, $Z \rightarrow \ell^+\ell^-$, diboson production, and $t\bar{t}$ production are estimated from the simulated samples described in Sect. 3. Predictions of the backgrounds to the W -boson and Z -boson production measurements arising from multijet production suffer from large theoretical uncertainties, and therefore the contribution to this background in the W -boson measurement is estimated from data. This is achieved by constructing a shape template for the background using a discriminating variable in a control region and then performing a template fit to the same distribution in the signal region to extract the background contribution. The choice of template variable is motivated by the difference between signal and background and by the available number of events. Previous ATLAS measurements at 7 TeV [10] and 13 TeV [21] found that multijet production makes a background contribution of less than 0.1% for Z -boson measurements; this is therefore neglected.

Electron candidates in multijet background events are typically misidentified candidates produced when jets mimic the signature of an electron, for example when a neutral pion and a charged pion overlap in the detector. Additional candidates can arise from 'non-prompt' electrons produced when a photon converts, and in decays of heavy-flavour hadrons. To construct a control region for the multijet template, a selection is used that differs from the W -boson selection described in Sect. 4 in only two respects: the medium electron identification criteria are inverted (while keeping the looser identification criteria) and the E_T^{miss} requirement is removed. By construction, this control region is statistically independent of the W -boson signal region. A template for the shape of the

multijet background in the E_T^{miss} distribution is then obtained from that distribution in the control region after subtraction of expected contributions from the signal and other backgrounds determined using MC samples. The normalisation of the multijet background template in the signal region is extracted by performing a χ^2 fit of the E_T^{miss} distribution (applying all signal criteria except the requirement on E_T^{miss}) to a sum of the templates for the multijet background, the signal, and all other backgrounds. The normalisation of the signal is allowed to vary freely in the fit as is the multijet background; however, the other backgrounds are only allowed to vary from their expected values by up to 5%, corresponding to the largest level of variation in predicted electroweak-boson production cross-sections obtained from varying the choice of PDF. The normalisation from this fit can then be used together with the inverted selection to construct multijet background distributions in any other variable that is not correlated with the electron identification criteria.

Muon candidates in multijet background events are typically ‘non-prompt’ muons produced in the decays of hadrons. The multijet background contribution to the $W \rightarrow \mu\nu$ selection is estimated by using the same method as described for the $W \rightarrow e\nu$ selection. In this case the control region is defined by inverting the isolation requirement and removing the requirement on m_T . The distribution used for the fits is m_T .

The overall number of multijet background events is estimated from a fit to the total W -boson sample. Comparisons between the fitted distributions and data for $W \rightarrow e\nu$ and $W \rightarrow \mu\nu$ are shown in Fig. 1. Fits to the separate W^+ -boson and W^- -boson samples are used in the evaluation of the systematic uncertainties, as described in Sect. 7. The final estimated multijet contributions are 30 ± 11 events for $W \rightarrow e^+\nu$ and $W \rightarrow e^-\nu$ and 2.5 ± 1.9 events for $W^+ \rightarrow \mu^+\nu$ and $W^- \rightarrow \mu^-\nu$. The relative contribution of the multijet events (1%) is lower than in 13 TeV (4%) and 7 TeV (3%) data. This is in agreement with expectations for this lower pile-up running, where the resolution in E_T^{miss} is improved compared to the higher pile-up running.

6 Correction for detector effects

The measurements in this paper are performed within specific fiducial regions and extrapolated to the total W -boson or Z -boson phase space. The fiducial regions are defined by the kinematic and geometric selection criteria given in Table 2; in simulations these are applied at the generator level before the emission of QED final-state radiation from the decay lepton(s) (QED Born level).

The fiducial W -boson/ Z -boson production cross-section is obtained from the number of observed events meeting the selection criteria after background contributions are sub-

tracted, $N_{W,Z}^{\text{sig}}$, using the following formula:

$$\sigma_{W,Z \rightarrow \ell\nu, \ell\ell}^{\text{fid}} = \frac{N_{W,Z}^{\text{sig}}}{C_{W,Z} \cdot \mathcal{L}_{\text{int}}},$$

where \mathcal{L}_{int} is the total integrated luminosity of the data samples used for the analysis. The factor $C_{W,Z}$ is the ratio of the number of generated events that satisfy the final selection criteria after event reconstruction to the number of generated events within the fiducial region. It includes the efficiency for triggering, reconstruction and identification of $W, Z \rightarrow \ell\nu, \ell^+\ell^-$ events falling within the acceptance. The different components of the efficiency are calculated using a mixture of MC simulation and measurements from data.

The total W -boson and Z -boson production cross-sections are obtained using the following formula:

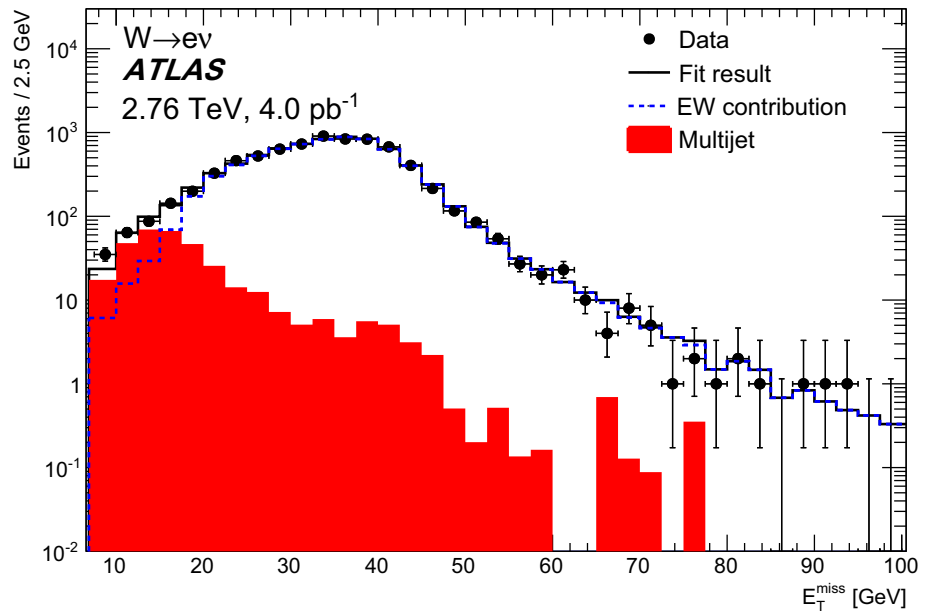
$$\begin{aligned} \sigma_{W,Z \rightarrow \ell\nu, \ell\ell}^{\text{tot}} &\equiv \sigma^{\text{tot}} \times B(W, Z \rightarrow \ell\nu, \ell\ell) \\ &= \frac{N_{W,Z}^{\text{sig}}}{A_{W,Z} \cdot C_{W,Z} \cdot \mathcal{L}_{\text{int}}}. \end{aligned}$$

The factor $B(W, Z \rightarrow \ell\nu, \ell\ell)$ is the per-lepton branching fraction of the vector boson. The factor $A_{W,Z}$ is the acceptance for W/Z -boson events being studied. It is defined as the fraction of generated events that satisfy the fiducial requirements. This acceptance is determined using MC signal samples, corrected to the generator QED Born level, and is used to extrapolate the measured cross-section in the fiducial region to the full phase space. The central values of $A_{W,Z}$ are around 0.6 for these measurements, compared with 0.5 at $\sqrt{s} = 7$ TeV and 0.4 at $\sqrt{s} = 13$ TeV, so the fiducial region is closer to the full phase space in this measurement than for those at higher centre-of-mass energies. This is due to a combination of higher p_T thresholds for leptons in other measurements, and more-central production of vector bosons at lower \sqrt{s} . The values of C_W are approximately 0.67 for the $W \rightarrow e\nu$ channels and 0.75 for the $W \rightarrow \mu\nu$ channels. The values of C_Z are 0.55 for the $Z \rightarrow e^+e^-$ channel and 0.79 for $Z \rightarrow \mu^+\mu^-$. The $C_{W,Z}$ values are a little higher than for previous measurements at $\sqrt{s} = 7$ TeV and $\sqrt{s} = 13$ TeV.

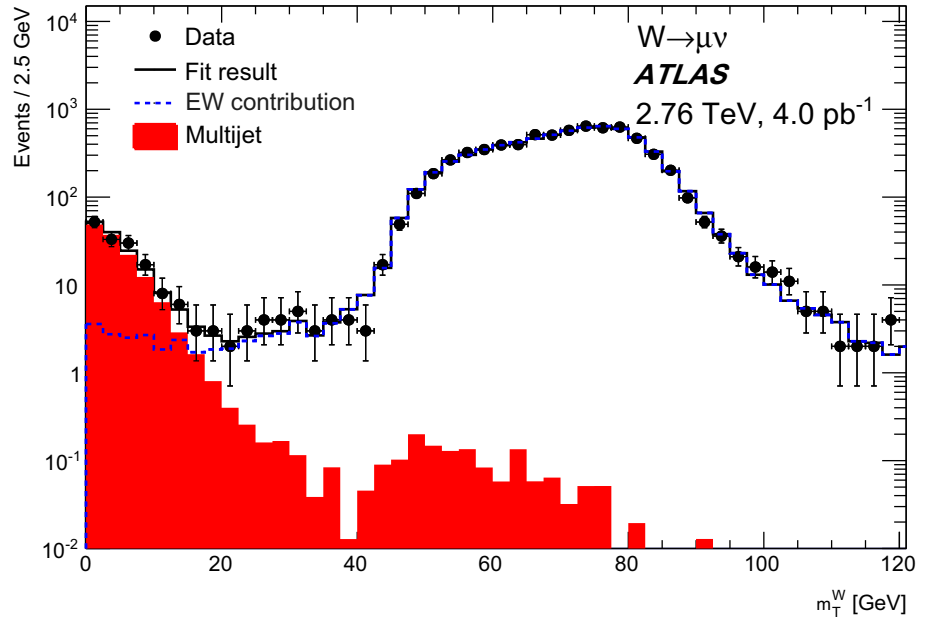
7 Systematic uncertainties

The systematic uncertainty in the electron reconstruction and identification efficiency is estimated using the tag-and-probe method in 8 TeV data [55,61] and extrapolated to the 2.76 TeV dataset. The extrapolation procedure results in absolute increases of $\pm 2\%$, due to uncertainties in the effect of the differing pile-up conditions in 2.76 TeV data relative to the 8 TeV data, as well as a different setting of the noise filtering in the LAr calorimeter of the 2.76 TeV data relative to the 8 TeV data. These uncertainties were estimated using a comparison between 7 TeV and 8 TeV data and MC samples,

Fig. 1 Distributions used to estimate the multijet background contribution in (a) the $W \rightarrow e\nu$ channel, and (b) the $W \rightarrow \mu\nu$ channel. The data is compared to the fit result



(a)



(b)

after having established that the central values of the efficiencies are the same for different centre-of-mass energies when the same LAr filter settings are used. A similar methodology had been used for internal estimates of the electron efficiency performance at 13 TeV before the start of Run-2 data taking and was found to give a good prediction of the efficiencies in data as well as a conservative estimate of the uncertainties. Transverse-momentum-dependent isolation corrections, calculated with the tag-and-probe method in 2.76 TeV data, are very close to 1, so the systematic uncertainty in the electron isolation requirement is set to the size of the correction

itself, that is $\pm 1\%$ for low p_T and $\pm 0.3\%$ for higher p_T . The electron energy scale has associated statistical uncertainties and systematic uncertainties arising from a possible bias in the calibration method, the choice of generator, the presampler energy scale, and imperfect knowledge of the material in front of the EM calorimeter [62]. The total energy-scale uncertainty is calculated as the sum in quadrature of these components.

Systematic uncertainties associated with the muon momentum can be divided into three major independent categories: momentum resolution of the MS track, momentum resolution

Table 2 Summary of the selection criteria that define the measured fiducial regions

W-boson fiducial region	Z-boson fiducial region
$p_T^\ell > 20 \text{ GeV}$	$p_T^{\ell^{+,-}} > 20 \text{ GeV}$
$ \eta^\ell < 2.4$	$ \eta^{\ell^{+,-}} < 2.4$
$E_T^{\text{miss}} > 25 \text{ GeV}$	$66 < m_{\ell^+\ell^-} < 116 \text{ GeV}$
$m_T > 40 \text{ GeV}$	

of the ID track, and an overall scale uncertainty [57]. The total momentum scale/resolution uncertainty is the sum in quadrature of these components. An η -independent uncertainty of approximately $\pm 1.1\%$ in the muon trigger efficiency, determined using the tag-and-probe method [57] in 2.76 TeV data, is taken into account. Furthermore, a p_T - and η -dependent uncertainty in the identification and reconstruction efficiencies of approximately $\pm 0.3\%$, derived using the tag-and-probe method on 8 TeV data is applied. The uncertainty in the p_T -dependent isolation correction in the muon channel, calculated with the tag-and-probe method in 2.76 TeV data, is about $\pm 0.6\%$ for low p_T and $\pm 0.5\%$ for higher p_T .

The luminosity uncertainty for the 2.76 TeV data is $\pm 3.1\%$. This is determined, following the same methodology as was used for the 7 TeV data recorded in 2011 [63], from a calibration of the luminosity scale derived from beam-separation scans performed during the 2.76 TeV operation of the LHC in 2013.

Systematic uncertainties in the E_T^{miss} arising from the smearing and bias corrections applied to obtain satisfactory modelling of the recoil [58] affect the C_W factors in the $W \rightarrow \ell\nu$ measurement, and are taken into account.

Uncertainties arising from the choice of PDF set are evaluated using the error sets of the initial CT10 PDF set (at 90% confidence level (CL)) and from comparison with the results obtained using the central PDF sets from ABKM09 [64], NNPDF23 [65], and ATLAS-epWZ12 [66]. The effect of this uncertainty on A_{W^+} (A_{W^-}) is estimated to be $\pm 1.0\%$ (1.2%), and the effect on A_Z is estimated to be $\pm 1.4\%$. The

effect on $C_{W,Z}$ is between $\pm 0.05\%$ and $\pm 0.4\%$ depending on the channel.

A summary of the systematic uncertainties in the $C_{W,Z}$ factors is shown in Table 3. The muon trigger, and electron reconstruction and identification uncertainties are dominant.

Uncertainties arising from the choice of event generator and parton shower models are estimated by comparing results obtained when using SHERPA 2.1 signal samples instead of the (nominal) POWHEG-BOX+PYTHIA 8. The effect of this uncertainty on $A_{W,Z}$ is estimated to be $\pm 0.9\%$.

The systematic uncertainty in the multijet background estimation can be divided into several components: the normalisation uncertainty from the χ^2 fit, the uncertainty in the modelling of electroweak processes by simulated samples in the fitted region, uncertainty from fit bias due to binning choice, and uncertainty from template shape. The scale normalisation uncertainty from the χ^2 fit is approximately $\pm 13\%$ for the $W \rightarrow e\nu$ channel. This uncertainty is neglected in the $W \rightarrow \mu\nu$ channel where the template bias is dominant. The mismodelling uncertainty is estimated by comparison of the fit results for ℓ^+ and ℓ^- , and for the combined ℓ^\pm candidates. The central value used is $0.5N^\pm$ with the uncertainties $N^+ - 0.5N^\pm$ and $N^- - 0.5N^\pm$, where N^+ is the fitted number of ℓ^+ background events, N^- is the fitted number of ℓ^- and N^\pm is the fitted total number of ℓ^\pm background events. In the $W \rightarrow e\nu$ channel this leads to an uncertainty of $\pm 28\%$ in the multijet background. In the $W \rightarrow \mu\nu$ channel the multijet template normalisation is derived from the fit in the small- m_T region, where electroweak contributions are negligible and there are many data events, and this source of systematic error is found to be negligible. The fit-bias uncertainty arising from the choice of bin width is estimated by repeating the fit with different binnings. This component is negligible in the $W \rightarrow \mu\nu$ case and $\pm 15\%$ in the $W \rightarrow e\nu$ case. The uncertainty due to a potential bias from template choice is estimated by employing different template selections. For the $W \rightarrow e\nu$ channel, different inverted-isolation criteria were investigated. The overall differences are considered negligible. For the $W \rightarrow \mu\nu$ channel, template vari-

Table 3 Relative systematic uncertainties (%) in the correction factors $C_{W,Z}$ in different channels

$\delta C/C$ (%)	$W^+ \rightarrow e^+\nu$	$W^- \rightarrow e^-\nu$	$Z \rightarrow e^+e^-$	$W^+ \rightarrow \mu^+\nu$	$W^- \rightarrow \mu^-\nu$	$Z \rightarrow \mu^+\mu^-$
Lepton trigger	0.14	0.13	< 0.01	1.07	1.07	0.03
Lepton reconstr. and ident.	2.31	2.33	4.55	0.30	0.32	0.62
Lepton isolation	0.71	0.71	1.41	0.51	0.51	1.01
Lepton scale and resolution	0.44	0.43	0.34	0.05	0.05	0.04
Recoil scale and resolution	0.25	0.20	–	0.22	0.22	–
PDF	0.22	0.29	0.11	0.11	0.20	0.06
MC statistical uncertainty	0.24	0.31	0.30	0.24	0.34	0.43
Total	2.5	2.5	4.8	1.3	1.3	1.3

Table 4 The correlation model for the grouped systematic uncertainties for the measurements of W -boson and Z -boson production. The entries in different rows are uncorrelated with each other. Entries in a row with the same letter are fully correlated. Entries in a row with a starred letter are mostly correlated with the entries with the same letter (most of the individual sources of uncertainties within a group are taken as correlated). Entries with different letters in a row are either fully or mostly uncorrelated with each other

Source	Muon channel			Electron channel		
	Z	W^+	W^-	Z	W^+	W^-
Muon trigger	A	A	A	–	–	–
Muon reconstruction/ID	A	A	A	–	–	–
Muon energy scale/resolution	A	A	A	–	–	–
Muon isolation	A	A	A	–	–	–
Electron trigger	–	–	–	A*	A*	A*
Electron reconstruction/ID	–	–	–	A	A	A
Electron energy scale/resolution	–	–	–	A	A	A
Electron isolation	–	–	–	A	A	A
Recoil related	–	A	A	–	A	A
EW background	A	B	B	A	B	B
Top-quark background	A	A	A	A	A	A
Multijet background	–	A	A	–	A	A
PDF	A	A	A	A	A	A

Table 5 The numbers of observed candidate events with the estimated numbers of selected electroweak (EW) plus top, and multijet background events, together with their total uncertainty. In addition, the number of background-subtracted signal events is shown with the first

uncertainty given being statistical and the second uncertainty being the total systematic uncertainty, obtained by summing in quadrature the EW+top and multijet uncertainties. Uncertainties shown as ± 0.0 have a magnitude less than 0.05.

Measurement Channel	Observed candidates	Background (EW + top)	Background (multijet)	Background-subtracted data N_W^{sig}
$W^+ \rightarrow e^+\nu$	3914	108 ± 6	30 ± 11	$3776 \pm 63 \pm 12$
$W^- \rightarrow e^-\bar{\nu}$	2209	74.2 ± 3.3	30 ± 11	$2105 \pm 47 \pm 12$
$W^+ \rightarrow \mu^+\nu$	4365	152 ± 7	2.5 ± 1.9	$4210 \pm 66 \pm 7$
$W^- \rightarrow \mu^-\bar{\nu}$	2460	108 ± 4	2.5 ± 1.9	$2350 \pm 50 \pm 5$
$Z \rightarrow e^+e^-$	430	1.3 ± 0.0	–	$428.7 \pm 20.7 \pm 0.0$
$Z \rightarrow \mu^+\mu^-$	646	1.6 ± 0.1	–	$644.4 \pm 25.4 \pm 0.1$

ations were estimated from fits that use $b\bar{b} + c\bar{c}$ MC samples as the multijet templates, leading to an uncertainty of $\pm 75\%$; this is the largest uncertainty in the multijet background in the $W \rightarrow \mu\nu$ channel.

Combining results and building ratios or asymmetries of results require a model for the correlations of particular systematic uncertainties between different measurements. Correlations arise mostly due to the fact that electrons, muons, and the recoil are reconstructed identically in the different measurements. Further correlations occur due to similarities in the analysis methodology such as the methods of signal and background estimation.

The systematic uncertainties from the electroweak background estimations are treated as uncorrelated between the W -boson and Z -boson measurements, and fully correlated among different flavour decay channels of the W and Z boson. The top-quark background is treated as fully correlated across all W -boson and Z -boson decay channels. The multijet background and recoil-related systematic uncertainties are also treated as fully correlated between all four W -

boson decay channels despite there being an expected uncorrelated component, since the statistical uncertainty is dominant in this case.

The systematic uncertainties due to the choice of PDF are treated as fully correlated between all W -boson and Z -boson channels. The uncertainties in electron and muon selection, reconstruction and efficiency are treated as fully correlated between all W -boson and Z -boson channels.

A simplified form of the correlation model with the grouped list of the sources of systematic errors is presented in Table 4.

8 Results

The numbers of events passing the event selections described in Sect. 4 are presented in Table 5, together with the estimated background contributions described in Sect. 5. The distribution of m_T for $W \rightarrow \ell\nu$ candidate events is shown in Fig. 2, compared with the expected distribution for signal plus back-

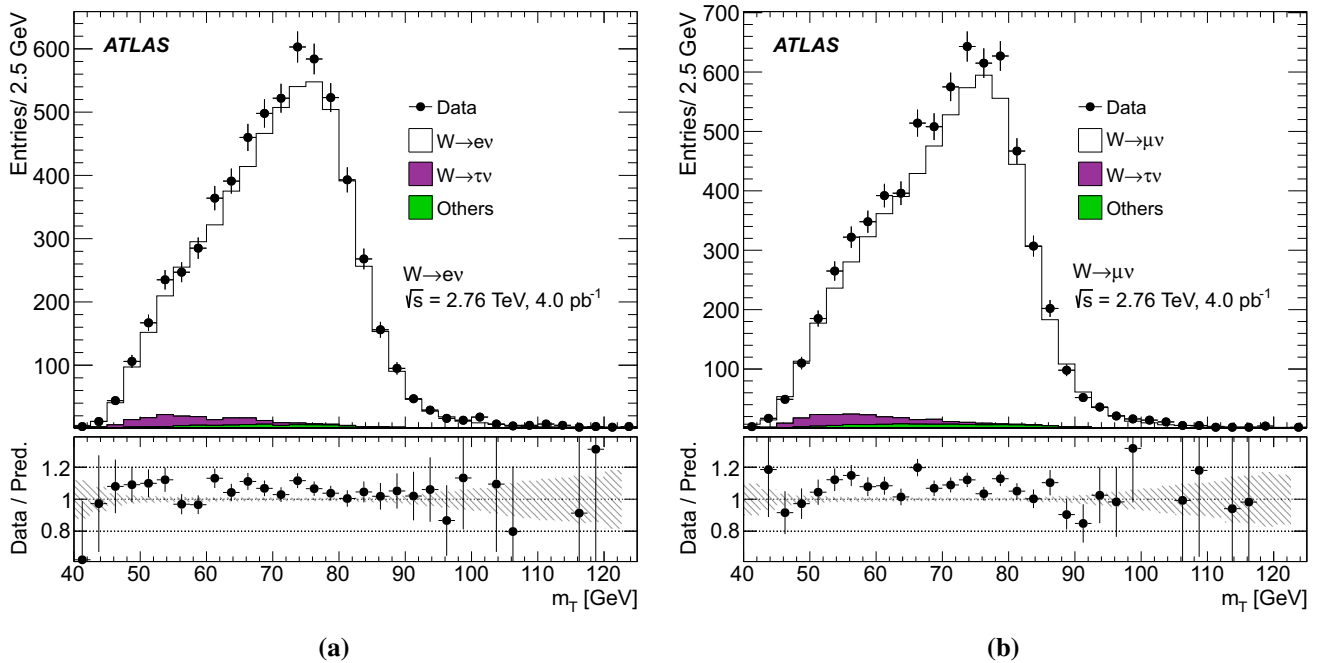


Fig. 2 The distribution of m_T for $W \rightarrow \ell\nu$ candidate events. The expected signal, normalised to the NNLO theoretical predictions, is shown as an unfilled histogram on top of the stacked background predictions. Backgrounds that do not originate from W production are grouped together into the ‘Others’ histogram. Systematic uncertainties

for the signal and background distributions are combined in the shaded band. Systematic uncertainties from the measurement of the integrated luminosity are not included. The lower panel shows the ratio of the data to the prediction

grounds, where the signal is normalised to the NNLO QCD prediction. Similarly, Fig. 3 shows the distribution of $m_{\ell\ell}$ for $Z \rightarrow \ell^+\ell^-$ candidate events compared with the expectations for signal. In this case, the background contributions are not shown, because they would not be visible in the figure if included.

The measured fiducial (σ^{fid}) and total (σ^{tot}) cross-sections in the electron and muon channels are presented separately in Table 6. For these measurements, the dominant contribution to the systematic uncertainty arises from the luminosity determination.

The results obtained from the electron and muon final states are consistent. The fiducial measurements from electron and muon final states are combined following the procedure described in Ref. [67] and the result is extrapolated to the full phase space to obtain the total cross-section. The total W -boson cross-section is calculated by summing the separate W^+ and W^- cross-sections. The results are shown in Table 7.

Theoretical predictions of the fiducial and total cross-sections are computed for comparison with the measured cross-sections using DYNLLO 1.5 [68] which provides calculations at NNLO in the strong-coupling constant, $\mathcal{O}(\alpha_s^2)$, including the boson decays into leptons ($\ell^+\nu$, $\ell^-\bar{\nu}$ or $\ell^+\ell^-$) with full spin correlations, finite width and interference

effects. These calculations allow kinematic requirements to be implemented for direct comparison with experimental data. The procedure used follows that used for the previous ATLAS measurement at $\sqrt{s} = 7$ TeV [10].

Corrections for NLO EW effects are calculated with FEWZ 3.1 [69–72], for the Z bosons and with SANC [73, 74] for the W bosons. The calculation was done in the G_μ EW scheme [75]. The following input parameters are taken from the Particle Data Group’s Review of Particle Properties 2014 edition [76]: the Fermi constant, the masses and widths of W and Z bosons as well as the elements of the CKM matrix. The cross-sections for vector bosons decaying into these leptonic final states are calculated such that they match the definition of the measured cross-sections in the data. Thus, from complete NLO EW corrections, the following components are included: virtual QED and weak corrections, real initial-state radiation (ISR), and interference between ISR and real final-state radiation (FSR) [77]. The calculated effect of these corrections on the cross-sections is $(-0.26 \pm 0.02)\%$ for $\sigma_{W^+}^{\text{fid}}$, $(-0.21 \pm 0.03)\%$ for $\sigma_{W^-}^{\text{fid}}$, and $(-0.25 \pm 0.12)\%$ for σ_Z^{fid} . DYNLLO is used for the central values of the predictions while FEWZ is used for the PDF variations and all other systematic variations such as QCD scale and α_s . The predictions are calculated using the CT14nnlo [78], NNPDF3.1 [79], MMHT14nnlo68cl [80], ABMP16 [81], HERAPDF2.0 [82],

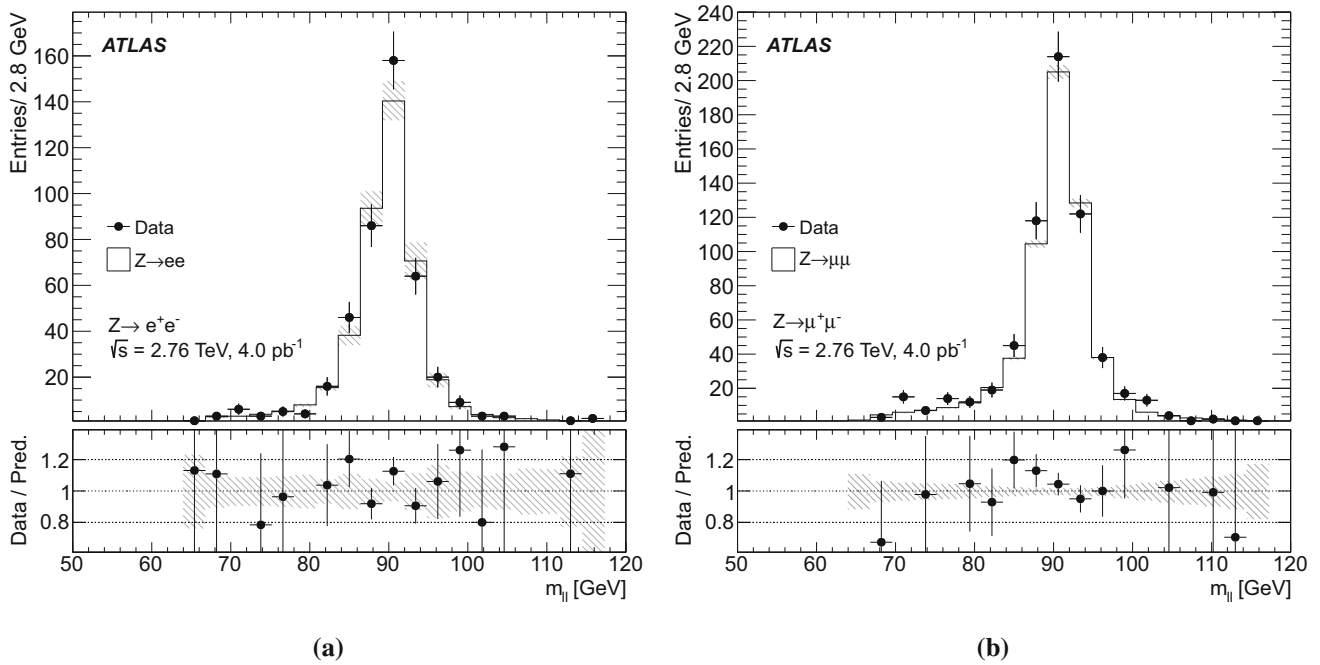


Fig. 3 The distribution of $m_{\ell\ell}$ for $Z \rightarrow \ell^+\ell^-$ candidate events. The expected signal, normalised to the NNLO theoretical predictions, is shown as an unfilled histogram. Systematic uncertainties for the signal and background distributions are combined in the shaded band. System-

atic uncertainties from the measurement of the integrated luminosity are not included. The background distributions are neglected here, but would not be visible if included. The lower panel shows the ratio of the data to the prediction

Table 6 Results of the fiducial and total cross-sections measurements of the W^+ -boson, W^- -boson, and Z-boson production cross-sections in the electron and muon channels. The cross-sections are shown with their statistical, systematic and luminosity uncertainties (and extrapolation uncertainty for total cross-section)

	Value \pm stat. \pm syst. \pm lumi. (\pm extr.)	Value \pm stat. \pm syst. \pm lumi. (\pm extr.)
	$W^+ \rightarrow e\nu$	$W^+ \rightarrow \mu\nu$
$\sigma_{W^+}^{\text{fid}}$ [pb]	$1416 \pm 24 \pm 36 \pm 44$	$1438 \pm 23 \pm 19 \pm 45$
$\sigma_{W^+}^{\text{tot}}$ [pb]	$2284 \pm 38 \pm 58 \pm 71$ (± 30)	$2319 \pm 36 \pm 30 \pm 72$ (± 30)
	$W^- \rightarrow e\nu$	$W^- \rightarrow \mu\nu$
$\sigma_{W^-}^{\text{fid}}$ [pb]	$789 \pm 18 \pm 20 \pm 25$	$799 \pm 17 \pm 11 \pm 25$
$\sigma_{W^-}^{\text{tot}}$ [pb]	$1385 \pm 31 \pm 36 \pm 43$ (± 21)	$1402 \pm 30 \pm 19 \pm 44$ (± 21)
	$Z \rightarrow ee$	$Z \rightarrow \mu\mu$
σ_Z^{fid} [pb]	$197.6 \pm 9.6 \pm 9.5 \pm 6.1$	$205.6 \pm 8.1 \pm 2.6 \pm 6.4$
σ_Z^{tot} [pb]	$313.6 \pm 15.2 \pm 15.0 \pm 9.7$ (± 5.3)	$326.3 \pm 12.9 \pm 4.1 \pm 10.1$ (± 5.5)

Table 7 Combined fiducial and total cross-section measurements for W^+ -boson, W^- -boson and Z-boson production. The cross-sections are shown with their statistical, systematic and luminosity uncertainties (and extrapolation uncertainty for total cross-section)

	Value \pm stat. \pm syst. \pm lumi. (\pm extr.)	Value \pm stat. \pm syst. \pm lumi. (\pm extr.)
	$W^+ \rightarrow \ell\nu$	$W^- \rightarrow \ell\nu$
σ_W^{fid} [pb]	$1433 \pm 16 \pm 17 \pm 44$	$798 \pm 12 \pm 10 \pm 25$
σ_W^{tot} [pb]	$2312 \pm 26 \pm 27 \pm 72$ (± 30)	$1399 \pm 21 \pm 17 \pm 43$ (± 21)
	$W \rightarrow \ell\nu$	
σ_W^{fid} [pb]	$2231 \pm 20 \pm 26 \pm 69$	
σ_W^{tot} [pb]	$3711 \pm 34 \pm 43 \pm 115$ (± 51)	
	$Z \rightarrow \ell\ell$	
σ_Z^{fid} [pb]	$203.7 \pm 6.2 \pm 3.2 \pm 6.3$	
σ_Z^{tot} [pb]	$323.4 \pm 9.8 \pm 5.0 \pm 10.0$ (± 5.5)	

Table 8 The predictions, using the CT14nnlo PDF set, for the cross-sections measured. The calculations are performed using DYNLLO 1.5 and FEWZ 3.1 as described in the text. The errors represent the PDF and scale uncertainties

Quantity	Predicted cross-section (pb)
$\sigma_{W^+}^{\text{fid}}$	1379 $^{+39}_{-40}$ $^{+6}_{-6}$
$\sigma_{W^-}^{\text{fid}}$	757.3 $^{+20.5}_{-24.5}$ $^{+3.1}_{-3.1}$
σ_Z^{fid}	196.0 $^{+5.0}_{-5.8}$ $^{+1.1}_{-1.3}$
$\sigma_{W^+}^{\text{tot}}$	2115 $^{+57}_{-60}$ $^{+9}_{-11}$
$\sigma_{W^-}^{\text{tot}}$	1266 $^{+32}_{-38}$ $^{+5}_{-6}$
σ_Z^{tot}	304.1 $^{+7.3}_{-8.2}$ $^{+1.1}_{-1.4}$

and ATLAS-epWZ12nnlo PDF sets. The dynamic scale, $m_{\ell\ell}$, and fixed scale, m_W , are used as the nominal renormalisation, μ_R , and factorisation, μ_F , scales for Z and W predictions, respectively.

Theoretical uncertainties in the predictions are also derived from the following sources:

PDF: these uncertainties are evaluated from the variations of the NNLO PDFs according to the recommended procedure for each PDF set. A table with all PDF uncertainties and their central values is shown in Appendix A; the PDF uncertainty from CT14nnlo was rescaled from 90% CL to 68% CL.

Scales: the scale uncertainties are defined by the envelope of the variations in which the scales are changed by factors of two subject to the constraint $0.5 \leq \mu_R/\mu_F \leq 2$.

α_s : the uncertainty due to α_s was estimated by varying the value of α_s used in the CT14nnlo PDF set by ± 0.001 , corresponding to a 68% CL variation.

The statistical uncertainties in these theoretical predictions are negligible.

The numerical values of the predictions for the CT14nnlo PDF set are presented in Table 8. The predictions for the acceptance factor $A_{W,Z}$ can differ by a few percent from those derived from simulated signal samples, this may be due to a poorer description of production of low p_T W-bosons by the fixed-order calculations. The predictions are shown in comparison with the combined W-boson and Z-boson production measurements, and with results from pp and p \bar{p} collisions at other centre-of-mass energies in Fig. 4. A comparison of the measurements with predictions from various different PDF sets is presented in Figs. 5 and 6. Overall there is good agreement.

Taking ratios of measurements leads to results that have significantly reduced systematic uncertainties due to full or partial cancellation of correlated systematic uncertainties, as discussed in Sect. 7. The ratios of the fiducial cross-sections

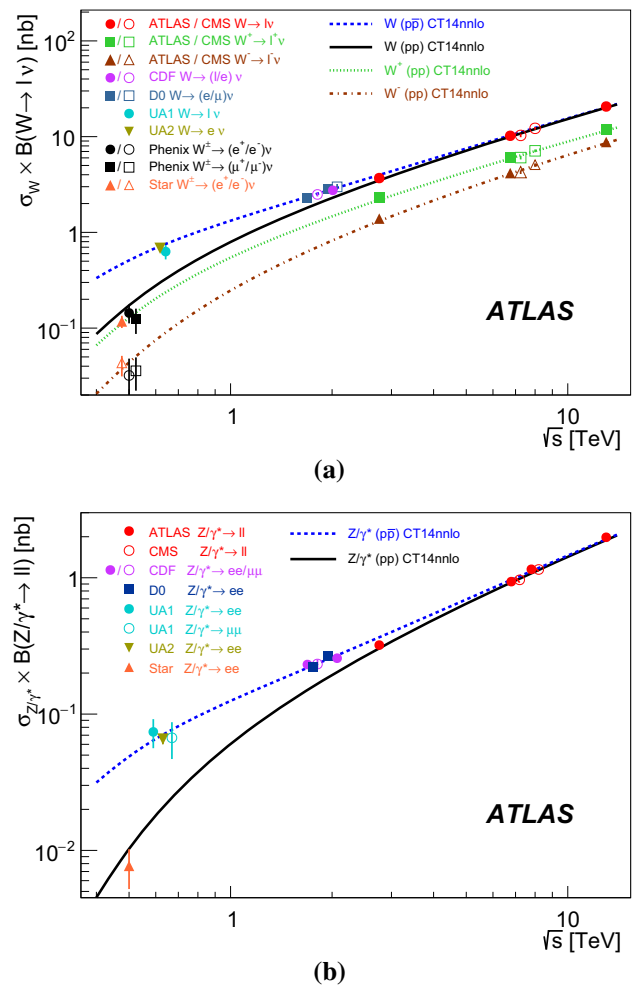


Fig. 4 The measured values of (a) $\sigma_W \times B(W \rightarrow \ell\nu)$ for W^+ bosons, W^- bosons and their sum and (b) $\sigma_{Z/\gamma^*} \times B(Z/\gamma^* \rightarrow \ell\ell)$ for proton–proton and proton–antiproton collisions as a function of \sqrt{s} . Data points at the same \sqrt{s} are staggered to improve readability. All data points are shown together with their total uncertainty. The theoretical calculations are performed at NNLO in QCD using DYNLLO 1.5 and FEWZ 3.1 as described in the text. The theoretical uncertainties are not shown

for W-boson and Z-boson production are presented, together with the ratio for W^+ -boson and W^- -boson production, in Fig. 7. It can be seen that the predictions from the different PDF sets are mostly in good agreement with the measurements. There is a slight (less than two standard deviations) tension between the data and the prediction using the ABMP16 PDF set. The measured values of the ratios are:

$$R_{W/Z} = 10.95 \pm 0.35 \text{ (stat.)} \pm 0.10 \text{ (syst.);}$$

$$R_{W^+/W^-} = 1.797 \pm 0.034 \text{ (stat.)} \pm 0.009 \text{ (syst.)}$$

The measurement of the ratio R_{W^+/W^-} is sensitive to the u_v and d_v valence quark distributions, while the ratio $R_{W/Z}$ can place constraints on the strange quark distributions. A common alternative way of presenting this information is in terms of the charge asymmetry, A_ℓ , in W-boson production:

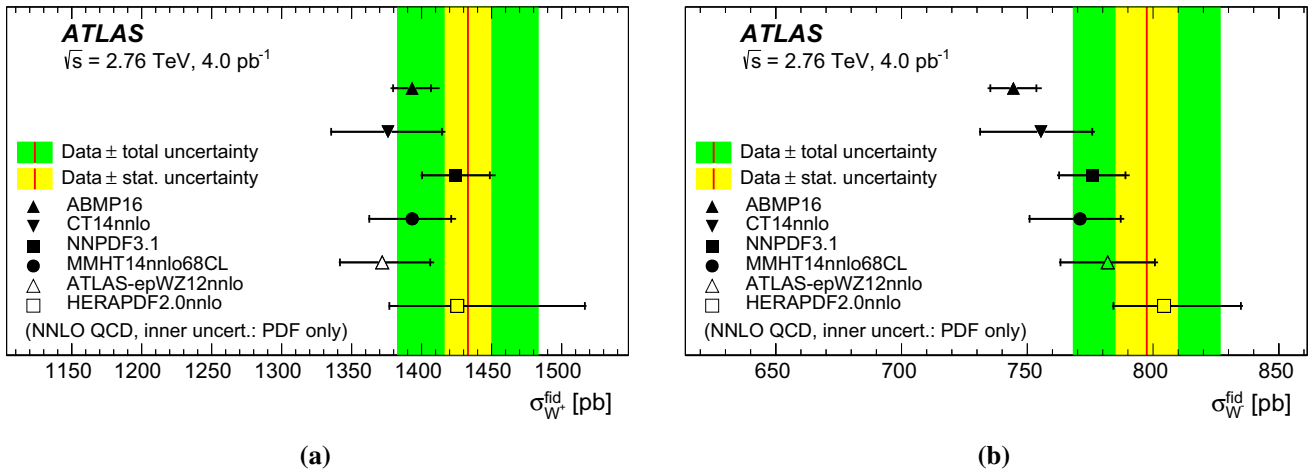


Fig. 5 NNLO predictions for the fiducial cross-section (a) $\sigma_{W^+}^{\text{fid}}$ and (b) $\sigma_{W^-}^{\text{fid}}$ for the six PDFs CT14nnlo, MMHT2014, NNPDF3.1, ATLASepWZ12, ABMP16 and, HERApdf2.0 compared with the measured fiducial cross-section as given in Table 7. The inner shaded band

represents the statistical uncertainty only, the outer band corresponds to the experimental uncertainty (including the luminosity uncertainty). The theory predictions are given with the corresponding PDF (total uncertainty shown by inner (outer) error bar

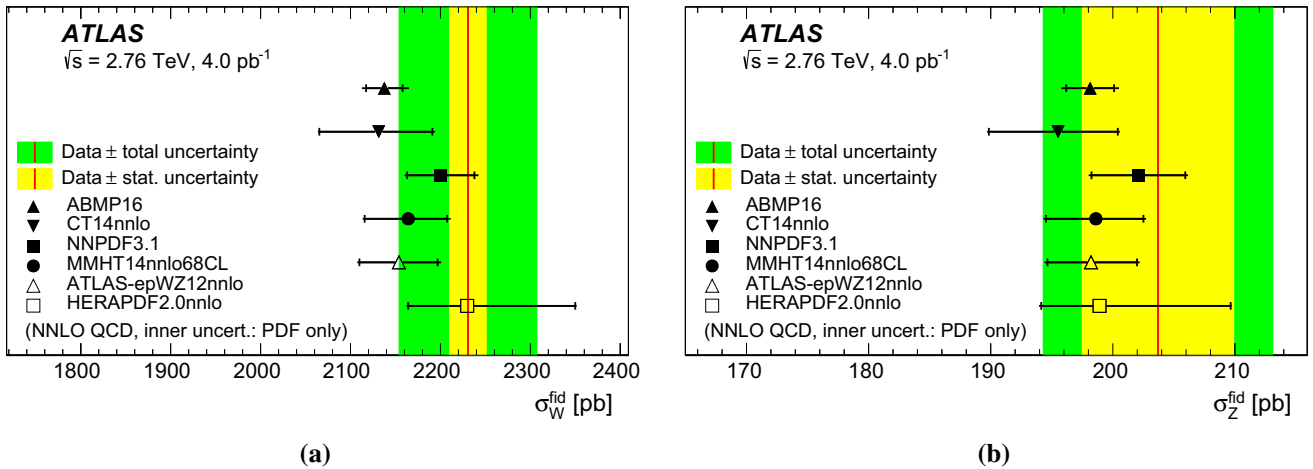


Fig. 6 NNLO predictions for the fiducial cross-sections (a) σ_W^{fid} and (b) σ_Z^{fid} for the six PDFs CT14nnlo, MMHT2014, NNPDF3.1, ATLASepWZ12, ABMP16 and, HERApdf2.0 compared with the measured fiducial cross-section as given in Table 7. The inner shaded band

represents the statistical uncertainty only, the outer band corresponds to the experimental uncertainty (including the luminosity uncertainty). The theory predictions are given with the corresponding PDF (total uncertainty shown by inner (outer) error bar

$$A_\ell = \frac{\sigma_{W^+}^{\text{fid}} - \sigma_{W^-}^{\text{fid}}}{\sigma_{W^+}^{\text{fid}} + \sigma_{W^-}^{\text{fid}}}$$

This observable also benefits from the cancellation of systematic uncertainties in the same way as the cross-section ratios. The measured value is:

$$A_\ell = 0.285 \pm 0.009(\text{stat.}) \pm 0.002(\text{syst.}).$$

The ratio of measured cross-sections in the electron and muon decay channels provides a test of lepton universality in W -boson decays. The measured ratios are:

$$R_{W^+} = \frac{\sigma_{W^+ \rightarrow e^+ \nu}^{\text{fid}}}{\sigma_{W^+ \rightarrow \mu^+ \nu}^{\text{fid}}} = 0.985 \pm 0.023 (\text{stat.}) \pm 0.028 (\text{syst.})$$

$$R_{W^-} = \frac{\sigma_{W^- \rightarrow e^- \bar{\nu}}^{\text{fid}}}{\sigma_{W^- \rightarrow \mu^- \bar{\nu}}^{\text{fid}}} = 0.988 \pm 0.030 (\text{stat.}) \pm 0.028 (\text{syst.})$$

$$R_W = \frac{\sigma_{W \rightarrow e \nu}^{\text{fid}}}{\sigma_{W \rightarrow \mu \nu}^{\text{fid}}} = 0.986 \pm 0.018 (\text{stat.}) \pm 0.028 (\text{syst.})$$

$$R_Z = \frac{\sigma_{Z \rightarrow e^+ e^-}^{\text{fid}}}{\sigma_{Z \rightarrow \mu^+ \mu^-}^{\text{fid}}} = 0.96 \pm 0.06 (\text{stat.}) \pm 0.05 (\text{syst.})$$

These results lie within one standard deviation of the Standard Model prediction and previous measurements by ATLAS.

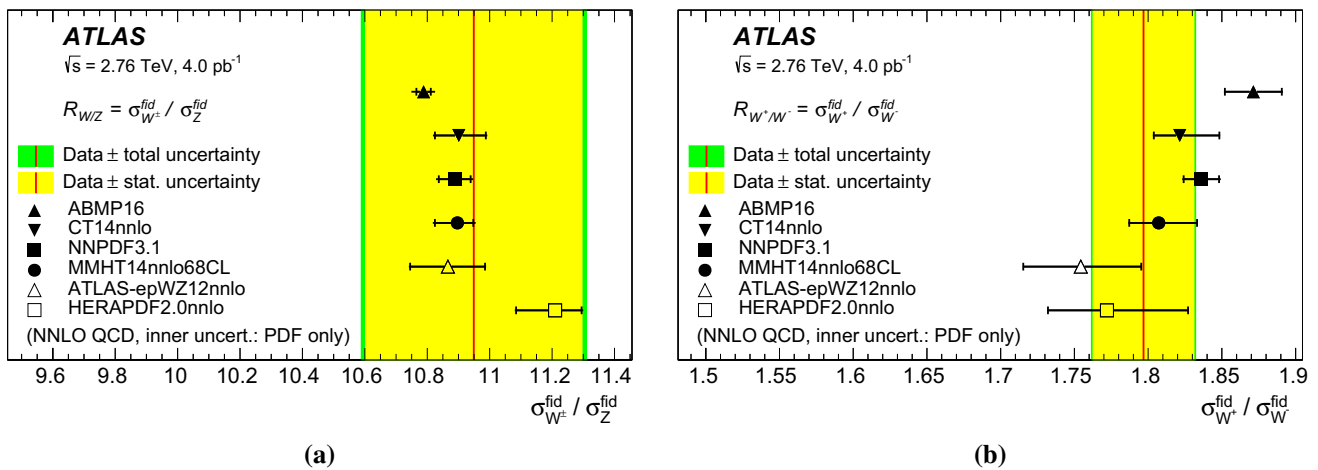


Fig. 7 The measured ratio of fiducial cross-sections for (a) W -boson production to Z -boson production, (b) W^+ -boson production to W^- -boson production. The measurements are compared with theoretical predictions at NNLO in QCD based on a selection of different PDF

9 Conclusion

This paper presents measurements of the $W \rightarrow \ell\nu$ and $Z \rightarrow \ell\ell$ production cross-sections based on about 12 400 W -boson and 1100 Z -boson candidates, after subtracting background events, reconstructed from $\sqrt{s} = 2.76$ TeV proton–proton collision data recorded by the ATLAS detector at the LHC, corresponding to integrated luminosity of 4.0 pb^{-1} . The total inclusive W -boson production cross-sections for the combined electron and muon channels are

$$\begin{aligned} \sigma_{W^+ \rightarrow \ell\nu}^{\text{tot}} &= 2312 \pm 26 \text{ (stat.)} \pm 27 \text{ (syst.)} \pm 72 \text{ (lumi.)} \\ &\pm 30 \text{ (extr.) pb,} \\ \sigma_{W^- \rightarrow \ell\nu}^{\text{tot}} &= 1399 \pm 21 \text{ (stat.)} \pm 17 \text{ (syst.)} \pm 43 \text{ (lumi.)} \\ &\pm 21 \text{ (extr.) pb,} \end{aligned}$$

and the total inclusive Z -boson cross-section in the combined electron and muon channels is:

$$\sigma_{Z \rightarrow \ell\ell}^{\text{tot}} = 323.4 \pm 9.8 \text{ (stat.)} \pm 5.0 \text{ (syst.)} \pm 10.0 \text{ (lumi.)} \pm 5.5 \text{ (extr.) pb.}$$

The results obtained, and the ratios and charge asymmetries constructed from them, are in agreement with theoretical calculations based on NNLO QCD.

Acknowledgements We thank CERN for the very successful operation of the LHC, as well as the support staff from our institutions without whom ATLAS could not be operated efficiently. We acknowledge the support of ANPCyT, Argentina; YerPhI, Armenia; ARC, Australia; BMWFW and FWF, Austria; ANAS, Azerbaijan; SSTC, Belarus; CNPq and FAPESP, Brazil; NSERC, NRC and CFI, Canada; CERN; CONICYT, Chile; CAS, MOST and NSFC, China; COLCIEN-CIAS, Colombia; MSMT CR, MPO CR and VSC CR, Czech Republic; DNRF and DNSRC, Denmark; IN2P3-CNRS, CEA-DRF/IRFU, France; SRNSFG, Georgia; BMBF, HGF, and MPG, Germany; GSRT, Greece; RGC, Hong Kong SAR, China; ISF and Benozziyo Center,

sets. The inner shaded band corresponds to statistical uncertainty while the outer band shows statistical and systematic uncertainties added in quadrature. The theory predictions are given with the corresponding PDF (total) uncertainty shown by inner (outer) error bar

Israel; INFN, Italy; MEXT and JSPS, Japan; CNRST, Morocco; NWO, Netherlands; RCN, Norway; MNiSW and NCN, Poland; FCT, Portugal; MNE/IFA, Romania; MES of Russia and NRC KI, Russian Federation; JINR; MESTD, Serbia; MSSR, Slovakia; ARRS and MIZŠ, Slovenia; DST/NRF, South Africa; MINECO, Spain; SRC and Wallenberg Foundation, Sweden; SERI, SNSF and Cantons of Bern and Geneva, Switzerland; MOST, Taiwan; TAEK, Turkey; STFC, United Kingdom; DOE and NSF, United States of America. In addition, individual groups and members have received support from BCKDF, CANARIE, CRC and Compute Canada, Canada; COST, ERC, ERDF, Horizon 2020, and Marie Skłodowska-Curie Actions, European Union; Investissements d’Avenir Labex and Idex, ANR, France; DFG and AvH Foundation, Germany; Herakleitos, Thales and Aristeia programmes co-financed by EU-ESF and the Greek NSRF, Greece; BSF-NSF and GIF, Israel; CERCA Programme Generalitat de Catalunya, Spain; The Royal Society and Leverhulme Trust, United Kingdom. The crucial computing support from all WLCG partners is acknowledged gratefully, in particular from CERN, the ATLAS Tier-1 facilities at TRIUMF (Canada), NDGF (Denmark, Norway, Sweden), CC-IN2P3 (France), KIT/GridKA (Germany), INFN-CNAF (Italy), NL-T1 (Netherlands), PIC (Spain), ASGC (Taiwan), RAL (UK) and BNL (USA), the Tier-2 facilities worldwide and large non-WLCG resource providers. Major contributors of computing resources are listed in Ref. [83].

Data Availability Statement This manuscript has no associated data or the data will not be deposited. [Authors’ comment: “All ATLAS scientific output is published in journals, and preliminary results are made available in Conference Notes. All are openly available, without restriction on use by external parties beyond copyright law and the standard conditions agreed by CERN. Data associated with journal publications are also made available: tables and data from plots (e.g. cross section values, likelihood profiles, selection efficiencies, cross section limits, ...) are stored in appropriate repositories such as HEPDATA (<http://hepdata.cedar.ac.uk/>). ATLAS also strives to make additional material related to the paper available that allows a reinterpretation of the data in the context of new theoretical models. For example, an extended encapsulation of the analysis is often provided for measurements in the framework of RIVET (<http://rivet.hepforge.org/>)”. This information is taken from the ATLAS Data Access Policy, which is a public document that can be downloaded from <http://opendata.cern.ch/record/413> [opendata.cern.ch].]

Table 9 The predictions at NNLO in QCD, using the MMHT14nnlo68cl, NNPDF31_nnlo_as_0118, ATLASepWZ12, HERAPDF2.0, and ABMP16 PDF sets, for the cross-sections measured in this study

Quantity	Predicted cross-section \pm PDF uncertainty (pb)				
	MMHT14	NNPDF31	ATLASepWZ12	HERAPDF20	ABMP16
$\sigma_{W^+}^{\text{fid}}$	1397_{-30}^{+29}	1428_{-24}^{+24}	1375_{-30}^{+34}	1429_{-49}^{+91}	1397_{-14}^{+14}
$\sigma_{W^-}^{\text{fid}}$	773_{-20}^{+17}	778_{-14}^{+14}	784_{-19}^{+19}	806_{-21}^{+31}	746_{-9}^{+9}
σ_Z^{fid}	199_{-4}^{+4}	203_{-4}^{+4}	199_{-4}^{+4}	199_{-5}^{+11}	$198.6_{-2.0}^{+2.0}$
$\sigma_{W^+}^{\text{tot}}$	2138_{-45}^{+43}	2271_{-36}^{+36}	2086_{-47}^{+54}	2140_{-70}^{+140}	2214_{-21}^{+21}
$\sigma_{W^-}^{\text{tot}}$	1295_{-33}^{+28}	1330_{-22}^{+22}	1296_{-29}^{+48}	1338_{-32}^{+52}	1283_{-16}^{+16}
σ_Z^{tot}	308_{-6}^{+6}	313_{-5}^{+5}	308_{-5}^{+6}	312_{-7}^{+16}	$305.7_{-3.0}^{+3.0}$

Open Access This article is distributed under the terms of the Creative Commons Attribution 4.0 International License (<http://creativecommons.org/licenses/by/4.0/>), which permits unrestricted use, distribution, and reproduction in any medium, provided you give appropriate credit to the original author(s) and the source, provide a link to the Creative Commons license, and indicate if changes were made. Funded by SCOAP³.

Appendix

A Theoretical predictions

This appendix presents the theoretical predictions used for comparison with the measurements in the main body of the paper. Table 9 shows the predictions using the MMHT14nnlo68cl, NNPDF31_nnlo_as_0118, ATLASepWZ12, HERAPDF2.0, and ABMP16 PDF sets with associated PDF uncertainties.

References

- V.N. Gribov, L.N. Lipatov, Deep inelastic e p scattering in perturbation theory. *Sov. J. Nucl. Phys.* **15**, 438 (1972)
- V.N. Gribov, L.N. Lipatov, Deep inelastic e p scattering in perturbation theory. *Yad. Fiz.* **15**, 781 (1972)
- L.N. Lipatov, The parton model and perturbation theory. *Sov. J. Nucl. Phys.* **20**, 94 (1975)
- L.N. Lipatov, The parton model and perturbation theory. *Yad. Fiz.* **20**, 181 (1974)
- G. Altarelli, G. Parisi, Asymptotic freedom in parton language. *Nucl. Phys. B* **126**, 298 (1977)
- Y.L. Dokshitzer, Calculation of the structure functions for deep inelastic scattering and e^+e^- annihilation by perturbation theory in quantum chromodynamics. *Sov. Phys. JETP* **46**, 641 (1977)
- Y.L. Dokshitzer, Calculation of the structure functions for deep inelastic scattering and e^+e^- annihilation by perturbation theory in quantum chromodynamics. *Zh. Eksp. Teor. Fiz.* **73**, 1216 (1972)
- L. Evans, P. Bryant, L.H.C. Machine, *JINST* **3**, S08001 (2008)
- ATLAS Collaboration, Measurements of W and Z boson production in pp collisions at $\sqrt{s} = 5.02$ TeV with the ATLAS detector. *Eur. Phys. J. C* **79**, 128 (2019). [arXiv:1810.08424](https://arxiv.org/abs/1810.08424) [hep-ex]
- ATLAS Collaboration, Precision measurement and interpretation of inclusive W^+ , W^- and Z/γ^* production cross sections with the ATLAS detector. *Eur. Phys. J. C* **77**, 367 (2017). [arXiv:1612.03016](https://arxiv.org/abs/1612.03016) [hep-ex]
- CMS Collaboration, Measurement of inclusive W and Z production cross sections in pp collisions at $\sqrt{s} = 7$ TeV. *JHEP* **10**, 132 (2011). [arXiv:1107.4789](https://arxiv.org/abs/1107.4789) [hep-ex]
- LHCb Collaboration, Measurement of the forward Z boson production cross-section in pp collisions at $\sqrt{s} = 7$ TeV. *JHEP* **08**, 039 (2015). [arXiv:1505.07024](https://arxiv.org/abs/1505.07024) [hep-ex]
- LHCb Collaboration, Measurement of the forward W boson cross-section in pp collisions at $\sqrt{s} = 7$ TeV. *JHEP* **12**, 079 (2014). [arXiv:1408.4354](https://arxiv.org/abs/1408.4354) [hep-ex]
- LHCb Collaboration, Measurement of the cross-section for $Z \rightarrow e^+e^-$ production in pp collisions at $\sqrt{s} = 7$ TeV. *JHEP* **02**, 106 (2013). [arXiv:1212.4620](https://arxiv.org/abs/1212.4620) [hep-ex]
- ATLAS Collaboration, Measurement of the transverse momentum and ϕ_η^* distributions of Drell–Yan lepton pairs in proton–proton collisions at $\sqrt{s} = 8$ TeV with the ATLAS detector. *Eur. Phys. J. C* **76**, 291 (2016). [arXiv:1512.02192](https://arxiv.org/abs/1512.02192) [hep-ex]
- CMS Collaboration, Measurement of inclusive W and Z boson production cross sections in pp collisions at $\sqrt{s} = 8$ TeV. *Phys. Rev. Lett.* **112**, 191802 (2014). [arXiv:1402.0923](https://arxiv.org/abs/1402.0923) [hep-ex]
- LHCb Collaboration, Measurement of forward W and Z boson production in pp collisions at $\sqrt{s} = 8$ TeV. *JHEP* **01**, 155 (2016). [arXiv:1511.08039](https://arxiv.org/abs/1511.08039) [hep-ex]
- LHCb Collaboration, Measurement of forward $W \rightarrow ev$ production in pp collisions at $\sqrt{s} = 8$ TeV. *JHEP* **10**, 030 (2016). [arXiv:1608.01484](https://arxiv.org/abs/1608.01484) [hep-ex]
- LHCb Collaboration, Measurement of forward $Z \rightarrow e^+e^-$ production at $\sqrt{s} = 8$ TeV. *JHEP* **05**, 109 (2015). [arXiv:1503.00963](https://arxiv.org/abs/1503.00963) [hep-ex]
- ATLAS Collaboration, Measurement of W^\pm and Z-boson production cross sections in pp collisions at $\sqrt{s} = 13$ TeV with the ATLAS detector. *Phys. Lett. B* **759**, 601 (2016). [arXiv:1603.09222](https://arxiv.org/abs/1603.09222) [hep-ex]
- ATLAS Collaboration, Measurements of top-quark pair to Z-boson cross-section ratios at $\sqrt{s} = 13, 8, 7$ TeV with the ATLAS detector. *JHEP* **02**, 117 (2017). [arXiv:1612.03636](https://arxiv.org/abs/1612.03636) [hep-ex]
- LHCb Collaboration, Measurement of the forward Z boson production cross-section in pp collisions at $\sqrt{s} = 13$ TeV. *JHEP* **09**, 136 (2016). [arXiv:1607.06495](https://arxiv.org/abs/1607.06495) [hep-ex]
- PHENIX Collaboration, Cross section and parity violating spin asymmetries of W^\pm boson production in polarized $p + p$ collisions at $\sqrt{s} = 500$ GeV. *Phys. Rev. Lett.* **106**, 062001 (2011). [arXiv:1009.0505](https://arxiv.org/abs/1009.0505) [hep-ex]
- STAR Collaboration, Measurement of the $W \rightarrow ev$ and $Z/\gamma^* \rightarrow e^+e^-$ production cross sections at mid-rapidity in proton–proton collisions at $\sqrt{s} = 500$ GeV. *Phys. Rev. D* **85**, 092010 (2012). [arXiv:1112.2980](https://arxiv.org/abs/1112.2980) [hep-ex]
- PHENIX Collaboration, Cross section and longitudinal single-spin asymmetry A_L for forward $W^\pm \rightarrow \mu^\pm\nu$ production in polarized p+p collisions at $\sqrt{s} = 510$ GeV. *Phys. Rev. D* **98**, 032007 (2018). [arXiv:1804.04181](https://arxiv.org/abs/1804.04181) [hep-ex]

26. CDF Collaboration, A measurement of the production and muonic decay rate of W and Z bosons in $p\bar{p}$ collisions at $\sqrt{s} = 1.8$ TeV. Phys. Rev. Lett. **69**, 28 (1992)
27. CDF Collaboration, Measurement of $\sigma B(W \rightarrow e\nu)$ and $\sigma B(Z^0 \rightarrow e^+e^-)$ in $p\bar{p}$ Collisions at $\sqrt{s} = 1.8$ TeV. Phys. Rev. Lett. **76**, 3070 (1996). [arXiv:hep-ex/9509010](#) [hep-ex]
28. CDF Collaboration, Measurement of Z^0 and Drell-Yan production cross section using dimuons in $p\bar{p}$ collisions at $\sqrt{s} = 1.8$ TeV. Phys. Rev. D **59**, 052002 (1999)
29. CDF Collaboration, Transverse momentum and total cross section of e^+e^- pairs in the Z-boson region from $p\bar{p}$ collisions at $\sqrt{s} = 1.8$ TeV. Phys. Rev. Lett. **84**, 845 (2000). [arXiv:hep-ex/0001021](#) [hep-ex]
30. CDF Collaboration, Measurements of inclusive W and Z cross sections in p anti-p collisions at $\sqrt{s} = 1.96$ -TeV. J. Phys. G **34**, 2457 (2007). [arXiv:hep-ex/0508029](#) [hep-ex]
31. D0 Collaboration, W and Z boson production in $p\bar{p}$ collisions at $\sqrt{s} = 1.8$ -TeV. Phys. Rev. Lett. **75**, 1456 (1995). [arXiv:hep-ex/9505013](#) [hep-ex]
32. UA1 Collaboration, Studies of intermediate vector boson production and decay in UA1 at the CERN proton-antiproton collider. Z. Phys. C **44**, 15 (1989)
33. UA2 Collaboration, A measurement of the W and Z production cross-sections and a determination of Γ_W at the CERN $p\bar{p}$ collider. Phys. Lett. B **276**, 365 (1992)
34. ATLAS Collaboration, The ATLAS Experiment at the CERN Large Hadron Collider, JINST 3 S08003 (2008)
35. ATLAS Collaboration, Performance of the ATLAS Trigger System in 2010. Eur. Phys. J. C **72**, 1849 (2012). [arXiv:1110.1530](#) [hep-ex]
36. P. Nason, A new method for combining NLO QCD with shower Monte Carlo algorithms. JHEP **11**, 040 (2004). [arXiv:hep-ph/0409146](#) [hep-ph]
37. S. Frixione, P. Nason, C. Oleari, Matching NLO QCD computations with parton shower simulations: the POWHEG method. JHEP **11**, 070 (2007). [arXiv:0709.2092](#) [hep-ph]
38. S. Alioli, P. Nason, C. Oleari, E. Re, A general framework for implementing NLO calculations in shower Monte Carlo programs: the POWHEG BOX. JHEP **06**, 043 (2010). [arXiv:1002.2581](#) [hep-ph]
39. S. Alioli, P. Nason, C. Oleari, E. Re, NLO vector-boson production matched with shower in POWHEG. JHEP **07**, 060 (2008). [arXiv:0805.4802](#) [hep-ph]
40. T. Sjöstrand, S. Mrenna, P.Z. Skands, A brief introduction to PYTHIA 8.1. Comput. Phys. Commun. **178**, 852 (2008). [arXiv:0710.3820](#) [hep-ph]
41. H.-L. Lai et al., New parton distributions for collider physics. Phys. Rev. D **82**, 074024 (2010). [arXiv:1007.2241](#) [hep-ph]
42. ATLAS Collaboration, ATLAS Pythia 8 tunes to 7 TeV data, ATL-PHYS-PUB-2014-021 (2014). <https://cds.cern.ch/record/1966419>
43. N. Davidson, T. Przedzinski, Z. Was, PHOTOS interface in C++: technical and physics documentation. Comput. Phys. Commun. **199**, 86 (2016). [arXiv:1011.0937](#) [hep-ph]
44. T. Gleisberg et al., Event generation with SHERPA 1.1. JHEP **02**, 007 (2009). [arXiv:0811.4622](#) [hep-ph]
45. S. Frixione, P. Nason, G. Ridolfi, A positive-weight next-to-leading-order Monte Carlo for heavy flavour hadroproduction. JHEP **09**, 126 (2007). [arXiv:0707.3088](#) [hep-ph]
46. T. Sjöstrand, S. Mrenna, P.Z. Skands, PYTHIA 6.4 physics and manual. JHEP **05**, 026 (2006). [arXiv:hep-ph/0603175](#) [hep-ph]
47. P.Z. Skands, Tuning Monte Carlo generators: the Perugia tunes. Phys. Rev. D **82**, 074018 (2010). [arXiv:1005.3457](#) [hep-ph]
48. N. Davidson, G. Nanava, T. Przedzinski, E. Richter-Was, Z. Was, Universal interface of TAUOLA technical and physics documentation. Comput. Phys. Commun. **183**, 821 (2012). [arXiv:1002.0543](#) [hep-ph]
49. G. Corcella et al., HERWIG 6.5 release note. [arXiv: hep-ph/0210213](#) [hep-ph]
50. J.M. Butterworth, J.R. Forshaw, M.H. Seymour, Multiparton interactions in photoproduction at HERA. Z. Phys. C **72**, 637 (1996). [arXiv:hep-ph/9601371](#) [hep-ph]
51. J. Pumplin et al., New generation of parton distributions with uncertainties from global QCD analysis. JHEP **07**, 012 (2002). [arXiv:hep-ph/0201195](#) [hep-ph]
52. ATLAS Collaboration, New ATLAS event generator tunes to 2010 data, ATL-PHYS-PUB-2011-008 (2011). <https://cds.cern.ch/record/1345343>
53. ATLAS Collaboration, The ATLAS simulation infrastructure. Eur. Phys. J. C **70**, 823 (2010). [arXiv:1005.4568](#) [physics.ins-det]
54. S. Agostinelli et al., GEANT4-A simulation toolkit. Nucl. Instrum. Methods A **506**, 250 (2003)
55. ATLAS Collaboration, Electron efficiency measurements with the ATLAS detector using 2012 LHC proton-proton collision data. Eur. Phys. J. C **77**, 195 (2017). [arXiv:1612.01456](#) [hep-ex]
56. ATLAS Collaboration, Improved electron reconstruction in ATLAS using the Gaussian Sum Filterbased model for bremsstrahlung, ATLAS-CONF-2012-047 (2012). <https://cds.cern.ch/record/1449796>
57. ATLAS Collaboration, Measurement of the muon reconstruction performance of the ATLAS detector using 2011 and 2012 LHC proton-proton collision data. Eur. Phys. J. C **74**, 3130 (2014). [arXiv:1407.3935](#) [hep-ex]
58. ATLAS Collaboration, Performance of algorithms that reconstruct missing transverse momentum in $\sqrt{s} = 8$ TeV proton-proton collisions in the ATLAS detector. Eur. Phys. J. C **77**, 241 (2017). [arXiv:1609.09324](#) [hep-ex]
59. ATLAS Collaboration, Topological cell clustering in the ATLAS calorimeters and its performance in LHC Run 1. Eur. Phys. J. C **77**, 490 (2017). [arXiv:1603.02934](#) [hep-ex]
60. ATLAS Collaboration, Measurement of the W-boson mass in pp collisions at $\sqrt{s} = 7$ TeV with the ATLAS detector. Eur. Phys. J. C **78**, 110 (2018). [arXiv:1701.07240](#) [hep-ex]
61. ATLAS Collaboration, Measurement of differential cross sections and W^+/W^- cross-section ratios for W boson production in association with jets at $\sqrt{s} = 8$ TeV with the ATLAS detector. JHEP **05**, 077 (2018). [arXiv:1711.03296](#) [hep-ex]
62. ATLAS Collaboration, Electron performance measurements with the ATLAS detector using the 2010 LHC proton-proton collision data. Eur. Phys. J. C **72**, 1909 (2012). [arXiv:1110.3174](#) [hep-ex]
63. ATLAS Collaboration, Improved luminosity determination in pp collisions at $\sqrt{s} = 7$ TeV using the ATLAS detector at the LHC. Eur. Phys. J. C **73**, 2518 (2013). [arXiv:1302.4393](#) [hep-ex]
64. S. Alekhin, J. Bluemlein, S. Klein, S. Moch, 3-, 4-, and 5-flavor next-to-next-to-leading order parton distribution from deep-inelastic-scattering data and at hadron colliders. Phys. Rev. D **81**, 014032 (2010). [arXiv:0908.2766](#) [hep-ph]
65. R.D. Ball et al., Parton distributions with LHC data. Nucl. Phys. B **867**, 244 (2013). [arXiv:1207.1303](#) [hep-ph]
66. ATLAS Collaboration, Determination of the strange-quark density of the proton from ATLAS measurements of the $W \rightarrow \ell\nu$ and $Z \rightarrow \ell\ell$ cross sections. Phys. Rev. Lett. **109**, 012001 (2012). [arXiv:1203.4051](#) [hep-ex]
67. A. Glazov, Averaging of DIS cross section data. AIP Conf. Proc. **792**, 237 (2005)
68. S. Catani, M. Grazzini, A next-to-next-to-leading order subtraction formalism in hadron collisions and its application to Higgs-Boson production at the large hadron collider. Phys. Rev. Lett. **98**, 222002 (2007). [arXiv:hep-ph/0703012](#) [hep-ph]
69. K. Melnikov, F. Petriello, Electroweak gauge boson production at hadron colliders through $O(\alpha_s^2)$. Phys. Rev. D **74**, 114017 (2006). [arXiv:hep-ph/0609070](#) [hep-ph]

70. R. Gavin, Y. Li, F. Petriello, S. Quackenbush, FEWZ 2.0: a code for hadronic Z production at next-to-next-to-leading order. *Comput. Phys. Commun.* **182**, 2388 (2011). [arXiv:1011.3540](https://arxiv.org/abs/1011.3540) [hep-ph]
71. R. Gavin, Y. Li, F. Petriello, S. Quackenbush, W physics at the LHC with FEWZ 2.1. *Comput. Phys. Commun.* **184**, 208 (2013). [arXiv:1201.5896](https://arxiv.org/abs/1201.5896) [hep-ph]
72. Y. Li, F. Petriello, Combining QCD and electroweak corrections to dilepton production in the framework of the FEWZ simulation code. *Phys. Rev. D* **86**, 094034 (2012). [arXiv:1208.5967](https://arxiv.org/abs/1208.5967) [hep-ph]
73. D. Bardin et al., SANC integrator in the progress: QCD and EW contributions. *JETP Lett.* **96**, 285 (2012). [arXiv:1207.4400](https://arxiv.org/abs/1207.4400) [hep-ph]
74. A.B. Arbuzov, R.R. Sadykov, Z. Was, QED Bremsstrahlung in decays of electroweak bosons. *Eur. Phys. J. C* **73**, 2625 (2013). [arXiv:1212.6783](https://arxiv.org/abs/1212.6783) [hep-ph]
75. W.F.L. Hollik, Radiative corrections in the standard model and their role for precision tests of the electroweak theory. *Fortsch. Phys.* **38**, 165 (1990)
76. K.A. Olive et al., Review of Particle Physics. *Chin. Phys. C* **38**, 090001 (2014)
77. S. Dittmaier, M. Huber, Radiative corrections to the neutral-current Drell–Yan process in the Standard Model and its minimal supersymmetric extension. *JHEP* **01**, 060 (2010). [arXiv:0911.2329](https://arxiv.org/abs/0911.2329) [hep-ph]
78. S. Dulat et al., New parton distribution functions from a global analysis of quantum chromodynamics. *Phys. Rev. D* **93**, 033006 (2016). [arXiv:1506.07443](https://arxiv.org/abs/1506.07443) [hep-ph]
79. R.D. Ball et al., Parton distributions from high-precision collider data. *Eur. Phys. J. C* **77**, 663 (2017). [arXiv:1706.00428](https://arxiv.org/abs/1706.00428) [hep-ph]
80. L.A. Harland-Lang, A.D. Martin, P. Motylinski, R.S. Thorne, Parton distributions in the LHC era: MMHT 2014 PDFs. *Eur. Phys. J. C* **75**, 204 (2015). [arXiv:1412.3989](https://arxiv.org/abs/1412.3989) [hep-ph]
81. S. Alekhin, J. Bluemlein, S. Moch, R. Placakyte, Parton distribution functions, α_s , and heavyquark masses for LHC Run II. *Phys. Rev. D* **96**, 014011 (2017). [arXiv:1701.05838](https://arxiv.org/abs/1701.05838) [hep-ph]
82. H1 and ZEUS Collaborations, Combination of measurements of inclusive deep inelastic $e^\pm p$ scattering cross sections and QCD analysis of HERA data. *Eur. Phys. J. C* **75**, 580 (2015). [arXiv:1506.06042](https://arxiv.org/abs/1506.06042) [hep-ex]
83. ATLAS Collaboration, ATLAS Computing Acknowledgements, ATL-GEN-PUB-2016-002. <https://cds.cern.ch/record/2202407>

ATLAS Collaboration

G. Aad¹⁰¹, B. Abbott¹²⁸, D. C. Abbott¹⁰², O. Abdinov^{13,*}, A. Abed Abud^{70a,70b}, K. Abeling⁵³, D. K. Abhayasinghe⁹³, S. H. Abidi¹⁶⁷, O. S. AbouZeid⁴⁰, N. L. Abraham¹⁵⁶, H. Abramowicz¹⁶¹, H. Abreu¹⁶⁰, Y. Abulaiti⁶, B. S. Acharya^{66a,66b,p}, B. Achkar⁵³, S. Adachi¹⁶³, L. Adam⁹⁹, C. Adam Bourdarios¹³², L. Adamczyk^{83a}, L. Adamek¹⁶⁷, J. Adelman¹²¹, M. Adersberger¹¹⁴, A. Adiguzel^{12c,ak}, S. Adorni⁵⁴, T. Adye¹⁴⁴, A. A. Affolder¹⁴⁶, Y. Afik¹⁶⁰, C. Agapopoulou¹³², M. N. Agaras³⁸, A. Aggarwal¹¹⁹, C. Agheorghiesei^{27c}, J. A. Aguilar-Saavedra^{140a,140f,aj}, F. Ahmadov⁷⁹, W. S. Ahmed¹⁰³, X. Ai^{15a}, G. Aielli^{73a,73b}, S. Akatsuka⁸⁵, T. P. A. Åkesson⁹⁶, E. Akilli⁵⁴, A. V. Akimov¹¹⁰, K. Al Khoury¹³², G. L. Alberghi^{23a,23b}, J. Albert¹⁷⁶, M. J. Alconada Verzini¹⁶¹, S. Alderweireldt³⁶, M. Aleksa³⁶, I. N. Aleksandrov⁷⁹, C. Alexa^{27b}, D. Alexandre¹⁹, T. Alexopoulos¹⁰, A. Alfonsi¹²⁰, M. Alhroob¹²⁸, B. Ali¹⁴², G. Alimonti^{68a}, J. Alison³⁷, S. P. Alkire¹⁴⁸, C. Allaire¹³², B. M. M. Allbrooke¹⁵⁶, B. W. Allen¹³¹, P. P. Allport²¹, A. Aloisio^{69a,69b}, A. Alonso⁴⁰, F. Alonso⁸⁸, C. Alpigiani¹⁴⁸, A. A. Alshehri⁵⁷, M. Alvarez Estevez⁹⁸, D. Álvarez Piqueras¹⁷⁴, M. G. Alvigi^{69a,69b}, Y. Amaral Coutinho^{80b}, A. Ambler¹⁰³, L. Ambroz¹³⁵, C. Amelung²⁶, D. Amidei¹⁰⁵, S. P. Amor Dos Santos^{140a}, S. Amoroso⁴⁶, C. S. Amrouche⁵⁴, F. An⁷⁸, C. Anastopoulos¹⁴⁹, N. Andari¹⁴⁵, T. Andeen¹¹, C. F. Anders^{61b}, J. K. Anders²⁰, A. Andreazza^{68a,68b}, V. Andrei^{61a}, C. R. Anelli¹⁷⁶, S. Angelidakis³⁸, A. Angerami³⁹, A. V. Anisenkov^{122a,122b}, A. Annovi^{71a}, C. Antel^{61a}, M. T. Anthony¹⁴⁹, M. Antonelli⁵¹, D. J. A. Antrim¹⁷¹, F. Anulli^{72a}, M. Aoki⁸¹, J. A. Aparisi Pozo¹⁷⁴, L. Aperio Bella³⁶, G. Arabidze¹⁰⁶, J. P. Araque^{140a}, V. Araujo Ferraz^{80b}, R. Araujo Pereira^{80b}, C. Arcangeletti⁵¹, A. T. H. Arce⁴⁹, F. A. Arduh⁸⁸, J-F. Arguin¹⁰⁹, S. Argyropoulos⁷⁷, J.-H. Arling⁴⁶, A. J. Armbruster³⁶, L. J. Armitage⁹², A. Armstrong¹⁷¹, O. Arnaez¹⁶⁷, H. Arnold¹²⁰, A. Artamonov^{111,*}, G. Artoni¹³⁵, S. Artz⁹⁹, S. Asai¹⁶³, N. Asbah⁵⁹, E. M. Asimakopoulou¹⁷², L. Asquith¹⁵⁶, K. Assamagan²⁹, R. Astalos^{28a}, R. J. Atkin^{33a}, M. Atkinson¹⁷³, N. B. Atlay¹⁵¹, H. Atmani¹³², K. Augsten¹⁴², G. Avolio³⁶, R. Avramidou^{60a}, M. K. Ayoub^{15a}, A. M. Azoulay^{168b}, G. Azuelos^{109,az}, M. J. Baca²¹, H. Bachacou¹⁴⁵, K. Bachas^{67a,67b}, M. Backes¹³⁵, F. Backman^{45a,45b}, P. Bagnaia^{72a,72b}, M. Bahmani⁸⁴, H. Bahrasemani¹⁵², A. J. Bailey¹⁷⁴, V. R. Bailey¹⁷³, J. T. Baines¹⁴⁴, M. Bajic⁴⁰, C. Bakalis¹⁰, O. K. Baker¹⁸³, P. J. Bakker¹²⁰, D. Bakshi Gupta⁸, S. Balaji¹⁵⁷, E. M. Baldin^{122a,122b}, P. Balek¹⁸⁰, F. Balli¹⁴⁵, W. K. Balunas¹³⁵, J. Balz⁹⁹, E. Banas⁸⁴, A. Bandyopadhyay²⁴, Sw. Banerjee^{181,j}, A. A. E. Bannoura¹⁸², L. Barak¹⁶¹, W. M. Barbe³⁸, E. L. Barberio¹⁰⁴, D. Barberis^{55a,55b}, M. Barbero¹⁰¹, T. Barillari¹¹⁵, M-S. Barisits³⁶, J. Barkeloo¹³¹, T. Barklow¹⁵³, R. Barnea¹⁶⁰, S. L. Barnes^{60c}, B. M. Barnett¹⁴⁴, R. M. Barnett¹⁸, Z. Barnovska-Blenessy^{60a}, A. Baroncelli^{60a}, G. Barone²⁹, A. J. Barr¹³⁵, L. Barranco Navarro^{45a,45b}, F. Barreiro⁹⁸, J. Barreiro Guimarães da Costa^{15a}, S. Barsov¹³⁸, R. Bartoldus¹⁵³, G. Bartolini¹⁰¹, A. E. Barton⁸⁹, P. Bartos^{28a}, A. Basalae⁴⁶, A. Bassalat^{132,as}, R. L. Bates⁵⁷, S. J. Batista¹⁶⁷, S. Batlamous^{35e}, J. R. Batley³², B. Batool¹⁵¹, M. Battaglia¹⁴⁶, M. Bauge^{72a,72b}, F. Bauer¹⁴⁵, K. T. Bauer¹⁷¹, H. S. Bawa^{31,n}, J. B. Beacham⁴⁹, T. Beau¹³⁶, P. H. Beauchemin¹⁷⁰, F. Becherer⁵², P. Bechtel²⁴, H. C. Beck⁵³, H. P. Beck^{20,i}, K. Becker⁵², M. Becker⁹⁹, C. Becot⁴⁶, A. Beddall^{12d}, A. J. Beddall^{12a}, V. A. Bednyakov⁷⁹, M. Bedognetti¹²⁰, C. P. Bee¹⁵⁵, T. A. Beermann⁷⁶, M. Begalli^{80b}, M. Beger²⁹, A. Behera¹⁵⁵, J. K. Behr⁴⁶, F. Beisiegel²⁴, A. S. Bell⁹⁴, G. Bella¹⁶¹, L. Bellagamba^{23b}, A. Bellerive³⁴, P. Bellos⁹, K. Beloborodov^{122a,122b}

K. Belotskiy¹¹², N. L. Belyaev¹¹², D. Bencheekroun^{35a}, N. Benekos¹⁰, Y. Benhammou¹⁶¹, D. P. Benjamin⁶, M. Benoit⁵⁴, J. R. Bensinger²⁶, S. Bentvelsen¹²⁰, L. Beresford¹³⁵, M. Beretta⁵¹, D. Berge⁴⁶, E. Bergeas Kuutmann¹⁷², N. Berger⁵, B. Bergmann¹⁴², L. J. Bergsten²⁶, J. Beringer¹⁸, S. Berlendis⁷, N. R. Bernard¹⁰², G. Bernardi¹³⁶, C. Bernius¹⁵³, T. Berry⁹³, P. Berta⁹⁹, C. Bertella^{15a}, I. A. Bertram⁸⁹, G. J. Besjes⁴⁰, O. Bessidskaia Bylund¹⁸², N. Besson¹⁴⁵, A. Bethani¹⁰⁰, S. Bethke¹¹⁵, A. Betti²⁴, A. J. Bevan⁹², J. Beyer¹¹⁵, R. Bi¹³⁹, R. M. Bianchi¹³⁹, O. Biebel¹¹⁴, D. Biedermann¹⁹, R. Bielski³⁶, K. Bierwagen⁹⁹, N. V. Biesuz^{71a,71b}, M. Biglietti^{74a}, T. R. V. Billoud¹⁰⁹, M. Bindi⁵³, A. Bingul^{12d}, C. Bini^{72a,72b}, S. Biondi^{23a,23b}, M. Birman¹⁸⁰, T. Bisanz⁵³, J. P. Biswal¹⁶¹, A. Bitadze¹⁰⁰, C. Bittrich⁴⁸, K. Bjørke¹³⁴, K. M. Black²⁵, T. Blazek^{28a}, I. Bloch⁴⁶, C. Blocker²⁶, A. Blue⁵⁷, U. Blumenschein⁹², G. J. Bobbink¹²⁰, V. S. Bobrovnikov^{122a,122b}, S. S. Bocchetta⁹⁶, A. Bocci⁴⁹, D. Boerner⁴⁶, D. Bogavac¹⁴, A. G. Bogdanchikov^{122a,122b}, C. Bohm^{45a}, V. Boisvert⁹³, P. Bokan^{53,172}, T. Bold^{83a}, A. S. Boldyrev¹¹³, A. E. Bolz^{61b}, M. Bomben¹³⁶, M. Bona⁹², J. S. Bonilla¹³¹, M. Boonekamp¹⁴⁵, H. M. Borecka-Bielska⁹⁰, A. Borisov¹²³, G. Borissov⁸⁹, J. Bortfeldt³⁶, D. Bortoletto¹³⁵, V. Bortolotto^{73a,73b}, D. Boscherini^{23b}, M. Bosman¹⁴, J. D. Bossio Sola¹⁰³, K. Bouaouda^{35a}, J. Boudreau¹³⁹, E. V. Bouhova-Thacker⁸⁹, D. Boumediene³⁸, S. K. Boutle⁵⁷, A. Boveia¹²⁶, J. Boyd³⁶, D. Boye^{33b.at}, I. R. Boyko⁷⁹, A. J. Bozson⁹³, J. Bracinik²¹, N. Brahimy¹⁰¹, G. Brandt¹⁸², O. Brandt^{61a}, F. Braren⁴⁶, B. Brau¹⁰², J. E. Brau¹³¹, W. D. Breaden Madden⁵⁷, K. Brendlinger⁴⁶, L. Brenner⁴⁶, R. Brenner¹⁷², S. Bressler¹⁸⁰, B. Brickwedde⁹⁹, D. L. Briglin²¹, D. Britton⁵⁷, D. Britzger¹¹⁵, I. Brock²⁴, R. Brock¹⁰⁶, G. Brooijmans³⁹, W. K. Brooks^{147c}, E. Brost¹²¹, J. H. Broughton²¹, P. A. Bruckman de Renstrom⁸⁴, D. Bruncko^{28b}, A. Bruni^{23b}, G. Bruni^{23b}, L. S. Bruni¹²⁰, S. Bruno^{73a,73b}, B. H. Brunt³², M. Bruschi^{23b}, N. Brusino¹³⁹, P. Bryant³⁷, L. Bryngemark⁹⁶, T. Buanes¹⁷, Q. Buat³⁶, P. Buchholz¹⁵¹, A. G. Buckley⁵⁷, I. A. Budagov⁷⁹, M. K. Bugge¹³⁴, F. Bühner⁵², O. Bulekov¹¹², T. J. Burch¹²¹, S. Burdin⁹⁰, C. D. Burgard¹²⁰, A. M. Burger¹²⁹, B. Burghgrave⁸, J. T. P. Burr⁴⁶, J. C. Burzynski¹⁰², V. Büscher⁹⁹, E. Buschmann⁵³, P. J. Bussey⁵⁷, J. M. Butler²⁵, C. M. Buttar⁵⁷, J. M. Butterworth⁹⁴, P. Butti³⁶, W. Buttinger³⁶, A. Buzatu¹⁵⁸, A. R. Buzykaev^{122a,122b}, G. Cabras^{23a,23b}, S. Cabrera Urbán¹⁷⁴, D. Caforio⁵⁶, H. Cai¹⁷³, V. M. M. Cairo¹⁵³, O. Cakir^{4a}, N. Calace³⁶, P. Calafiura¹⁸, A. Calandri¹⁰¹, G. Calderini¹³⁶, P. Calfayan⁶⁵, G. Callea⁵⁷, L. P. Caloba^{80b}, S. Calvente Lopez⁹⁸, D. Calvet³⁸, S. Calvet³⁸, T. P. Calvet¹⁵⁵, M. Calvetti^{71a,71b}, R. Camacho Toro¹³⁶, S. Camarda³⁶, D. Camarero Munoz⁹⁸, P. Camari^{73a,73b}, D. Cameron¹³⁴, R. Caminal Armadans¹⁰², C. Camincher³⁶, S. Campana³⁶, M. Campanelli⁹⁴, A. Camplani⁴⁰, A. Campoverde¹⁵¹, V. Canale^{69a,69b}, A. Canesse¹⁰³, M. Cano Bret^{60c}, J. Cantero¹²⁹, T. Cao¹⁶¹, Y. Cao¹⁷³, M. D. M. Capeans Garrido³⁶, M. Capua^{41a,41b}, R. Cardarelli^{73a}, F. Cardillo¹⁴⁹, G. Carducci^{41a,41b}, I. Carli¹⁴³, T. Carli³⁶, G. Carlino^{69a}, B. T. Carlson¹³⁹, L. Carminati^{68a,68b}, R. M. D. Carney^{45a,45b}, S. Caron¹¹⁹, E. Carquin^{147c}, S. Carrá⁴⁶, J. W. S. Carter¹⁶⁷, M. P. Casado^{14.f}, A. F. Casha¹⁶⁷, D. W. Casper¹⁷¹, R. Castelijm¹²⁰, F. L. Castillo¹⁷⁴, V. Castillo Gimenez¹⁷⁴, N. F. Castro^{140a,140e}, A. Catinaccio³⁶, J. R. Catmore¹³⁴, A. Cattai³⁶, J. Caudron²⁴, V. Cavaliere²⁹, E. Cavallaro¹⁴, M. Cavalli-Sforza¹⁴, V. Cavasinni^{71a,71b}, E. Celebi^{12b}, F. Ceradini^{74a,74b}, L. Cerda Alberich¹⁷⁴, K. Cerny¹³⁰, A. S. Cerqueira^{80a}, A. Cerri¹⁵⁶, L. Cerrito^{73a,73b}, F. Cerutti¹⁸, A. Cervelli^{23a,23b}, S. A. Cetin^{12b}, D. Chakraborty¹²¹, S. K. Chan⁵⁹, W. S. Chan¹²⁰, W. Y. Chan⁹⁰, J. D. Chapman³², B. Chargeishvili^{159b}, D. G. Charlton²¹, T. P. Charman⁹², C. C. Chau³⁴, S. Che¹²⁶, A. Chegwidden¹⁰⁶, S. Chekanov⁶, S. V. Chekulaev^{168a}, G. A. Chelkov^{79.ay}, M. A. Chelstowska³⁶, B. Chen⁷⁸, C. Chen^{60a}, C. H. Chen⁷⁸, H. Chen²⁹, J. Chen^{60a}, J. Chen³⁹, S. Chen¹³⁷, S. J. Chen^{15c}, X. Chen^{15b.ax}, Y. Chen⁸², Y.-H. Chen⁴⁶, H. C. Cheng^{63a}, H. J. Cheng^{15a,15d}, A. Cheplakov⁷⁹, E. Cheremushkina¹²³, R. Cherkaoui El Moursli^{35e}, E. Cheu⁷, K. Cheung⁶⁴, T. J. A. Chevaléras¹⁴⁵, L. Chevalier¹⁴⁵, V. Chiarella⁵¹, G. Chiarelli^{71a}, G. Chiodini^{67a}, A. S. Chisholm^{21,36}, A. Chitan^{27b}, I. Chiu¹⁶³, Y. H. Chiu¹⁷⁶, M. V. Chizhov⁷⁹, K. Choi⁶⁵, A. R. Chomont^{72a,72b}, S. Chouridou¹⁶², Y. S. Chow¹²⁰, M. C. Chu^{63a}, X. Chu^{15a}, J. Chudoba¹⁴¹, A. J. Chuinard¹⁰³, J. J. Chwastowski⁸⁴, L. Chytka¹³⁰, K. M. Ciesla⁸⁴, D. Cinca⁴⁷, V. Cindro⁹¹, I. A. Cioară^{27b}, A. Ciocio¹⁸, F. Ciroto^{69a,69b}, Z. H. Citron^{180.1}, M. Citterio^{68a}, D. A. Ciubotaru^{27b}, B. M. Ciungu¹⁶⁷, A. Clark⁵⁴, M. R. Clark³⁹, P. J. Clark⁵⁰, C. Clement^{45a,45b}, Y. Coadou¹⁰¹, M. Cokal^{66a,66c}, A. Coccaro^{55b}, J. Cochran⁷⁸, H. Cohen¹⁶¹, A. E. C. Coimbra³⁶, L. Colasurdo¹¹⁹, B. Cole³⁹, A. P. Colijn¹²⁰, J. Collot⁵⁸, P. Conde Muiño^{140a.g}, E. Coniavitis⁵², S. H. Connell^{33b}, I. A. Connelly⁵⁷, S. Constantinescu^{27b}, F. Conventi^{69a,aaa}, A. M. Cooper-Sarkar¹³⁵, F. Cormier¹⁷⁵, K. J. R. Cormier¹⁶⁷, L. D. Corpe⁹⁴, M. Corradi^{72a,72b}, E. E. Corrigan⁹⁶, F. Corriveau^{103.af}, A. Cortes-Gonzalez³⁶, M. J. Costa¹⁷⁴, F. Costanza⁵, D. Costanzo¹⁴⁹, G. Cowan⁹³, J. W. Cowley³², J. Crane¹⁰⁰, K. Cranmer¹²⁴, S. J. Crawley⁵⁷, R. A. Creager¹³⁷, S. Crépe-Renaudin⁵⁸, F. Crescioli¹³⁶, M. Cristinziani²⁴, V. Croft¹²⁰, G. Crosetti^{41a,41b}, A. Cueto⁵, T. Cuhadar Donszelmann¹⁴⁹, A. R. Cukierman¹⁵³, S. Czekierra⁸⁴, P. Czodrowski³⁶, M. J. Da Cunha Sargedas De Sousa^{60b}, J. V. Da Fonseca Pinto^{80b}, C. Da Via¹⁰⁰, W. Dabrowski^{83a}, T. Dado^{28a}, S. Dahbi^{35e}, T. Dai¹⁰⁵, C. Dallapiccola¹⁰², M. Dam⁴⁰, G. D'amen^{23a,23b}, V. D'Amico^{74a,74b}, J. Damp⁹⁹, J. R. Dandoy¹³⁷, M. F. Daneri³⁰, N. P. Dang^{181.j}, N. S. Dann¹⁰⁰, M. Danninger¹⁷⁵, V. Dao³⁶, G. Darbo^{55b}, O. Dartsis⁵, A. Dattagupta¹³¹, T. Daubney⁴⁶, S. D'Auria^{68a,68b}, W. Davey²⁴, C. David⁴⁶, T. Davidek¹⁴³, D. R. Davis⁴⁹, I. Dawson¹⁴⁹, K. De⁸, R. De Asmundis^{69a}, M. De Beurs¹²⁰, S. De Castro^{23a,23b}, S. De Cecco^{72a,72b}, N. De Groot¹¹⁹, P. de Jong¹²⁰, H. De la Torre¹⁰⁶, A. De Maria^{15c}, D. De Pedis^{72a}, A. De Salvo^{72a}, U. De Sanctis^{73a,73b}, M. De Santis^{73a,73b}

A. De Santo¹⁵⁶, K. De Vasconcelos Corga¹⁰¹, J. B. De Vivie De Regie¹³², C. Debenedetti¹⁴⁶, D. V. Dedovich⁷⁹, A. M. Deiana⁴², M. Del Gaudio^{41a,41b}, J. Del Peso⁹⁸, Y. Delabat Diaz⁴⁶, D. Delgove¹³², F. Deliot^{145,s}, C. M. Delitzsch⁷, M. Della Pietra^{69a,69b}, D. Della Volpe⁵⁴, A. Dell'Acqua³⁶, L. Dell'Asta^{73a,73b}, M. Delmastro⁵, C. Delporte¹³², P. A. Delsart⁵⁸, D. A. DeMarco¹⁶⁷, S. Demers¹⁸³, M. Demichev⁷⁹, G. Demontigny¹⁰⁹, S. P. Denisov¹²³, D. Denysiuk¹²⁰, L. D'Eramo¹³⁶, D. Derendarz⁸⁴, J. E. Derkaoui^{35d}, F. Derue¹³⁶, P. Dervan⁹⁰, K. Desch²⁴, C. Deterre⁴⁶, K. Dette¹⁶⁷, C. Deutsch²⁴, M. R. Devesa³⁰, P. O. Deviveiros³⁶, A. Dewhurst¹⁴⁴, S. Dhaliwal²⁶, F. A. Di Bello⁵⁴, A. Di Ciaccio^{73a,73b}, L. Di Ciaccio⁵, W. K. Di Clemente¹³⁷, C. Di Donato^{69a,69b}, A. Di Girolamo³⁶, G. Di Gregorio^{71a,71b}, B. Di Micco^{74a,74b}, R. Di Nardo¹⁰², K. F. Di Petrillo⁵⁹, R. Di Sipio¹⁶⁷, D. Di Valentino³⁴, C. Diaconu¹⁰¹, F. A. Dias⁴⁰, T. Dias Do Vale^{140a}, M. A. Diaz^{147a}, J. Dickinson¹⁸, E. B. Diehl¹⁰⁵, J. Dietrich¹⁹, S. Díez Cornell⁴⁶, A. Dimitrievska¹⁸, W. Ding^{15b}, J. Dingfelder²⁴, F. Dittus³⁶, F. Djama¹⁰¹, T. Djobava^{159b}, J. I. Djuvsland¹⁷, M. A. B. Do Vale^{80c}, M. Dobre^{27b}, D. Dodsworth²⁶, C. Doglioni⁹⁶, J. Dolejsi¹⁴³, Z. Dolezal¹⁴³, M. Donadelli^{80d}, J. Donini³⁸, A. D'onofrio⁹², M. D'Onofrio⁹⁰, J. Dopke¹⁴⁴, A. Doria^{69a}, M. T. Dova⁸⁸, A. T. Doyle⁵⁷, E. Drechsler¹⁵², E. Dreyer¹⁵², T. Dreyer⁵³, A. S. Drobac¹⁷⁰, Y. Duan^{60b}, F. Dubinin¹¹⁰, M. Dubovsky^{28a}, A. Dubreuil⁵⁴, E. Duchovni¹⁸⁰, G. Duckeck¹¹⁴, A. Ducourthial¹³⁶, O. A. Ducu¹⁰⁹, D. Duda¹¹⁵, A. Dudarev³⁶, A. C. Dudder⁹⁹, E. M. Duffield¹⁸, L. Duflo¹³², M. Dührssen³⁶, C. Dülsen¹⁸², M. Dumancic¹⁸⁰, A. E. Dumitriu^{27b}, A. K. Duncan⁵⁷, M. Dunford^{61a}, A. Duperrin¹⁰¹, H. Duran Yildiz^{4a}, M. Düren⁵⁶, A. Durglishvili^{159b}, D. Duschinger⁴⁸, B. Dutta⁴⁶, D. Duvnjak¹, G. I. Dyckes¹³⁷, M. Dyndal³⁶, S. Dysch¹⁰⁰, B. S. Dziedzic⁸⁴, K. M. Ecker¹¹⁵, R. C. Edgar¹⁰⁵, T. Eifert³⁶, G. Eigen¹⁷, K. Einsweiler¹⁸, T. Ekelof¹⁷², H. El Jarrari^{35e}, M. El Kacimi^{35c}, R. El Kosseifi¹⁰¹, V. Ellajosyula¹⁷², M. Ellert¹⁷², F. Ellinghaus¹⁸², A. A. Elliot⁹², N. Ellis³⁶, J. Elmsheuser²⁹, M. Elsing³⁶, D. Emelianov¹⁴⁴, A. Emerman³⁹, Y. Enari¹⁶³, J. S. Ennis¹⁷⁸, M. B. Epland⁴⁹, J. Erdmann⁴⁷, A. Ereditato²⁰, M. Errenst³⁶, M. Escalier¹³², C. Escobar¹⁷⁴, O. Estrada Pastor¹⁷⁴, E. Etzion¹⁶¹, H. Evans⁶⁵, A. Ezhilov¹³⁸, F. Fabbri⁵⁷, L. Fabbri^{23a,23b}, V. Fabiani¹¹⁹, G. Facini⁹⁴, R. M. Faisca Rodrigues Pereira^{140a}, R. M. Fakhruddinov¹²³, S. Falciano^{72a}, P. J. Falke⁵, S. Falke⁵, J. Faltova¹⁴³, Y. Fang^{15a}, Y. Fang^{15a}, G. Fanourakis⁴⁴, M. Fanti^{68a,68b}, A. Farbin⁸, A. Farilla^{74a}, E. M. Farina^{70a,70b}, T. Faroouque¹⁰⁶, S. Farrell¹⁸, S. M. Farrington¹⁷⁸, P. Farthouat³⁶, F. Fassi^{35e}, P. Fassnacht³⁶, D. Fassouliotis⁹, M. Fauci Giannelli⁵⁰, W. J. Fawcett³², L. Fayard¹³², O. L. Fedin^{138,q}, W. Fedorko¹⁷⁵, M. Feickert⁴², S. Feigl¹³⁴, L. Felgioni¹⁰¹, A. Fell¹⁴⁹, C. Feng^{60b}, E. J. Feng³⁶, M. Feng⁴⁹, M. J. Fenton⁵⁷, A. B. Fenyuk¹²³, J. Ferrando⁴⁶, A. Ferrante¹⁷³, A. Ferrari¹⁷², P. Ferrari¹²⁰, R. Ferrari^{70a}, D. E. Ferreira de Lima^{61b}, A. Ferrer¹⁷⁴, D. Ferrere⁵⁴, C. Ferretti¹⁰⁵, F. Fiedler⁹⁹, A. Filipčić⁹¹, F. Filthaut¹¹⁹, K. D. Finelli²⁵, M. C. N. Fiolhais^{140a,140c,a}, L. Fiorini¹⁷⁴, F. Fischer¹¹⁴, W. C. Fisher¹⁰⁶, I. Fleck¹⁵¹, P. Fleischmann¹⁰⁵, R. R. M. Fletcher¹³⁷, T. Flick¹⁸², B. M. Flierl¹¹⁴, L. Flores¹³⁷, L. R. Flores Castillo^{63a}, F. M. Follega^{75a,75b}, N. Fomin¹⁷, J. H. Foo¹⁶⁷, G. T. Forcolin^{75a,75b}, A. Formica¹⁴⁵, F. A. Förster¹⁴, A. C. Forti¹⁰⁰, A. G. Foster²¹, M. G. Foti¹³⁵, D. Fournier¹³², H. Fox⁸⁹, P. Francavilla^{71a,71b}, S. Francescato^{72a,72b}, M. Franchini^{23a,23b}, S. Franchino^{61a}, D. Francis³⁶, L. Franconi²⁰, M. Franklin⁵⁹, A. N. Fray⁹², B. Freund¹⁰⁹, W. S. Freund^{80b}, E. M. Freundlich⁴⁷, D. C. Frizzell¹²⁸, D. Froidevaux³⁶, J. A. Frost¹³⁵, C. Fukunaga¹⁶⁴, E. Fullana Torregrosa¹⁷⁴, E. Fumagalli^{55a,55b}, T. Fusayasu¹¹⁶, J. Fuster¹⁷⁴, A. Gabrielli^{23a,23b}, A. Gabrielli¹⁸, G. P. Gach^{83a}, S. Gadatsch⁵⁴, P. Gadow¹¹⁵, G. Gagliardi^{55a,55b}, L. G. Gagnon¹⁰⁹, C. Galea^{27b}, B. Galhardo^{140a}, G. E. Gallardo¹³⁵, E. J. Gallas¹³⁵, B. J. Gallop¹⁴⁴, P. Gallus¹⁴², G. Galster⁴⁰, R. Gamboa Goni⁹², K. K. Gan¹²⁶, S. Ganguly¹⁸⁰, J. Gao^{60a}, Y. Gao⁹⁰, Y. S. Gao^{31,n}, C. García¹⁷⁴, J. E. García Navarro¹⁷⁴, J. A. García Pascual^{15a}, C. Garcia-Argos⁵², M. Garcia-Sciveres¹⁸, R. W. Gardner³⁷, N. Garelli¹⁵³, S. Gargiulo⁵², V. Garonne¹³⁴, K. Gasnikova⁴⁶, A. Gaudiello^{55a,55b}, G. Gaudio^{70a}, I. L. Gavrilenko¹¹⁰, A. Gavrilyuk¹¹¹, C. Gay¹⁷⁵, G. Gaycken²⁴, E. N. Gazis¹⁰, A. A. Geanta^{27b}, C. N. P. Gee¹⁴⁴, J. Geisen⁵³, M. Geisen⁹⁹, M. P. Geisler^{61a}, C. Gemme^{55b}, M. H. Genest⁵⁸, C. Geng¹⁰⁵, S. Gentile^{72a,72b}, S. George⁹³, T. Gerialis⁴⁴, L. O. Gerlach⁵³, P. Gessinger-Befurt⁹⁹, G. Gessner⁴⁷, S. Ghasemi¹⁵¹, M. Ghasemi Bostanabad¹⁷⁶, A. Ghosh⁷⁷, B. Giacobbe^{23b}, S. Giagu^{72a,72b}, N. Giangiacomi^{23a,23b}, P. Giannetti^{71a}, A. Giannini^{69a,69b}, S. M. Gibson⁹³, M. Gignac¹⁴⁶, D. Gillberg³⁴, G. Gilles¹⁸², D. M. Gingrich^{3,az}, M. P. Giordani^{66a,66c}, F. M. Giorgi^{23b}, P. F. Giraud¹⁴⁵, G. Giugliarelli^{66a,66c}, D. Giugni^{68a}, F. Giuli^{73a,73b}, S. Gkaitatzis¹⁶², I. Gkialas^{9,i}, E. L. Gkoukousis¹⁴, P. Gkoutoumis¹⁰, L. K. Gladilin¹¹³, C. Glasman⁹⁸, J. Glatzer¹⁴, P. C. F. Glaysher⁴⁶, A. Glazov⁴⁶, M. Goblirsch-Kolb²⁶, S. Goldfarb¹⁰⁴, T. Golling⁵⁴, D. Golubkov¹²³, A. Gomes^{140a,140b}, R. Goncalves Gama⁵³, R. Gonçalves^{140a,140b}, G. Gonella⁵², L. Gonella²¹, A. Gongadze⁷⁹, F. Gonnella²¹, J. L. Gonski⁵⁹, S. González de la Hoz¹⁷⁴, S. Gonzalez-Sevilla⁵⁴, G. R. Gonzalvo Rodriguez¹⁷⁴, L. Goossens³⁶, P. A. Gorbounov¹¹¹, H. A. Gordon²⁹, B. Gorini³⁶, E. Gorini^{67a,67b}, A. Gorišek⁹¹, A. T. Goshaw⁴⁹, M. I. Gostkin⁷⁹, C. A. Gottardo²⁴, M. Gouighri^{35b}, D. Goujdami^{35c}, A. G. Goussiou¹⁴⁸, N. Govender^{33b,b}, C. Goy⁵, E. Gozani¹⁶⁰, I. Grabowska-Bold^{83a}, E. C. Graham⁹⁰, J. Gramling¹⁷¹, E. Gramstad¹³⁴, S. Grancagnolo¹⁹, M. Grandi¹⁵⁶, V. Gratchev¹³⁸, P. M. Gravila^{27f}, F. G. Gravili^{67a,67b}, C. Gray⁵⁷, H. M. Gray¹⁸, C. Grefe²⁴, K. Gregersen⁹⁶, I. M. Gregor⁴⁶, P. Grenier¹⁵³, K. Grevtsov⁴⁶, C. Grieco¹⁴, N. A. Grieser¹²⁸, J. Griffiths⁸, A. A. Grillo¹⁴⁶, K. Grimm^{31,m}, S. Grinstein^{14,z}, J.-F. Grivaz¹³², S. Groh⁹⁹, E. Gross¹⁸⁰, J. Grosse-Knetter⁵³, Z. J. Grout⁹⁴, C. Grud¹⁰⁵, A. Grummer¹¹⁸, L. Guan¹⁰⁵, W. Guan¹⁸¹, J. Guenther³⁶, A. Guerguichon¹³², F. Guescini¹¹⁵, D. Guest¹⁷¹, R. Gugel⁵²,

T. Guillemain⁵, S. Guindon³⁶, U. Gul⁵⁷, J. Guo^{60c}, W. Guo¹⁰⁵, Y. Guo^{60a,u}, Z. Guo¹⁰¹, R. Gupta⁴⁶, S. Gurbuz^{12c}, G. Gustavino¹²⁸, P. Gutierrez¹²⁸, C. Gutsche⁹⁴, C. Guyot¹⁴⁵, M. P. Guzik^{83a}, C. Gwenlan¹³⁵, C. B. Gwilliam⁹⁰, A. Haas¹²⁴, C. Haber¹⁸, H. K. Hadavand⁸, N. Haddad^{35e}, A. Hader^{60a}, S. Hageböck³⁶, M. Hagihara¹⁶⁹, M. Haleem¹⁷⁷, J. Haley¹²⁹, G. Halladjian¹⁰⁶, G. D. Hallewell¹⁰¹, K. Hamacher¹⁸², P. Hamal¹³⁰, K. Hamano¹⁷⁶, H. Hamdaoui^{35e}, G. N. Hamity¹⁴⁹, K. Han^{60a,am}, L. Han^{60a}, S. Han^{15a,15d}, K. Hanagaki^{81,x}, M. Hance¹⁴⁶, D. M. Handl¹¹⁴, B. Haney¹³⁷, R. Hankache¹³⁶, E. Hansen⁹⁶, J. B. Hansen⁴⁰, J. D. Hansen⁴⁰, M. C. Hansen²⁴, P. H. Hansen⁴⁰, E. C. Hanson¹⁰⁰, K. Hara¹⁶⁹, A. S. Hard¹⁸¹, T. Harenberg¹⁸², S. Harkusha¹⁰⁷, P. F. Harrison¹⁷⁸, N. M. Hartmann¹¹⁴, Y. Hasegawa¹⁵⁰, A. Hasib⁵⁰, S. Hassani¹⁴⁵, S. Haug²⁰, R. Hauser¹⁰⁶, L. B. Havener³⁹, M. Havranek¹⁴², C. M. Hawkes²¹, R. J. Hawkings³⁶, D. Hayden¹⁰⁶, C. Hayes¹⁵⁵, R. L. Hayes¹⁷⁵, C. P. Hays¹³⁵, J. M. Hays⁹², H. S. Hayward⁹⁰, S. J. Haywood¹⁴⁴, F. He^{60a}, M. P. Heath⁵⁰, V. Hedberg⁹⁶, L. Heelan⁸, S. Heer²⁴, K. K. Heidegger⁵², W. D. Heidorn⁷⁸, J. Heilman³⁴, S. Heim⁴⁶, T. Heim¹⁸, B. Heinemann^{46,au}, J. J. Heinrich¹³¹, L. Heinrich³⁶, C. Heinz⁵⁶, J. Hejbal¹⁴¹, L. Helary^{61b}, A. Held¹⁷⁵, S. Hellesund¹³⁴, C. M. Helling¹⁴⁶, S. Hellman^{45a,45b}, C. Helsen³⁶, R. C. W. Henderson⁸⁹, Y. Heng¹⁸¹, S. Henkelmann¹⁷⁵, A. M. Henriques Correia³⁶, G. H. Herbert¹⁹, H. Herde²⁶, V. Herget¹⁷⁷, Y. Hernández Jiménez^{33c}, H. Herr⁹⁹, M. G. Herrmann¹¹⁴, T. Herrmann⁴⁸, G. Herten⁵², R. Hertenberger¹¹⁴, L. Hervas³⁶, T. C. Herwig¹³⁷, G. G. Hesketh⁹⁴, N. P. Hessey^{168a}, A. Higashida¹⁶³, S. Higashino⁸¹, E. Higón-Rodríguez¹⁷⁴, K. Hildebrand³⁷, E. Hill¹⁷⁶, J. C. Hill³², K. K. Hill²⁹, K. H. Hiller⁴⁶, S. J. Hillier²¹, M. Hils⁴⁸, I. Hinchliffe¹⁸, F. Hinterkeuser²⁴, M. Hirose¹³³, S. Hirose⁵², D. Hirschebuehl¹⁸², B. Hiti⁹¹, O. Hladik¹⁴¹, D. R. Hlaluku^{33c}, X. Hoad⁵⁰, J. Hobbs¹⁵⁵, N. Hod¹⁸⁰, M. C. Hodgkinson¹⁴⁹, A. Hoecker³⁶, F. Hoenig¹¹⁴, D. Hohn⁵², D. Hohov¹³², T. R. Holmes³⁷, M. Holzbock¹¹⁴, L.B.A.H Hommels³², S. Honda¹⁶⁹, T. Honda⁸¹, T. M. Hong¹³⁹, A. Hönle¹¹⁵, B. H. Hooberman¹⁷³, W. H. Hopkins⁶, Y. Horii¹¹⁷, P. Horn⁴⁸, L. A. Horyn³⁷, J.-Y. Hostachy⁵⁸, A. Hostiuc¹⁴⁸, S. Hou¹⁵⁸, A. Houmada^{35a}, J. Howarth¹⁰⁰, J. Hoya⁸⁸, M. Hrabovsky¹³⁰, J. Hrdinka⁷⁶, I. Hristova¹⁹, J. Hrivnac¹³², A. Hrynevich¹⁰⁸, T. Hryn'ova⁵, P. J. Hsu⁶⁴, S.-C. Hsu¹⁴⁸, Q. Hu²⁹, S. Hu^{60c}, Y. Huang^{15a}, Z. Hubacek¹⁴², F. Hubaut¹⁰¹, M. Huebner²⁴, F. Huegging²⁴, T. B. Huffman¹³⁵, M. Huhtinen³⁶, R. F. H. Hunter³⁴, P. Huo¹⁵⁵, A. M. Hupe³⁴, N. Huseynov^{79,ah}, J. Huston¹⁰⁶, J. Huth⁵⁹, R. Hyneman¹⁰⁵, S. Hyrych^{28a}, G. Iacobucci⁵⁴, G. Iakovidis²⁹, I. Ibragimov¹⁵¹, L. Iconomidou-Fayard¹³², Z. Idrissi^{35e}, P. Iengo³⁶, R. Ignazzi⁴⁰, O. Igonkina^{120,ab,*}, R. Iguchi¹⁶³, T. Iizawa⁵⁴, Y. Ikegami⁸¹, M. Ikeno⁸¹, D. Iliadis¹⁶², N. Ilic¹¹⁹, F. Iltzsche⁴⁸, G. Introzzi^{70a,70b}, M. Iodice^{74a}, K. Iordanidou^{168a}, V. Ippolito^{72a,72b}, M. F. Isacson¹⁷², M. Ishino¹⁶³, M. Ishitsuka¹⁶⁵, W. Islam¹²⁹, C. Issever¹³⁵, S. Istin¹⁶⁰, F. Ito¹⁶⁹, J. M. Iturbe Ponce^{63a}, R. Iuppa^{75a,75b}, A. Ivina¹⁸⁰, H. Iwasaki⁸¹, J. M. Izen⁴³, V. Izzo^{69a}, P. Jacka¹⁴¹, P. Jackson¹, R. M. Jacobs²⁴, B. P. Jaeger¹⁵², V. Jain², G. Jäkel¹⁸², K. B. Jakobi⁹⁹, K. Jakobs⁵², S. Jakobsen⁷⁶, T. Jakoubek¹⁴¹, J. Jamieson⁵⁷, K. W. Janas^{83a}, R. Jansky⁵⁴, J. Janssen²⁴, M. Janus⁵³, P. A. Janus^{83a}, G. Jarlskog⁹⁶, N. Javadov^{79,ah}, T. Javůrek³⁶, M. Javurkova⁵², F. Jeanneau¹⁴⁵, L. Jeanty¹³¹, J. Jejelava^{159a,ai}, A. Jelinskas¹⁷⁸, P. Jenni^{52,c}, J. Jeong⁴⁶, N. Jeong⁴⁶, S. Jézéquel⁵, H. Ji¹⁸¹, J. Jia¹⁵⁵, H. Jiang⁷⁸, Y. Jiang^{60a}, Z. Jiang^{153,r}, S. Jiggins⁵², F. A. Jimenez Morales³⁸, J. Jimenez Pena¹⁷⁴, S. Jin^{15c}, A. Jinaru^{27b}, O. Jinnouchi¹⁶⁵, H. Jivan^{33c}, P. Johansson¹⁴⁹, K. A. Johns⁷, C. A. Johnson⁶⁵, K. Jon-And^{45a,45b}, R. W. L. Jones⁸⁹, S. D. Jones¹⁵⁶, S. Jones⁷, T. J. Jones⁹⁰, J. Jongmanns^{61a}, P. M. Jorge^{140a}, J. Jovicevic³⁶, X. Ju¹⁸, J. J. Junggeburth¹¹⁵, A. Juste Rozas^{14,z}, A. Kaczmarska⁸⁴, M. Kado^{72a,72b}, H. Kagan¹²⁶, M. Kagan¹⁵³, C. Kahra⁹⁹, T. Kajii¹⁷⁹, E. Kajomovitz¹⁶⁰, C. W. Kalderon⁹⁶, A. Kaluza⁹⁹, A. Kamenshchikov¹²³, L. Kanjir⁹¹, Y. Kano¹⁶³, V. A. Kantserov¹¹², J. Kanzaki⁸¹, L. S. Kaplan¹⁸¹, D. Kar^{33c}, M. J. Kareem^{168b}, E. Karentzos¹⁰, S. N. Karpov⁷⁹, Z. M. Karpova⁷⁹, V. Kartvelishvili⁸⁹, A. N. Karyukhin¹²³, L. Kashif¹⁸¹, R. D. Kass¹²⁶, A. Kastanas^{45a,45b}, Y. Kataoka¹⁶³, C. Kato^{60c,60d}, J. Katzy⁴⁶, K. Kawade⁸², K. Kawagoe⁸⁷, T. Kawaguchi¹¹⁷, T. Kawamoto¹⁶³, G. Kawamura⁵³, E. F. Kay¹⁷⁶, V. F. Kazanin^{122a,122b}, R. Keeler¹⁷⁶, R. Kehoe⁴², J. S. Keller³⁴, E. Kellermann⁹⁶, D. Kelsey¹⁵⁶, J. J. Kempster²¹, J. Kendrick²¹, O. Kepka¹⁴¹, S. Kersten¹⁸², B. P. Kerševan⁹¹, S. Ketabchi Haghighat¹⁶⁷, M. Khader¹⁷³, F. Khalil-Zada¹³, M. Khandoga¹⁴⁵, A. Khanov¹²⁹, A. G. Kharlamov^{122a,122b}, T. Kharlamova^{122a,122b}, E. E. Khoda¹⁷⁵, A. Khodinov¹⁶⁶, T. J. Khoo⁵⁴, E. Khramov⁷⁹, J. Khubua^{159b}, S. Kido⁸², M. Kiehn⁵⁴, C. R. Kilby⁹³, Y. K. Kim³⁷, N. Kimura^{66a,66c}, O. M. Kind¹⁹, B. T. King^{90,*}, D. Kirchmeier⁴⁸, J. Kirkl¹⁴⁴, A. E. Kiryunin¹¹⁵, T. Kishimoto¹⁶³, D. P. Kisiuk¹⁶⁷, V. Kitali⁴⁶, O. Kivernyk⁵, E. Kladiava^{28b,*}, T. Klapdor-Kleingrothaus⁵², M. Klassen^{61a}, M. H. Klein¹⁰⁵, M. Klein⁹⁰, U. Klein⁹⁰, K. Kleinknecht⁹⁹, P. Klimek¹²¹, A. Klimentov²⁹, T. Klingl²⁴, T. Klioutchnikova³⁶, F. F. Klitzner¹¹⁴, P. Kluit¹²⁰, S. Kluth¹¹⁵, E. Kneringer⁷⁶, E. B. F. G. Knoop¹⁰¹, A. Knue⁵², D. Kobayashi⁸⁷, T. Kobayashi¹⁶³, M. Kobel⁴⁸, M. Kocian¹⁵³, P. Kodys¹⁴³, P. T. Koenig²⁴, T. Koffas³⁴, N. M. Köhler¹¹⁵, T. Koi¹⁵³, M. Kolb^{61b}, I. Koletsou⁵, T. Komarek¹³⁰, T. Kondo⁸¹, N. Kondrashova^{60c}, K. Köneke⁵², A. C. König¹¹⁹, T. Kono¹²⁵, R. Konoplich^{124,ap}, V. Konstantinides⁹⁴, N. Konstantinidis⁹⁴, B. Konya⁹⁶, R. Kopeliansky⁶⁵, S. Koperny^{83a}, K. Korcyl⁸⁴, K. Kordas¹⁶², G. Koren¹⁶¹, A. Korn⁹⁴, I. Korolkov¹⁴, E. V. Korolkova¹⁴⁹, N. Korotkova¹¹³, O. Kortner¹¹⁵, S. Kortner¹¹⁵, T. Kosek¹⁴³, V. V. Kostyukhin²⁴, A. Kotwal⁴⁹, A. Koulouris¹⁰, A. Kourkouveli-Charalampidi^{70a,70b}, C. Kourkouvelis⁹, E. Kourlitis¹⁴⁹, V. Kouskoura²⁹, A. B. Kowalewska⁸⁴, R. Kowalewski¹⁷⁶, C. Kozakai¹⁶³, W. Kozanecki¹⁴⁵, A. S. Kozhin¹²³, V. A. Kramarenko¹¹³, G. Kramberger⁹¹, D. Krasnopevtsev^{60a}, M. W. Krasny¹³⁶, A. Krasznahorkay³⁶, D. Krauss¹¹⁵, J. A. Kremer^{83a}

J. Kretzschmar⁹⁰, P. Krieger¹⁶⁷, F. Krieter¹¹⁴, A. Krishnan^{61b}, K. Krizka¹⁸, K. Kroeninger⁴⁷, H. Kroha¹¹⁵, J. Kroll¹⁴¹, J. Kroll¹³⁷, J. Krstic¹⁶, U. Kruchonak⁷⁹, H. Krüger²⁴, N. Krumnack⁷⁸, M. C. Kruse⁴⁹, J. A. Krzysiak⁸⁴, T. Kubota¹⁰⁴, S. Kuday^{4b}, J. T. Kuechler⁴⁶, S. Kuehn³⁶, A. Kugel^{61a}, T. Kuhl⁴⁶, V. Kukhtin⁷⁹, R. Kukla¹⁰¹, Y. Kulchitsky^{107,al}, S. Kuleshov^{147c}, Y. P. Kulinich¹⁷³, M. Kuna⁵⁸, T. Kunigo⁸⁵, A. Kupco¹⁴¹, T. Kupfer⁴⁷, O. Kuprash⁵², H. Kurashige⁸², L. L. Kurchaninov^{168a}, Y. A. Kurochkin¹⁰⁷, A. Kurova¹¹², M. G. Kurth^{15a,15d}, E. S. Kuwertz³⁶, M. Kuze¹⁶⁵, A. K. Kvam¹⁴⁸, J. Kvita¹³⁰, T. Kwan¹⁰³, A. La Rosa¹¹⁵, L. La Rotonda^{41a,41b}, F. La Ruffa^{41a,41b}, C. Lacasta¹⁷⁴, F. Lacava^{72a,72b}, D. P. J. Lack¹⁰⁰, H. Lacker¹⁹, D. Lacour¹³⁶, E. Ladygin⁷⁹, R. Lafaye⁵, B. Laforge¹³⁶, T. Lagouri^{33c}, S. Lai⁵³, S. Lammers⁶⁵, W. Lamp⁷, C. Lampoudis¹⁶², E. Lançon²⁹, U. Landgraf⁵², M. P. J. Landon⁹², M. C. Lanfermann⁵⁴, V. S. Lang⁴⁶, J. C. Lange⁵³, R. J. Langenberg³⁶, A. J. Lankford¹⁷¹, F. Lanni²⁹, K. Lantzsch²⁴, A. Lanza^{70a}, A. Lapertosa^{55a,55b}, S. Laplace¹³⁶, J. F. Laporte¹⁴⁵, T. Lari^{68a}, F. Lasagni Manghi^{23a,23b}, M. Lassnig³⁶, T. S. Lau^{63a}, A. Laudrain¹³², A. Laurier³⁴, M. Lavorgna^{69a,69b}, M. Lazzaroni^{68a,68b}, B. Le¹⁰⁴, E. Le Guirriec¹⁰¹, M. LeBlanc⁷, T. LeCompte⁶, F. Ledroit-Guillon⁵⁸, C. A. Lee²⁹, G. R. Lee¹⁷, L. Lee⁵⁹, S. C. Lee¹⁵⁸, S. J. Lee³⁴, B. Lefebvre^{168a}, M. Lefebvre¹⁷⁶, F. Legger¹¹⁴, C. Leggett¹⁸, K. Lehmann¹⁵², N. Lehmann¹⁸², G. Lehmann Miotto³⁶, W. A. Leight⁴⁶, A. Leisos^{162,y}, M. A. L. Leite^{80d}, C. E. Leitgeb¹¹⁴, R. Leitner¹⁴³, D. Lellouch^{180,*}, K. J. C. Leney⁴², T. Lenz²⁴, B. Lenzi³⁶, R. Leone⁷, S. Leone^{71a}, C. Leonidopoulos⁵⁰, A. Leopold¹³⁶, G. Lerner¹⁵⁶, C. Leroy¹⁰⁹, R. Les¹⁶⁷, C. G. Lester³², M. Levchenko¹³⁸, J. Levêque⁵, D. Levin¹⁰⁵, L. J. Levinson¹⁸⁰, D. J. Lewis²¹, B. Li^{15b}, B. Li¹⁰⁵, C-Q. Li^{60a}, F. Li^{60c}, H. Li^{60a}, H. Li^{60b}, J. Li^{60c}, K. Li¹⁵³, L. Li^{60c}, M. Li^{15a}, Q. Li^{15a,15d}, Q. Y. Li^{60a}, S. Li^{60c,60d}, X. Li⁴⁶, Y. Li⁴⁶, Z. Li^{60b}, Z. Liang^{15a}, B. Liberti^{73a}, A. Liblong¹⁶⁷, K. Lie^{63c}, S. Liem¹²⁰, C. Y. Lin³², K. Lin¹⁰⁶, T. H. Lin⁹⁹, R. A. Linck⁶⁵, J. H. Lindon²¹, A. L. Lioni⁵⁴, E. Lipeles¹³⁷, A. Lipniacka¹⁷, M. Lisovy^{61b}, T. M. Liss^{173,aw}, A. Lister¹⁷⁵, A. M. Litke¹⁴⁶, J. D. Little⁸, B. Liu^{78,ae}, B. L. Liu⁶, H. B. Liu²⁹, H. Liu¹⁰⁵, J. B. Liu^{60a}, J. K. K. Liu¹³⁵, K. Liu¹³⁶, M. Liu^{60a}, P. Liu¹⁸, Y. Liu^{15a,15d}, Y. L. Liu¹⁰⁵, Y. W. Liu^{60a}, M. Livan^{70a,70b}, A. Lleres⁵⁸, J. Llorente Merino^{15a}, S. L. Lloyd⁹², C. Y. Lo^{63b}, F. Lo Sterzo⁴², E. M. Lobodzinska⁴⁶, P. Loch⁷, S. Loffredo^{73a,73b}, T. Lohse¹⁹, K. Lohwasser¹⁴⁹, M. Lokajicek¹⁴¹, J. D. Long¹⁷³, R. E. Long⁸⁹, L. Longo³⁶, K. A. Looper¹²⁶, J. A. Lopez^{147c}, I. Lopez Paz¹⁰⁰, A. Lopez Solis¹⁴⁹, J. Lorenz¹¹⁴, N. Lorenzo Martinez⁵, M. Losada²², P. J. Lösel¹¹⁴, A. Lösle⁵², X. Lou⁴⁶, X. Lou^{15a}, A. Lounis¹³², J. Love⁶, P. A. Love⁸⁹, J. J. Lozano Bahilo¹⁷⁴, M. Lu^{60a}, Y. J. Lu⁶⁴, H. J. Lubatti¹⁴⁸, C. Luci^{72a,72b}, A. Lucotte⁵⁸, C. Luedtke⁵², F. Luehring⁶⁵, I. Luise¹³⁶, L. Luminari^{72a}, B. Lund-Jensen¹⁵⁴, M. S. Lutz¹⁰², D. Lynn²⁹, R. Lysak¹⁴¹, E. Lytken⁹⁶, F. Lyu^{15a}, V. Lyubushkin⁷⁹, T. Lyubushkina⁷⁹, H. Ma²⁹, L. L. Ma^{60b}, Y. Ma^{60b}, G. Maccarrone⁵¹, A. Macchiolo¹¹⁵, C. M. Macdonald¹⁴⁹, J. Machado Miguens¹³⁷, D. Madaffari¹⁷⁴, R. Madar³⁸, W. F. Mader⁴⁸, N. Madysa⁴⁸, J. Maeda⁸², K. Maekawa¹⁶³, S. Maeland¹⁷, T. Maeno²⁹, M. Maerker⁴⁸, A. S. Maevskiy¹¹³, V. Magerl⁵², N. Magini⁷⁸, D. J. Mahon³⁹, C. Maidantchik^{80b}, T. Maier¹¹⁴, A. Maio^{140a,140b,140d}, K. Maj⁸⁴, O. Majersky^{28a}, S. Majewski¹³¹, Y. Makida⁸¹, N. Makovec¹³², B. Malaescu¹³⁶, Pa. Malecki⁸⁴, V. P. Maleev¹³⁸, F. Malek⁵⁸, U. Mallik⁷⁷, D. Malon⁶, C. Malone³², S. Maltezos¹⁰, S. Malyukov⁷⁹, J. Mamuzic¹⁷⁴, G. Mancini⁵¹, I. Mandić⁹¹, L. Manhaes de Andrade Filho^{80a}, I. M. Maniatis¹⁶², J. Manjarres Ramos⁴⁸, K. H. Mankinen⁹⁶, A. Mann¹¹⁴, A. Manousos⁷⁶, B. Mansoulie¹⁴⁵, I. Mantos¹⁶², S. Manzoni¹²⁰, A. Marantis¹⁶², G. Marceca³⁰, L. Marchese¹³⁵, G. Marchiori¹³⁶, M. Marcisovsky¹⁴¹, C. Marcon⁹⁶, C. A. Marin Tobon³⁶, M. Marjanovic³⁸, Z. Marshall¹⁸, M.U.F. Martensson¹⁷², S. Marti-Garcia¹⁷⁴, C. B. Martin¹²⁶, T. A. Martin¹⁷⁸, V. J. Martin⁵⁰, B. Martin dit Latour¹⁷, L. Martinelli^{74a,74b}, M. Martinez^{14,z}, V. I. Martinez Outschoorn¹⁰², S. Martin-Haugh¹⁴⁴, V. S. Martoiu^{27b}, A. C. Martyniuk⁹⁴, A. Marzin³⁶, S. R. Maschek¹¹⁵, L. Masetti⁹⁹, T. Mashimo¹⁶³, R. Mashinistov¹¹⁰, J. Masik¹⁰⁰, A. L. Maslennikov^{122a,122b}, L. H. Mason¹⁰⁴, L. Massa^{73a,73b}, P. Massarotti^{69a,69b}, P. Mastrandrea^{71a,71b}, A. Mastroberardino^{41a,41b}, T. Masubuchi¹⁶³, A. Matic¹¹⁴, P. Mättig²⁴, J. Maurer^{27b}, B. Maček⁹¹, D. A. Maximov^{122a,122b}, R. Mazini¹⁵⁸, I. Maznas¹⁶², S. M. Mazza¹⁴⁶, S. P. Mc Kee¹⁰⁵, T. G. McCarthy¹¹⁵, L. I. McClymont⁹⁴, W. P. McCormack¹⁸, E. F. McDonald¹⁰⁴, J. A. McFayden³⁶, M. A. McKay⁴², K. D. McLean¹⁷⁶, S. J. McMahon¹⁴⁴, P. C. McNamara¹⁰⁴, C. J. McNicol¹⁷⁸, R. A. McPherson^{176,af}, J. E. Mdhului^{33c}, Z. A. Meadows¹⁰², S. Meehan¹⁴⁸, T. Megy⁵², S. Mehlhase¹¹⁴, A. Mehta⁹⁰, T. Meideck⁵⁸, B. Meirose⁴³, D. Melini¹⁷⁴, B. R. Mellado Garcia^{33c}, J. D. Mellenthin⁵³, M. Melo^{28a}, F. Meloni⁴⁶, A. Melzer²⁴, S. B. Menary¹⁰⁰, E. D. Mendes Gouveia^{140a,140e}, L. Meng³⁶, X. T. Meng¹⁰⁵, S. Menke¹¹⁵, E. Meoni^{41a,41b}, S. Mergelmeyer¹⁹, S. A. M. Merkt¹³⁹, C. Merlassino²⁰, P. Mermod⁵⁴, L. Merola^{69a,69b}, C. Meroni^{68a}, O. Meshkov^{113,110}, J. K. R. Meshreki¹⁵¹, A. Messina^{72a,72b}, J. Metcalfe⁶, A. S. Mete¹⁷¹, C. Meyer⁶⁵, J. Meyer¹⁶⁰, J-P. Meyer¹⁴⁵, H. Meyer Zu Theenhausen^{61a}, F. Miano¹⁵⁶, R. P. Middleton¹⁴⁴, L. Mijović⁵⁰, G. Mikenberg¹⁸⁰, M. Mikestikova¹⁴¹, M. Mikuz⁹¹, H. Mildner¹⁴⁹, M. Milesi¹⁰⁴, A. Milic¹⁶⁷, D. A. Millar⁹², D. W. Miller³⁷, A. Milov¹⁸⁰, D. A. Milstead^{45a,45b}, R. A. Mina^{153,r}, A. A. Minaenko¹²³, M. Miñano Moya¹⁷⁴, I. A. Minashvili^{159b}, A. I. Mincer¹²⁴, B. Mindur^{83a}, M. Mineev⁷⁹, Y. Minegishi¹⁶³, Y. Ming¹⁸¹, L. M. Mir¹⁴, A. Mirto^{67a,67b}, K. P. Mistry¹³⁷, T. Mitani¹⁷⁹, J. Mitrevski¹¹⁴, V. A. Mitsou¹⁷⁴, M. Mittal^{60c}, A. Miucci²⁰, P. S. Miyagawa¹⁴⁹, A. Mizukami⁸¹, J. U. Mjörnmark⁹⁶, T. Mkrtychyan¹⁸⁴, M. Mlynarikova¹⁴³, T. Moa^{45a,45b}, K. Mochizuki¹⁰⁹, P. Mogg⁵², S. Mohapatra³⁹, R. Moles-Valls²⁴, M. C. Mondragon¹⁰⁶, K. Mönig⁴⁶, J. Monk⁴⁰, E. Monnier¹⁰¹, A. Montalbano¹⁵², J. Montejo Berlingen³⁶

M. Montella⁹⁴, F. Monticelli⁸⁸, S. Monzani^{68a}, N. Morange¹³², D. Moreno²², M. Moreno Llácer³⁶, C. Moreno Martinez¹⁴, P. Morettini^{55b}, M. Morgenstern¹²⁰, S. Morgenstern⁴⁸, D. Mori¹⁵², M. Morii⁵⁹, M. Morinaga¹⁷⁹, V. Morisbak¹³⁴, A. K. Morley³⁶, G. Mornacchi³⁶, A. P. Morris⁹⁴, L. Morvaj¹⁵⁵, P. Moschovakos³⁶, B. Moser¹²⁰, M. Mosidze^{159b}, T. Moskalets¹⁴⁵, H. J. Moss¹⁴⁹, J. Moss^{31.o}, K. Motohashi¹⁶⁵, E. Mountricha³⁶, E. J. W. Moyses¹⁰², S. Muanza¹⁰¹, J. Mueller¹³⁹, R. S. P. Mueller¹¹⁴, D. Muenstermann⁸⁹, G. A. Mullier⁹⁶, J. L. Munoz Martinez¹⁴, F. J. Munoz Sanchez¹⁰⁰, P. Murin^{28b}, W. J. Murray^{178,144}, A. Murrone^{68a,68b}, M. Muškinja¹⁸, C. Mwewa^{33a}, A. G. Myagkov^{123.aq}, J. Myers¹³¹, M. Myska¹⁴², B. P. Nachman¹⁸, O. Nackendorst⁴⁷, A. Nag Nag⁴⁸, K. Nagai¹³⁵, K. Nagano⁸¹, Y. Nagasaka⁶², M. Nagel⁵², E. Nagy¹⁰¹, A. M. Nairz³⁶, Y. Nakahama¹¹⁷, K. Nakamura⁸¹, T. Nakamura¹⁶³, I. Nakano¹²⁷, H. Nanjo¹³³, F. Napolitano^{61a}, R. F. Naranjo Garcia⁴⁶, R. Narayan⁴², D. I. Narrias Villar^{61a}, I. Naryshkin¹³⁸, T. Naumann⁴⁶, G. Navarro²², H. A. Neal^{105.*}, P. Y. Nechaeva¹¹⁰, F. Nechansky⁴⁶, T. J. Neep²¹, A. Negri^{70a,70b}, M. Negrini^{23b}, C. Nellist⁵³, M. E. Nelson¹³⁵, S. Nemecek¹⁴¹, P. Nemethy¹²⁴, M. Nessi^{36.e}, M. S. Neubauer¹⁷³, M. Neumann¹⁸², P. R. Newman²¹, T. Y. Ng^{63c}, Y. S. Ng¹⁹, Y. W. Y. Ng¹⁷¹, H. D. N. Nguyen¹⁰¹, T. Nguyen Manh¹⁰⁹, E. Nibigira³⁸, R. B. Nickerson¹³⁵, R. Nicolaidou¹⁴⁵, D. S. Nielsen⁴⁰, J. Nielsen¹⁴⁶, N. Nikiforou¹¹, V. Nikolaenko^{123.aq}, I. Nikolic-Audit¹³⁶, K. Nikolopoulos²¹, P. Nilsson²⁹, H. R. Nindhito⁵⁴, Y. Ninomiya⁸¹, A. Nisati^{72a}, N. Nishu^{60c}, R. Nisius¹¹⁵, I. Nitsche⁴⁷, T. Nitta¹⁷⁹, T. Nobe¹⁶³, Y. Noguchi⁸⁵, I. Nomidis¹³⁶, M. A. Nomura²⁹, M. Nordberg³⁶, N. Norjoharuddeen¹³⁵, T. Novak⁹¹, O. Novgorodova⁴⁸, R. Novotny¹⁴², L. Nozka¹³⁰, K. Ntekas¹⁷¹, E. Nurse⁹⁴, F. G. Oakham^{34.az}, H. Oberlack¹¹⁵, J. Ocariz¹³⁶, A. Ochi⁸², I. Ochoa³⁹, J. P. Ochoa-Ricoux^{147a}, K. O'Connor²⁶, S. Oda⁸⁷, S. Odaka⁸¹, S. Oerdek⁵³, A. Ogrodnik^{83a}, A. Oh¹⁰⁰, S. H. Oh⁴⁹, C. C. Ohm¹⁵⁴, H. Oide^{55a,55b}, M. L. Ojeda¹⁶⁷, H. Okawa¹⁶⁹, Y. Okazaki⁸⁵, Y. Okumura¹⁶³, T. Okuyama⁸¹, A. Olariu^{27b}, L. F. Oleiro Seabra^{140a}, S. A. Olivares Pino^{147a}, D. Oliveira Damazio²⁹, J. L. Oliver¹, M. J. R. Olsson¹⁷¹, A. Olszewski⁸⁴, J. Olszowska⁸⁴, D. C. O'Neil¹⁵², A. Onofre^{140a,140e}, K. Onogi¹¹⁷, P. U. E. Onyisi¹¹, H. Oppen¹³⁴, M. J. Oreglia³⁷, G. E. Orellana⁸⁸, D. Orestano^{74a,74b}, N. Orlando¹⁴, R. S. Orr¹⁶⁷, V. O'Shea⁵⁷, R. Ospanov^{60a}, G. Otero y Garzon³⁰, H. Otono⁸⁷, M. Ouchrif^{35d}, J. Ouellette²⁹, F. Ould-Saada¹³⁴, A. Ouraou¹⁴⁵, Q. Ouyang^{15a}, M. Owen⁵⁷, R. E. Owen²¹, V. E. Ozcan^{12c}, N. Ozturk⁸, J. Pacalt¹³⁰, H. A. Pacey³², K. Pachal⁴⁹, A. Pacheco Pages¹⁴, C. Padilla Aranda¹⁴, S. Pagan Griso¹⁸, M. Paganini¹⁸³, G. Palacino⁶⁵, S. Palazzo⁵⁰, S. Palestini³⁶, M. Palka^{83b}, D. Pallin³⁸, I. Panagoulas¹⁰, C. E. Pandini³⁶, J. G. Panduro Vazquez⁹³, P. Pani⁴⁶, G. Panizzo^{66a,66c}, L. Paolozzi⁵⁴, C. Papadatos¹⁰⁹, K. Papageorgiou^{9.i}, A. Paramonov⁶, D. Paredes Hernandez^{63b}, S. R. Paredes Saenz¹³⁵, B. Parida¹⁶⁶, T. H. Park¹⁶⁷, A. J. Parker⁸⁹, M. A. Parker³², F. Parodi^{55a,55b}, E. W. P. Parrish¹²¹, J. A. Parsons³⁹, U. Parzefall⁵², L. Pascual Dominguez¹³⁶, V. R. Pascuzzi¹⁶⁷, J. M. P. Pasner¹⁴⁶, E. Pasqualucci^{72a}, S. Passaggio^{55b}, F. Pastore⁹³, P. Pasuwan^{45a,45b}, S. Pataria⁹⁹, J. R. Pater¹⁰⁰, A. Pathak¹⁸¹, T. Pauly³⁶, B. Pearson¹¹⁵, M. Pedersen¹³⁴, L. Pedraza Diaz¹¹⁹, R. Pedro^{140a}, T. Peiffer⁵³, S. V. Peleganchuk^{122a,122b}, O. Penc¹⁴¹, H. Peng^{60a}, B. S. Peralva^{80a}, M. M. Perego¹³², A. P. Pereira Peixoto^{140a}, D. V. Perepelitsa²⁹, F. Peri¹⁹, L. Perini^{68a,68b}, H. Pernegger³⁶, S. Perrella^{69a,69b}, K. Peters⁴⁶, R. F. Y. Peters¹⁰⁰, B. A. Petersen³⁶, T. C. Petersen⁴⁰, E. Petit¹⁰¹, A. Petridis¹, C. Petridou¹⁶², P. Petroff¹³², M. Petrov¹³⁵, F. Petrucci^{74a,74b}, M. Pettee¹⁸³, N. E. Pettersson¹⁰², K. Petukhova¹⁴³, A. Peyaud¹⁴⁵, R. Pezoa^{147c}, L. Pezzotti^{70a,70b}, T. Pham¹⁰⁴, F. H. Phillips¹⁰⁶, P. W. Phillips¹⁴⁴, M. W. Phipps¹⁷³, G. Piacquadio¹⁵⁵, E. Pianori¹⁸, A. Picazio¹⁰², R. H. Pickles¹⁰⁰, R. Piegaia³⁰, D. Pietreanu^{27b}, J. E. Pilcher³⁷, A. D. Pilkington¹⁰⁰, M. Pinamonti^{73a,73b}, J. L. Pinfold³, M. Pitt¹⁸⁰, L. Pizzimento^{73a,73b}, M.-A. Pleier²⁹, V. Pleskot¹⁴³, E. Plotnikova⁷⁹, D. Pluth⁷⁸, P. Podberzko^{122a,122b}, R. Poettgen⁹⁶, R. Poggi⁵⁴, L. Poggioli¹³², I. Pogrebnyak¹⁰⁶, D. Pohl²⁴, I. Pokharel⁵³, G. Polesello^{70a}, A. Poley¹⁸, A. Policicchio^{72a,72b}, R. Polifka¹⁴³, A. Polini^{23b}, C. S. Pollard⁴⁶, V. Polychronakos²⁹, D. Ponomarenko¹¹², L. Pontecorvo³⁶, S. Popa^{27a}, G. A. Popeneciu^{27d}, D. M. Portillo Quintero⁵⁸, S. Pospisil¹⁴², K. Potamianos⁴⁶, I. N. Potrap⁷⁹, C. J. Potter³², H. Potti¹¹, T. Poulsen⁹⁶, J. Poveda³⁶, T. D. Powell¹⁴⁹, G. Pownall⁴⁶, M. E. Pozo Astigarraga³⁶, P. Pralavorio¹⁰¹, S. Prell⁷⁸, D. Price¹⁰⁰, M. Primavera^{67a}, S. Prince¹⁰³, M. L. Proffitt¹⁴⁸, N. Proklova¹¹², K. Prokofiev^{63c}, F. Prokoshin⁷⁹, S. Protopopescu²⁹, J. Proudfoot⁶, M. Przybycien^{83a}, D. Pudzha¹³⁸, A. Puri¹⁷³, P. Puzo¹³², J. Qian¹⁰⁵, Y. Qin¹⁰⁰, A. Quadt⁵³, M. Queitsch-Maitland⁴⁶, A. Qureshi¹, P. Rados¹⁰⁴, F. Ragusa^{68a,68b}, G. Rahal⁹⁷, J. A. Raine⁵⁴, S. Rajagopalan²⁹, A. Ramirez Morales⁹², K. Ran^{15a,15d}, T. Rashid¹³², S. Raspopov⁵, M. G. Ratti^{68a,68b}, D. M. Rauch⁴⁶, F. Rauscher¹¹⁴, S. Rave⁹⁹, B. Ravina¹⁴⁹, I. Ravinovich¹⁸⁰, J. H. Rawling¹⁰⁰, M. Raymond³⁶, A. L. Read¹³⁴, N. P. Readoff⁵⁸, M. Reale^{67a,67b}, D. M. Rebuzzi^{70a,70b}, A. Redelbach¹⁷⁷, G. Redlinger²⁹, K. Reeves⁴³, L. Rehnisch¹⁹, J. Reichert¹³⁷, D. Reikher¹⁶¹, A. Reiss⁹⁹, A. Rej¹⁵¹, C. Rembser³⁶, M. Renda^{27b}, M. Rescigno^{72a}, S. Resconi^{68a}, E. D. Resseguie¹³⁷, S. Rettie¹⁷⁵, E. Reynolds²¹, O. L. Rezanova^{122a,122b}, P. Reznicek¹⁴³, E. Ricci^{75a,75b}, R. Richter¹¹⁵, S. Richter⁴⁶, E. Richter-Was^{83b}, O. Ricken²⁴, M. Rideli¹³⁶, P. Rieck¹¹⁵, C. J. Riegel¹⁸², O. Rifki⁴⁶, M. Rijssenbeek¹⁵⁵, A. Rimoldi^{70a,70b}, M. Rimoldi⁴⁶, L. Rinaldi^{23b}, G. Ripellino¹⁵⁴, B. Ristic⁸⁹, E. Ritsch³⁶, I. Riu¹⁴, J. C. Rivera Vergara¹⁷⁶, F. Rizatdinova¹²⁹, E. Rizvi⁹², C. Rizzi³⁶, R. T. Roberts¹⁰⁰, S. H. Robertson^{103.af}, M. Robin⁴⁶, D. Robinson³², J. E. M. Robinson⁴⁶, C. M. Robles Gajardo^{147c}, A. Robson⁵⁷, E. Rocco⁹⁹, C. Roda^{71a,71b}, S. Rodriguez Bosca¹⁷⁴, A. Rodriguez Perez¹⁴, D. Rodriguez Rodriguez¹⁷⁴, A. M. Rodriguez Vera^{168b}, S. Roe³⁶, O. Røhne¹³⁴, R. Röhrig¹¹⁵, C. P. A. Roland⁶⁵, J. Roloff⁵⁹

A. Romaniouk¹¹², M. Romano^{23a,23b}, N. Rompotis⁹⁰, M. Ronzani¹²⁴, L. Roos¹³⁶, S. Rosati^{72a}, K. Rosbach⁵², G. Rosin¹⁰², B. J. Rosser¹³⁷, E. Rossi⁴⁶, E. Rossi^{74a,74b}, E. Rossi^{69a,69b}, L. P. Rossi^{55b}, L. Rossini^{68a,68b}, R. Rosten¹⁴, M. Rotaru^{27b}, J. Rothberg¹⁴⁸, D. Rousseau¹³², G. Rovelli^{70a,70b}, D. Roy^{33c}, A. Rozanov¹⁰¹, Y. Rozen¹⁶⁰, X. Ruan^{33c}, F. Rubbo¹⁵³, F. Rühr⁵², A. Ruiz-Martinez¹⁷⁴, A. Rummler³⁶, Z. Rurikova⁵², N. A. Rusakovich⁷⁹, H. L. Russell¹⁰³, L. Rustige^{38,47}, J. P. Rutherford⁷, E. M. Rüttinger^{46,k}, M. Rybar³⁹, G. Rybkin¹³², A. Ryzhov¹²³, G. F. Rzehorz⁵³, P. Sabatini⁵³, G. Sabato¹²⁰, S. Sacerdoti¹³², H.F.-W. Sadrozinski¹⁴⁶, R. Sadykov⁷⁹, F. Safai Tehrani^{72a}, B. Safarzadeh Samani¹⁵⁶, P. Saha¹²¹, S. Saha¹⁰³, M. Sahinsoy^{61a}, A. Sahu¹⁸², M. Saimpert⁴⁶, M. Saito¹⁶³, T. Saito¹⁶³, H. Sakamoto¹⁶³, A. Sakharov^{124,ap}, D. Salamani⁵⁴, G. Salamanna^{74a,74b}, J. E. Salazar Loyola^{147c}, P. H. Sales De Bruin¹⁷², A. Salnikov¹⁵³, J. Salt¹⁷⁴, D. Salvatore^{41a,41b}, F. Salvatore¹⁵⁶, A. Salvucci^{63a,63b,63c}, A. Salzburger³⁶, J. Samarati³⁶, D. Sammel⁵², D. Sampsonidis¹⁶², D. Sampsonidou¹⁶², J. Sánchez¹⁷⁴, A. Sanchez Pineda^{66a,66c}, H. Sandaker¹³⁴, C. O. Sander⁴⁶, I. G. Sanderswood⁸⁹, M. Sandhoff¹⁸², C. Sandoval²², D. P. C. Sankey¹⁴⁴, M. Sannino^{55a,55b}, Y. Sano¹¹⁷, A. Sansoni⁵¹, C. Santoni³⁸, H. Santos^{140a,140b}, S. N. Santpur¹⁸, A. Santra¹⁷⁴, A. Saponov⁷⁹, J. G. Saraiva^{140a,140d}, O. Sasaki⁸¹, K. Sato¹⁶⁹, E. Sauvan⁵, P. Savard^{167,az}, N. Savic¹¹⁵, R. Sawada¹⁶³, C. Sawyer¹⁴⁴, L. Sawyer^{95,an}, C. Sbarra^{23b}, A. Sbrizzi^{23a}, T. Scanlon⁹⁴, J. Schaarschmidt¹⁴⁸, P. Schacht¹¹⁵, B. M. Schachtner¹¹⁴, D. Schaefer³⁷, L. Schaefer¹³⁷, J. Schaeffer⁹⁹, S. Schaepe³⁶, U. Schäfer⁹⁹, A. C. Schaffer¹³², D. Schaile¹¹⁴, R. D. Schamberger¹⁵⁵, N. Scharmberg¹⁰⁰, V. A. Schegelsky¹³⁸, D. Scheirich¹⁴³, F. Schenck¹⁹, M. Schernau¹⁷¹, C. Schiavi^{55a,55b}, S. Schier¹⁴⁶, L. K. Schildgen²⁴, Z. M. Schillaci²⁶, E. J. Schioppa³⁶, M. Schioppa^{41a,41b}, K. E. Schleicher⁵², S. Schlenker³⁶, K. R. Schmidt-Sommerfeld¹¹⁵, K. Schmieden³⁶, C. Schmitt⁹⁹, S. Schmitt⁴⁶, S. Schmitz⁹⁹, J. C. Schmoeckel⁴⁶, U. Schnoor⁵², L. Schoeffel¹⁴⁵, A. Schoening^{61b}, P. G. Scholer⁵², E. Schopf¹³⁵, M. Schott⁹⁹, J. F. P. Schouwenberg¹¹⁹, J. Schovancova³⁶, S. Schramm⁵⁴, F. Schroeder¹⁸², A. Schulte⁹⁹, H.-C. Schultz-Coulon^{61a}, M. Schumacher⁵², B. A. Schumm¹⁴⁶, Ph. Schune¹⁴⁵, A. Schwartzman¹⁵³, T. A. Schwarz¹⁰⁵, Ph. Schwemling¹⁴⁵, R. Schwienhorst¹⁰⁶, A. Sciandra¹⁴⁶, G. Sciolla²⁶, M. Scodreggio⁴⁶, M. Scornajenghi^{41a,41b}, F. Scuri^{71a}, F. Scutti¹⁰⁴, L. M. Scyboz¹¹⁵, C. D. Sebastiani^{72a,72b}, P. Seema¹⁹, S. C. Seidel¹¹⁸, A. Seiden¹⁴⁶, T. Seiss³⁷, J. M. Seixas^{80b}, G. Sekhniaidze^{69a}, K. Sekhon¹⁰⁵, S. J. Sekula⁴², N. Semprini-Cesari^{23a,23b}, S. Sen⁴⁹, S. Senkin³⁸, C. Serfon⁷⁶, L. Serin¹³², L. Serkin^{66a,66b}, M. Sessa^{60a}, H. Severini¹²⁸, T. Šfiligoj⁹¹, F. Sforza¹⁷⁰, A. Sfyrla⁵⁴, E. Shabalina⁵³, J. D. Shahinian¹⁴⁶, N. W. Shaikh^{45a,45b}, D. Shaked Renous¹⁸⁰, L. Y. Shan^{15a}, R. Shang¹⁷³, J. T. Shank²⁵, M. Shapiro¹⁸, A. Sharma¹³⁵, A. S. Sharma¹, P. B. Shatalov¹¹¹, K. Shaw¹⁵⁶, S. M. Shaw¹⁰⁰, A. Shcherbakova¹³⁸, Y. Shen¹²⁸, N. Sherafati³⁴, A. D. Sherman²⁵, P. Sherwood⁹⁴, L. Shi^{158,av}, S. Shimizu⁸¹, C. O. Shimmin¹⁸³, Y. Shimogama¹⁷⁹, M. Shimojima¹¹⁶, I. P. J. Shipsey¹³⁵, S. Shirabe⁸⁷, M. Shiyakova^{79,ac}, J. Shlomi¹⁸⁰, A. Shmeleva¹¹⁰, M. J. Shochet³⁷, J. Shojaii¹⁰⁴, D. R. Shope¹²⁸, S. Shrestha¹²⁶, E. Shulga¹⁸⁰, P. Sicho¹⁴¹, A. M. Sickles¹⁷³, P. E. Sidebo¹⁵⁴, E. Sideras Haddad^{33c}, O. Sidiropoulou³⁶, A. Sidoti^{23a,23b}, F. Siegert⁴⁸, Dj. Sijacki¹⁶, M. Jr. Silva¹⁸¹, M. V. Silva Oliveira^{80a}, S. B. Silverstein^{45a}, S. Simion¹³², E. Simioni⁹⁹, R. Simoniello⁹⁹, S. Simsek^{12b}, P. Sinervo¹⁶⁷, V. Sinetckii^{113,110}, N. B. Sinev¹³¹, M. Sioli^{23a,23b}, I. Siral¹⁰⁵, S. Yu. Sivoklov¹¹³, J. Sjölin^{45a,45b}, E. Skorda⁹⁶, P. Skubic¹²⁸, M. Slawinska⁸⁴, K. Sliwa¹⁷⁰, R. Slovak¹⁴³, V. Smakhtin¹⁸⁰, B. H. Smart¹⁴⁴, J. Smiesko^{28a}, N. Smirnov¹¹², S. Yu. Smirnov¹¹², Y. Smirnov¹¹², L. N. Smirnova^{113,v}, O. Smirnova⁹⁶, J. W. Smith⁵³, M. Smizanska⁸⁹, K. Smolek¹⁴², A. Smykiewicz⁸⁴, A. A. Snesarev¹¹⁰, H. L. Snoek¹²⁰, I. M. Snyder¹³¹, S. Snyder²⁹, R. Sobie^{176,af}, A. M. Soffa¹⁷¹, A. Soffer¹⁶¹, A. Sogaard⁵⁰, F. Sohns⁵³, C. A. Solans Sanchez³⁶, E. Yu. Soldatov¹¹², U. Soldevila¹⁷⁴, A. A. Solodkov¹²³, A. Soloshenko⁷⁹, O. V. Solovyanov¹²³, V. Solovyev¹³⁸, P. Sommer¹⁴⁹, H. Son¹⁷⁰, W. Song¹⁴⁴, W. Y. Song^{168b}, A. Sopczak¹⁴², F. Sopkova^{28b}, C. L. Sotiropoulou^{71a,71b}, S. Sottocornola^{70a,70b}, R. Soualah^{66a,66c,h}, A. M. Soukharev^{122a,122b}, D. South⁴⁶, S. Spagnolo^{67a,67b}, M. Spalla¹¹⁵, M. Spangenberg¹⁷⁸, F. Spanò⁹³, D. Sperlich⁵², T. M. Spieker^{61a}, R. Spighi^{23b}, G. Spigo³⁶, M. Spina¹⁵⁶, D. P. Spiteri⁵⁷, M. Spousta¹⁴³, A. Stabile^{68a,68b}, B. L. Stamas¹²¹, R. Stamen^{61a}, M. Stamenkovic¹²⁰, E. Stanecka⁸⁴, R. W. Stanek⁶, B. Stanislaus¹³⁵, M. M. Stanitzki⁴⁶, M. Stankaityte¹³⁵, B. Stapf¹²⁰, E. A. Starchenko¹²³, G. H. Stark¹⁴⁶, J. Stark⁵⁸, S. H. Stark⁴⁰, P. Staroba¹⁴¹, P. Starovoitov^{61a}, S. Stärz¹⁰³, R. Staszewski⁸⁴, G. Stavropoulos⁴⁴, M. Stegler⁴⁶, P. Steinberg²⁹, A. L. Steinhebel¹³¹, B. Stelzer¹⁵², H. J. Stelzer¹³⁹, O. Stelzer-Chilton^{168a}, H. Stenzel⁵⁶, T. J. Stevenson¹⁵⁶, G. A. Stewart³⁶, M. C. Stockton³⁶, G. Stoicea^{27b}, M. Stolarski^{140a}, P. Stolte⁵³, S. Stonjek¹¹⁵, A. Straessner⁴⁸, J. Strandberg¹⁵⁴, S. Strandberg^{45a,45b}, M. Strauss¹²⁸, P. Strizenc^{28b}, R. Ströhmer¹⁷⁷, D. M. Strom¹³¹, R. Stroynowski⁴², A. Strubig⁵⁰, S. A. Stucci²⁹, B. Stugu¹⁷, J. Stupak¹²⁸, N. A. Styles⁴⁶, D. Su¹⁵³, S. Suchek^{61a}, V. V. Sulin¹¹⁰, M. J. Sullivan⁹⁰, D. M. S. Sultan⁵⁴, S. Sultansoy^{4c}, T. Sumida⁸⁵, S. Sun¹⁰⁵, X. Sun³, K. Suruliz¹⁵⁶, C. J. E. Suster¹⁵⁷, M. R. Sutton¹⁵⁶, S. Suzuki⁸¹, M. Svatos¹⁴¹, M. Swiatlowski³⁷, S. P. Swift², T. Swirski¹⁷⁷, A. Sydorenko⁹⁹, I. Sykora^{28a}, M. Sykora¹⁴³, T. Sykora¹⁴³, D. Ta⁹⁹, K. Tackmann^{46,aa}, J. Taenzer¹⁶¹, A. Taffard¹⁷¹, R. Tafirout^{168a}, H. Takai²⁹, R. Takashima⁸⁶, K. Takeda⁸², T. Takeshita¹⁵⁰, E. P. Takeva⁵⁰, Y. Takubo⁸¹, M. Talby¹⁰¹, A. A. Talyshev^{122a,122b}, N. M. Tamir¹⁶¹, J. Tanaka¹⁶³, M. Tanaka¹⁶⁵, R. Tanaka¹³², S. Tapia Araya¹⁷³, S. Tapprogge⁹⁹, A. Tarek Abouelfadl Mohamed¹³⁶, S. Tarem¹⁶⁰, G. Tarna^{27b,d}, G. F. Tartarelli^{68a}, P. Tas¹⁴³, M. Tasevsky¹⁴¹, T. Tashiro⁸⁵, E. Tassi^{41a,41b}, A. Tavares Delgado^{140a,140b}, Y. Tayalati^{35e}, A. J. Taylor⁵⁰, G. N. Taylor¹⁰⁴, W. Taylor^{168b}

A. S. Tee⁸⁹, R. Teixeira De Lima¹⁵³, P. Teixeira-Dias⁹³, H. Ten Kate³⁶, J. J. Teoh¹²⁰, S. Terada⁸¹, K. Terashi¹⁶³, J. Terron⁹⁸, S. Terzo¹⁴, M. Testa⁵¹, R. J. Teuscher^{167,af}, S. J. Thais¹⁸³, T. Theveneaux-Pelzer⁴⁶, F. Thiele⁴⁰, D. W. Thomas⁹³, J. O. Thomas⁴², J. P. Thomas²¹, A. S. Thompson⁵⁷, P. D. Thompson²¹, L. A. Thomsen¹⁸³, E. Thomson¹³⁷, Y. Tian³⁹, R. E. Ticse Torres⁵³, V. O. Tikhomirov^{110,ar}, Yu. A. Tikhonov^{122a,122b}, S. Timoshenko¹¹², P. Tipton¹⁸³, S. Tisserant¹⁰¹, K. Todome^{23a,23b}, S. Todorova-Nova⁵, S. Todt⁴⁸, J. Tojo⁸⁷, S. Tokár^{28a}, K. Tokushuku⁸¹, E. Tolley¹²⁶, K. G. Tomiwa^{33c}, M. Tomoto¹¹⁷, L. Tompkins^{153,r}, B. Tong⁵⁹, P. Tornambe¹⁰², E. Torrence¹³¹, H. Torres⁴⁸, E. Torró Pastor¹⁴⁸, C. Tosciri¹³⁵, J. Toth^{101,ad}, D. R. Tovey¹⁴⁹, A. Traeel¹⁷, C. J. Treado¹²⁴, T. Trefzger¹⁷⁷, F. Tresoldi¹⁵⁶, A. Tricoli²⁹, I. M. Trigger^{168a}, S. Trincaz-Duvoid¹³⁶, W. Trischuk¹⁶⁷, B. Trocmé⁵⁸, A. Trofymov¹⁴⁵, C. Troncon^{68a}, M. Trovatelli¹⁷⁶, F. Trovato¹⁵⁶, L. Truong^{33b}, M. Trzebinski⁸⁴, A. Trzupek⁸⁴, F. Tsai⁴⁶, J.C.-L. Tseng¹³⁵, P. V. Tsiarshka^{107,al}, A. Tsirigotis¹⁶², N. Tsirintanis⁹, V. Tsiskaridze¹⁵⁵, E. G. Tskhadadze^{159a}, M. Tsopoulou¹⁶², I. I. Tsukerman¹¹¹, V. Tsulaia¹⁸, S. Tsuno⁸¹, D. Tsybychev¹⁵⁵, Y. Tu^{63b}, A. Tudorache^{27b}, V. Tudorache^{27b}, T. T. Tulbure^{27a}, A. N. Tuna⁵⁹, S. Turchikhin⁷⁹, D. Turgeman¹⁸⁰, I. Turk Cakir^{4b,w}, R. J. Turner²¹, R. T. Turra^{68a}, P. M. Tuts³⁹, S. Tzamarias¹⁶², E. Tzovara⁹⁹, G. Ucchielli⁴⁷, K. Uchida¹⁶³, I. Ueda⁸¹, M. Ughetto^{45a,45b}, F. Ukegawa¹⁶⁹, G. Unal³⁶, A. Undrus²⁹, G. Unel¹⁷¹, F. C. Ungaro¹⁰⁴, Y. Unno⁸¹, K. Uno¹⁶³, J. Urban^{28b}, P. Urquijo¹⁰⁴, G. Usai⁸, J. Usui⁸¹, Z. Uysal^{12d}, L. Vacavant¹⁰¹, V. Vacek¹⁴², B. Vachon¹⁰³, K. O. H. Vadla¹³⁴, A. Vaidya⁹⁴, C. Valderanis¹¹⁴, E. Valdes Santurio^{45a,45b}, M. Valente⁵⁴, S. Valentini^{23a,23b}, A. Valero¹⁷⁴, L. Valéry⁴⁶, R. A. Vallance²¹, A. Vallier³⁶, J. A. Valls Ferrer¹⁷⁴, T. R. Van Daalen¹⁴, P. Van Gemmeren⁶, I. Van Vulpen¹²⁰, M. Vanadia^{73a,73b}, W. Vandelli³⁶, A. Vaniachine¹⁶⁶, D. Vannicola^{72a,72b}, R. Vari^{72a}, E. W. Varnes⁷, C. Varni^{55a,55b}, T. Varol⁴², D. Varouchas¹³², K. E. Varvell¹⁵⁷, M. E. Vasile^{27b}, G. A. Vasquez¹⁷⁶, J. G. Vasquez¹⁸³, F. Vazeille³⁸, D. Vazquez Furelos¹⁴, T. Vazquez Schroeder³⁶, J. Veatch⁵³, V. Vecchio^{74a,74b}, M. J. Veen¹²⁰, L. M. Veloce¹⁶⁷, F. Veloso^{140a,140c}, S. Veneziano^{72a}, A. Ventura^{67a,67b}, N. Venturi³⁶, A. Verbitskiy¹¹⁵, V. Vercesi^{70a}, M. Verducci^{74a,74b}, C. M. Vergel Infante⁷⁸, C. Vergis²⁴, W. Verkerke¹²⁰, A. T. Vermeulen¹²⁰, J. C. Vermeulen¹²⁰, M. C. Vetterli^{152,az}, N. Viaux Maira^{147c}, M. Vicente Barreto Pinto⁵⁴, T. Vickey¹⁴⁹, O. E. Vickey Boeriu¹⁴⁹, G. H. A. Viehhauser¹³⁵, L. Vigani¹³⁵, M. Villa^{23a,23b}, M. Villaplana Perez^{68a,68b}, E. Vilucchi⁵¹, M. G. Vincter³⁴, V. B. Vinogradov⁷⁹, A. Vishwakarma⁴⁶, C. Vittori^{23a,23b}, I. Vivarelli¹⁵⁶, M. Vogel¹⁸², P. Vokac¹⁴², S. E. von Buddenbrock^{33c}, E. Von Toerne²⁴, V. Vorobel¹⁴³, K. Vorobev¹¹², M. Vos¹⁷⁴, J. H. Vosseveld⁹⁰, M. Vozak¹⁰⁰, N. Vranjes¹⁶, M. Vranjes Milosavljevic¹⁶, V. Vrba¹⁴², M. Vreeswijk¹²⁰, R. Vuillermet³⁶, I. Vukotic³⁷, P. Wagner²⁴, W. Wagner¹⁸², J. Wagner-Kuhr¹¹⁴, H. Wahlberg⁸⁸, K. Wakamiya⁸², V. M. Walbrecht¹¹⁵, J. Walder⁸⁹, R. Walker¹¹⁴, S. D. Walker⁹³, W. Walkowiak¹⁵¹, V. Wallangen^{45a,45b}, A. M. Wang⁵⁹, C. Wang^{60b}, F. Wang¹⁸¹, H. Wang¹⁸, H. Wang³, J. Wang¹⁵⁷, J. Wang^{61b}, P. Wang⁴², Q. Wang¹²⁸, R.-J. Wang⁹⁹, R. Wang^{60a}, R. Wang⁶, S. M. Wang¹⁵⁸, W. T. Wang^{60a}, W. Wang^{15c,ag}, W. X. Wang^{60a,ag}, Y. Wang^{60a,ao}, Z. Wang^{60c}, C. Wanotayaroj⁴⁶, A. Warburton¹⁰³, C. P. Ward³², D. R. Wardrop⁹⁴, N. Warrack⁵⁷, A. Washbrook⁵⁰, A. T. Watson²¹, M. F. Watson²¹, G. Watts¹⁴⁸, B. M. Waugh⁹⁴, A. F. Webb¹¹, S. Webb⁹⁹, C. Weber¹⁸³, M. S. Weber²⁰, S. A. Weber³⁴, S. M. Weber^{61a}, A. R. Weidberg¹³⁵, J. Weingarten⁴⁷, M. Weirich⁹⁹, C. Weiser⁵², P. S. Wells³⁶, T. Wenaus²⁹, T. Wengler³⁶, S. Wenig³⁶, N. Vermes²⁴, M. D. Werner⁷⁸, M. Wessels^{61a}, T. D. Weston²⁰, K. Whalen¹³¹, N. L. Whallon¹⁴⁸, A. M. Wharton⁸⁹, A. S. White¹⁰⁵, A. White⁸, M. J. White¹, D. Whiteson¹⁷¹, B. W. Whitmore⁸⁹, F. J. Wickens¹⁴⁴, W. Wiedenmann¹⁸¹, M. Wielers¹⁴⁴, N. Wieseotte⁹⁹, C. Wiglesworth⁴⁰, L. A. M. Wiik-Fuchs⁵², F. Wilk¹⁰⁰, H. G. Wilkens³⁶, L. J. Wilkins⁹³, H. H. Williams¹³⁷, S. Williams³², C. Willis¹⁰⁶, S. Willocq¹⁰², J. A. Wilson²¹, I. Wingerter-Seez⁵, E. Winkels¹⁵⁶, F. Winklmeier¹³¹, O. J. Winston¹⁵⁶, B. T. Winter⁵², M. Wittgen¹⁵³, M. Wobisch⁹⁵, A. Wolf⁹⁹, T. M. H. Wolf¹²⁰, R. Wolff¹⁰¹, R. W. Wölker¹³⁵, J. Wollrath⁵², M. W. Wolter⁸⁴, H. Wolters^{140a,140c}, V. W. S. Wong¹⁷⁵, N. L. Woods¹⁴⁶, S. D. Worm²¹, B. K. Wosiek⁸⁴, K. W. Woźniak⁸⁴, K. Wraight⁵⁷, S. L. Wu¹⁸¹, X. Wu⁵⁴, Y. Wu^{60a}, T. R. Wyatt¹⁰⁰, B. M. Wynne⁵⁰, S. Xella⁴⁰, Z. Xi¹⁰⁵, L. Xia¹⁷⁸, D. Xu^{15a}, H. Xu^{60a,d}, L. Xu²⁹, T. Xu¹⁴⁵, W. Xu¹⁰⁵, Z. Xu^{60b}, Z. Xu¹⁵³, B. Yabsley¹⁵⁷, S. Yacoob^{33a}, K. Yajima¹³³, D. P. Yallup⁹⁴, D. Yamaguchi¹⁶⁵, Y. Yamaguchi¹⁶⁵, A. Yamamoto⁸¹, T. Yamanaka¹⁶³, F. Yamane⁸², M. Yamatani¹⁶³, T. Yamazaki¹⁶³, Y. Yamazaki⁸², Z. Yan²⁵, H. J. Yang^{60c,60d}, H. T. Yang¹⁸, S. Yang⁷⁷, X. Yang^{58,60b}, Y. Yang¹⁶³, W.-M. Yao¹⁸, Y. C. Yap⁴⁶, Y. Yasu⁸¹, E. Yatsenko^{60c,60d}, J. Ye⁴², S. Ye²⁹, I. Yeletsikh⁷⁹, M. R. Yexley⁸⁹, E. Yigitbasi²⁵, K. Yorita¹⁷⁹, K. Yoshihara¹³⁷, C. J. S. Young³⁶, C. Young¹⁵³, J. Yu⁷⁸, R. Yuan^{60b}, X. Yue^{61a}, S. P. Y. Yuen²⁴, B. Zabinski⁸⁴, G. Zacharis¹⁰, E. Zaffaroni⁵⁴, J. Zahreddine¹³⁶, A. M. Zaitsev^{123,aq}, T. Zakareishvili^{159b}, N. Zakharchuk³⁴, S. Zambito⁵⁹, D. Zanzi³⁶, D. R. Zaripovas⁵⁷, S. V. Zeißner⁴⁷, C. Zeitnitz¹⁸², G. Zemaityte¹³⁵, J. C. Zeng¹⁷³, O. Zenin¹²³, T. Ženiš^{28a}, D. Zerwas¹³², M. Zgubič¹³⁵, D. F. Zhang^{15b}, F. Zhang¹⁸¹, G. Zhang^{60a}, G. Zhang^{15b}, H. Zhang^{15c}, J. Zhang⁶, L. Zhang^{15c}, L. Zhang^{60a}, M. Zhang¹⁷³, R. Zhang^{60a}, R. Zhang²⁴, X. Zhang^{60b}, Y. Zhang^{15a,15d}, Z. Zhang^{63a}, Z. Zhang¹³², P. Zhao⁴⁹, Y. Zhao^{60b}, Z. Zhao^{60a}, A. Zhemchugov⁷⁹, Z. Zheng¹⁰⁵, D. Zhong¹⁷³, B. Zhou¹⁰⁵, C. Zhou¹⁸¹, M. S. Zhou^{15a,15d}, M. Zhou¹⁵⁵, N. Zhou^{60c}, Y. Zhou⁷, C. G. Zhu^{60b}, H. L. Zhu^{60a}, H. Zhu^{15a}, J. Zhu¹⁰⁵, Y. Zhu^{60a}, X. Zhuang^{15a}, K. Zhukov¹¹⁰, V. Zhulanov^{122a,122b}, D. Zieminska⁶⁵, N. I. Zimine⁷⁹, S. Zimmermann⁵², Z. Zinonos¹¹⁵, M. Ziolkowski¹⁵¹, L. Živković¹⁶, G. Zobernig¹⁸¹, A. Zoccoli^{23a,23b}, K. Zoch⁵³, T. G. Zorbas¹⁴⁹, R. Zou³⁷, L. Zwalinski³⁶

- ¹ Department of Physics, University of Adelaide, Adelaide, Australia
- ² Physics Department, SUNY Albany, Albany, NY, USA
- ³ Department of Physics, University of Alberta, Edmonton, AB, Canada
- ⁴ (a)Department of Physics, Ankara University, Ankara, Turkey; (b)Istanbul Aydin University, Istanbul, Turkey; (c)Division of Physics, TOBB University of Economics and Technology, Ankara, Turkey
- ⁵ LAPP, Université Grenoble Alpes, Université Savoie Mont Blanc, CNRS/IN2P3, Annecy, France
- ⁶ High Energy Physics Division, Argonne National Laboratory, Argonne, IL, USA
- ⁷ Department of Physics, University of Arizona, Tucson, AZ, USA
- ⁸ Department of Physics, University of Texas at Arlington, Arlington, TX, USA
- ⁹ Physics Department, National and Kapodistrian University of Athens, Athens, Greece
- ¹⁰ Physics Department, National Technical University of Athens, Zografou, Greece
- ¹¹ Department of Physics, University of Texas at Austin, Austin, TX, USA
- ¹² (a)Bahcesehir University, Faculty of Engineering and Natural Sciences, Istanbul, Turkey; (b)Istanbul Bilgi University, Faculty of Engineering and Natural Sciences, Istanbul, Turkey; (c)Department of Physics, Bogazici University, Istanbul, Turkey; (d)Department of Physics Engineering, Gaziantep University, Gaziantep, Turkey
- ¹³ Institute of Physics, Azerbaijan Academy of Sciences, Baku, Azerbaijan
- ¹⁴ Institut de Física d'Altes Energies (IFAE), Barcelona Institute of Science and Technology, Barcelona, Spain
- ¹⁵ (a)Institute of High Energy Physics, Chinese Academy of Sciences, Beijing, China; (b)Physics Department, Tsinghua University, Beijing, China; (c)Department of Physics, Nanjing University, Nanjing, China; (d)University of Chinese Academy of Science (UCAS), Beijing, China
- ¹⁶ Institute of Physics, University of Belgrade, Belgrade, Serbia
- ¹⁷ Department for Physics and Technology, University of Bergen, Bergen, Norway
- ¹⁸ Physics Division, Lawrence Berkeley National Laboratory and University of California, Berkeley, CA, USA
- ¹⁹ Institut für Physik, Humboldt Universität zu Berlin, Berlin, Germany
- ²⁰ Albert Einstein Center for Fundamental Physics and Laboratory for High Energy Physics, University of Bern, Bern, Switzerland
- ²¹ School of Physics and Astronomy, University of Birmingham, Birmingham, UK
- ²² Facultad de Ciencias y Centro de Investigaciones, Universidad Antonio Nariño, Bogota, Colombia
- ²³ (a)INFN Bologna and Università di Bologna, Dipartimento di Fisica, Bologna, Italy; (b)INFN Sezione di Bologna, Bologna, Italy
- ²⁴ Physikalisches Institut, Universität Bonn, Bonn, Germany
- ²⁵ Department of Physics, Boston University, Boston, MA, USA
- ²⁶ Department of Physics, Brandeis University, Waltham, MA, USA
- ²⁷ (a)Transilvania University of Brasov, Brasov, Romania; (b)Horia Hulubei National Institute of Physics and Nuclear Engineering, Bucharest, Romania; (c)Department of Physics, Alexandru Ioan Cuza University of Iasi, Iasi, Romania; (d)National Institute for Research and Development of Isotopic and Molecular Technologies, Physics Department, Cluj-Napoca, Romania; (e)University Politehnica Bucharest, Bucharest, Romania; (f)West University in Timisoara, Timisoara, Romania
- ²⁸ (a)Faculty of Mathematics, Physics and Informatics, Comenius University, Bratislava, Slovakia; (b)Department of Subnuclear Physics, Institute of Experimental Physics of the Slovak Academy of Sciences, Kosice, Slovak Republic
- ²⁹ Physics Department, Brookhaven National Laboratory, Upton, NY, USA
- ³⁰ Departamento de Física, Universidad de Buenos Aires, Buenos Aires, Argentina
- ³¹ California State University, Long Beach, CA, USA
- ³² Cavendish Laboratory, University of Cambridge, Cambridge, UK
- ³³ (a)Department of Physics, University of Cape Town, Cape Town, South Africa; (b)Department of Mechanical Engineering Science, University of Johannesburg, Johannesburg, South Africa; (c)School of Physics, University of the Witwatersrand, Johannesburg, South Africa
- ³⁴ Department of Physics, Carleton University, Ottawa, ON, Canada
- ³⁵ (a)Faculté des Sciences Ain Chock, Réseau Universitaire de Physique des Hautes Energies-Université Hassan II, Casablanca, Morocco; (b)Faculté des Sciences, Université Ibn-Tofail, Kénitra, Morocco; (c)Faculté des Sciences Semlalia, Université Cadi Ayyad, LPHEA-Marrakech, Marrakesh, Morocco; (d)Faculté des Sciences, Université Mohamed Premier and LTPM, Oujda, Morocco; (e)Faculté des sciences, Université Mohammed V, Rabat, Morocco
- ³⁶ CERN, Geneva, Switzerland

- 37 Enrico Fermi Institute, University of Chicago, Chicago, IL, USA
- 38 LPC, Université Clermont Auvergne, CNRS/IN2P3, Clermont-Ferrand, France
- 39 Nevis Laboratory, Columbia University, Irvington, NY, USA
- 40 Niels Bohr Institute, University of Copenhagen, Copenhagen, Denmark
- 41 (a)Dipartimento di Fisica, Università della Calabria, Rende, Italy; (b)INFN Gruppo Collegato di Cosenza, Laboratori Nazionali di Frascati, Frascati, Italy
- 42 Physics Department, Southern Methodist University, Dallas, TX, USA
- 43 Physics Department, University of Texas at Dallas, Richardson, TX, USA
- 44 National Centre for Scientific Research “Demokritos”, Agia Paraskevi, Greece
- 45 (a)Department of Physics, Stockholm University, Stockholm, Sweden; (b)Oskar Klein Centre, Stockholm, Sweden
- 46 Deutsches Elektronen-Synchrotron DESY, Hamburg and Zeuthen, Germany
- 47 Lehrstuhl für Experimentelle Physik IV, Technische Universität Dortmund, Dortmund, Germany
- 48 Institut für Kern- und Teilchenphysik, Technische Universität Dresden, Dresden, Germany
- 49 Department of Physics, Duke University, Durham, NC, USA
- 50 SUPA-School of Physics and Astronomy, University of Edinburgh, Edinburgh, UK
- 51 INFN e Laboratori Nazionali di Frascati, Frascati, Italy
- 52 Physikalisches Institut, Albert-Ludwigs-Universität Freiburg, Freiburg, Germany
- 53 II. Physikalisches Institut, Georg-August-Universität Göttingen, Göttingen, Germany
- 54 Département de Physique Nucléaire et Corpusculaire, Université de Genève, Geneva, Switzerland
- 55 (a)Dipartimento di Fisica, Università di Genova, Genoa, Italy; (b)INFN Sezione di Genova, Genoa, Italy
- 56 II. Physikalisches Institut, Justus-Liebig-Universität Giessen, Giessen, Germany
- 57 SUPA-School of Physics and Astronomy, University of Glasgow, Glasgow, UK
- 58 LPSC, Université Grenoble Alpes, CNRS/IN2P3, Grenoble INP, Grenoble, France
- 59 Laboratory for Particle Physics and Cosmology, Harvard University, Cambridge, MA, USA
- 60 (a)Department of Modern Physics and State Key Laboratory of Particle Detection and Electronics, University of Science and Technology of China, Hefei, China; (b)Institute of Frontier and Interdisciplinary Science and Key Laboratory of Particle Physics and Particle Irradiation (MOE), Shandong University, Qingdao, China; (c)School of Physics and Astronomy, Shanghai Jiao Tong University, KLPPAC-MoE, SKLPPC, Shanghai, China; (d)Tsung-Dao Lee Institute, Shanghai, China
- 61 (a)Kirchhoff-Institut für Physik, Ruprecht-Karls-Universität Heidelberg, Heidelberg, Germany; (b)Physikalisches Institut, Ruprecht-Karls-Universität Heidelberg, Heidelberg, Germany
- 62 Faculty of Applied Information Science, Hiroshima Institute of Technology, Hiroshima, Japan
- 63 (a)Department of Physics, Chinese University of Hong Kong, Shatin, NT, Hong Kong; (b)Department of Physics, University of Hong Kong, Hong Kong, China; (c)Department of Physics and Institute for Advanced Study, Hong Kong University of Science and Technology, Clear Water Bay, Kowloon, Hong Kong, China
- 64 Department of Physics, National Tsing Hua University, Hsinchu, Taiwan
- 65 Department of Physics, Indiana University, Bloomington, IN, USA
- 66 (a)INFN Gruppo Collegato di Udine, Sezione di Trieste, Udine, Italy; (b)ICTP, Trieste, Italy; (c)Dipartimento Politecnico di Ingegneria e Architettura, Università di Udine, Udine, Italy
- 67 (a)INFN Sezione di Lecce, Lecce, Italy; (b)Dipartimento di Matematica e Fisica, Università del Salento, Lecce, Italy
- 68 (a)INFN Sezione di Milano, Milan, Italy; (b)Dipartimento di Fisica, Università di Milano, Milan, Italy
- 69 (a)INFN Sezione di Napoli, Naples, Italy; (b)Dipartimento di Fisica, Università di Napoli, Naples, Italy
- 70 (a)INFN Sezione di Pavia, Pavia, Italy; (b)Dipartimento di Fisica, Università di Pavia, Pavia, Italy
- 71 (a)INFN Sezione di Pisa, Pisa, Italy; (b)Dipartimento di Fisica E. Fermi, Università di Pisa, Pisa, Italy
- 72 (a)INFN Sezione di Roma, Rome, Italy; (b)Dipartimento di Fisica, Sapienza Università di Roma, Rome, Italy
- 73 (a)INFN Sezione di Roma Tor Vergata, Rome, Italy; (b)Dipartimento di Fisica, Università di Roma Tor Vergata, Rome, Italy
- 74 (a)INFN Sezione di Roma Tre, Rome, Italy; (b)Dipartimento di Matematica e Fisica, Università Roma Tre, Rome, Italy
- 75 (a)INFN-TIFPA, Trento, Italy; (b)Università degli Studi di Trento, Trento, Italy
- 76 Institut für Astro- und Teilchenphysik, Leopold-Franzens-Universität, Innsbruck, Austria
- 77 University of Iowa, Iowa City, IA, USA
- 78 Department of Physics and Astronomy, Iowa State University, Ames, IA, USA
- 79 Joint Institute for Nuclear Research, Dubna, Russia

- 80 (a)Departamento de Engenharia Elétrica, Universidade Federal de Juiz de Fora (UFJF), Juiz de Fora, Brazil ; (b)Universidade Federal do Rio De Janeiro COPPE/EE/IF, Rio de Janeiro, Brazil; (c)Universidade Federal de São João del Rei (UFSJ), São João del Rei, Brazil; (d)Instituto de Física, Universidade de São Paulo, São Paulo, Brazil
- 81 KEK, High Energy Accelerator Research Organization, Tsukuba, Japan
- 82 Graduate School of Science, Kobe University, Kobe, Japan
- 83 (a)AGH University of Science and Technology, Faculty of Physics and Applied Computer Science, Krakow, Poland; (b)Marian Smoluchowski Institute of Physics, Jagiellonian University, Krakow, Poland
- 84 Institute of Nuclear Physics Polish Academy of Sciences, Krakow, Poland
- 85 Faculty of Science, Kyoto University, Kyoto, Japan
- 86 Kyoto University of Education, Kyoto, Japan
- 87 Research Center for Advanced Particle Physics and Department of Physics, Kyushu University, Fukuoka, Japan
- 88 Instituto de Física La Plata, Universidad Nacional de La Plata and CONICET, La Plata, Argentina
- 89 Physics Department, Lancaster University, Lancaster, UK
- 90 Oliver Lodge Laboratory, University of Liverpool, Liverpool, UK
- 91 Department of Experimental Particle Physics, Jožef Stefan Institute and Department of Physics, University of Ljubljana, Ljubljana, Slovenia
- 92 School of Physics and Astronomy, Queen Mary University of London, London, UK
- 93 Department of Physics, Royal Holloway University of London, Egham, UK
- 94 Department of Physics and Astronomy, University College London, London, UK
- 95 Louisiana Tech University, Ruston, LA, USA
- 96 Fysiska institutionen, Lunds universitet, Lund, Sweden
- 97 Centre de Calcul de l'Institut National de Physique Nucléaire et de Physique des Particules (IN2P3), Villeurbanne, France
- 98 Departamento de Física Teórica C-15 and CIAFF, Universidad Autónoma de Madrid, Madrid, Spain
- 99 Institut für Physik, Universität Mainz, Mainz, Germany
- 100 School of Physics and Astronomy, University of Manchester, Manchester, UK
- 101 CPPM, Aix-Marseille Université, CNRS/IN2P3, Marseille, France
- 102 Department of Physics, University of Massachusetts, Amherst, MA, USA
- 103 Department of Physics, McGill University, Montreal, QC, Canada
- 104 School of Physics, University of Melbourne, Victoria, Australia
- 105 Department of Physics, University of Michigan, Ann Arbor, MI, USA
- 106 Department of Physics and Astronomy, Michigan State University, East Lansing, MI, USA
- 107 B.I. Stepanov Institute of Physics, National Academy of Sciences of Belarus, Minsk, Belarus
- 108 Research Institute for Nuclear Problems of Byelorussian State University, Minsk, Belarus
- 109 Group of Particle Physics, University of Montreal, Montreal, QC, Canada
- 110 P.N. Lebedev Physical Institute of the Russian Academy of Sciences, Moscow, Russia
- 111 Institute for Theoretical and Experimental Physics of the National Research Centre Kurchatov Institute, Moscow, Russia
- 112 National Research Nuclear University MEPhI, Moscow, Russia
- 113 D.V. Skobel'syn Institute of Nuclear Physics, M.V. Lomonosov Moscow State University, Moscow, Russia
- 114 Fakultät für Physik, Ludwig-Maximilians-Universität München, Munich, Germany
- 115 Max-Planck-Institut für Physik (Werner-Heisenberg-Institut), Munich, Germany
- 116 Nagasaki Institute of Applied Science, Nagasaki, Japan
- 117 Graduate School of Science and Kobayashi-Maskawa Institute, Nagoya University, Nagoya, Japan
- 118 Department of Physics and Astronomy, University of New Mexico, Albuquerque, NM, USA
- 119 Institute for Mathematics, Astrophysics and Particle Physics, Radboud University Nijmegen/Nikhef, Nijmegen, The Netherlands
- 120 Nikhef National Institute for Subatomic Physics and University of Amsterdam, Amsterdam, The Netherlands
- 121 Department of Physics, Northern Illinois University, DeKalb, IL, USA
- 122 (a)Budker Institute of Nuclear Physics and NSU, SB RAS, Novosibirsk, Russia; (b)Novosibirsk State University, Novosibirsk, Russia
- 123 Institute for High Energy Physics of the National Research Centre, Kurchatov Institute, Protvino, Russia
- 124 Department of Physics, New York University, New York, NY, USA
- 125 Ochanomizu University, Otsuka, Bunkyo-ku, Tokyo, Japan

- 126 Ohio State University, Columbus, OH, USA
- 127 Faculty of Science, Okayama University, Okayama, Japan
- 128 Homer L. Dodge Department of Physics and Astronomy, University of Oklahoma, Norman, OK, USA
- 129 Department of Physics, Oklahoma State University, Stillwater, OK, USA
- 130 Palacký University, RCPTM, Joint Laboratory of Optics, Olomouc, Czech Republic
- 131 Center for High Energy Physics, University of Oregon, Eugene, OR, USA
- 132 LAL, Université Paris-Sud, CNRS/IN2P3, Université Paris-Saclay, Orsay, France
- 133 Graduate School of Science, Osaka University, Osaka, Japan
- 134 Department of Physics, University of Oslo, Oslo, Norway
- 135 Department of Physics, Oxford University, Oxford, UK
- 136 LPNHE, Sorbonne Université, Université de Paris, CNRS/IN2P3, Paris, France
- 137 Department of Physics, University of Pennsylvania, Philadelphia, PA, USA
- 138 Konstantinov Nuclear Physics Institute of National Research Centre “Kurchatov Institute”, PNPI, St. Petersburg, Russia
- 139 Department of Physics and Astronomy, University of Pittsburgh, Pittsburgh, PA, USA
- 140 (a) Laboratório de Instrumentação e Física Experimental de Partículas-LIP, Lisbon, Portugal; (b) Departamento de Física, Faculdade de Ciências, Universidade de Lisboa, Lisbon, Portugal; (c) Departamento de Física, Universidade de Coimbra, Coimbra, Portugal; (d) Centro de Física Nuclear da Universidade de Lisboa, Lisbon, Portugal; (e) Departamento de Física, Universidade do Minho, Braga, Portugal; (f) Universidad de Granada, Granada, Spain; (g) Dep Física and CEFITEC of Faculdade de Ciências e Tecnologia, Universidade Nova de Lisboa, Caparica, Portugal; (h) Instituto Superior Técnico, Universidade de Lisboa, Lisbon, Portugal
- 141 Institute of Physics of the Czech Academy of Sciences, Prague, Czech Republic
- 142 Czech Technical University in Prague, Prague, Czech Republic
- 143 Charles University, Faculty of Mathematics and Physics, Prague, Czech Republic
- 144 Particle Physics Department, Rutherford Appleton Laboratory, Didcot, UK
- 145 IRFU, CEA, Université Paris-Saclay, Gif-sur-Yvette, France
- 146 Santa Cruz Institute for Particle Physics, University of California Santa Cruz, Santa Cruz, CA, USA
- 147 (a) Departamento de Física, Pontificia Universidad Católica de Chile, Santiago, Chile; (b) Department of Physics, Universidad Andres Bello, Santiago, Chile; (c) Departamento de Física, Universidad Técnica Federico Santa María, Valparaíso, Chile
- 148 Department of Physics, University of Washington, Seattle, WA, USA
- 149 Department of Physics and Astronomy, University of Sheffield, Sheffield, UK
- 150 Department of Physics, Shinshu University, Nagano, Japan
- 151 Department Physik, Universität Siegen, Siegen, Germany
- 152 Department of Physics, Simon Fraser University, Burnaby, BC, Canada
- 153 SLAC National Accelerator Laboratory, Stanford, CA, USA
- 154 Physics Department, Royal Institute of Technology, Stockholm, Sweden
- 155 Departments of Physics and Astronomy, Stony Brook University, Stony Brook, NY, USA
- 156 Department of Physics and Astronomy, University of Sussex, Brighton, UK
- 157 School of Physics, University of Sydney, Sydney, Australia
- 158 Institute of Physics, Academia Sinica, Taipei, Taiwan
- 159 (a) E. Andronikashvili Institute of Physics, Iv. Javakhishvili Tbilisi State University, Tbilisi, Georgia; (b) High Energy Physics Institute, Tbilisi State University, Tbilisi, Georgia
- 160 Department of Physics, Technion, Israel Institute of Technology, Haifa, Israel
- 161 Raymond and Beverly Sackler School of Physics and Astronomy, Tel Aviv University, Tel Aviv, Israel
- 162 Department of Physics, Aristotle University of Thessaloniki, Thessaloniki, Greece
- 163 International Center for Elementary Particle Physics and Department of Physics, University of Tokyo, Tokyo, Japan
- 164 Graduate School of Science and Technology, Tokyo Metropolitan University, Tokyo, Japan
- 165 Department of Physics, Tokyo Institute of Technology, Tokyo, Japan
- 166 Tomsk State University, Tomsk, Russia
- 167 Department of Physics, University of Toronto, Toronto, ON, Canada
- 168 (a) TRIUMF, Vancouver, BC, Canada; (b) Department of Physics and Astronomy, York University, Toronto, ON, Canada
- 169 Division of Physics and Tomonaga Center for the History of the Universe, Faculty of Pure and Applied Sciences, University of Tsukuba, Tsukuba, Japan

- ¹⁷⁰ Department of Physics and Astronomy, Tufts University, Medford, MA, USA
- ¹⁷¹ Department of Physics and Astronomy, University of California Irvine, Irvine, CA, USA
- ¹⁷² Department of Physics and Astronomy, University of Uppsala, Uppsala, Sweden
- ¹⁷³ Department of Physics, University of Illinois, Urbana, IL, USA
- ¹⁷⁴ Instituto de Física Corpuscular (IFIC), Centro Mixto Universidad de Valencia - CSIC, Valencia, Spain
- ¹⁷⁵ Department of Physics, University of British Columbia, Vancouver, BC, Canada
- ¹⁷⁶ Department of Physics and Astronomy, University of Victoria, Victoria, BC, Canada
- ¹⁷⁷ Fakultät für Physik und Astronomie, Julius-Maximilians-Universität Würzburg, Würzburg, Germany
- ¹⁷⁸ Department of Physics, University of Warwick, Coventry, UK
- ¹⁷⁹ Waseda University, Tokyo, Japan
- ¹⁸⁰ Department of Particle Physics, Weizmann Institute of Science, Rehovot, Israel
- ¹⁸¹ Department of Physics, University of Wisconsin, Madison, WI, USA
- ¹⁸² Fakultät für Mathematik und Naturwissenschaften, Fachgruppe Physik, Bergische Universität Wuppertal, Wuppertal, Germany
- ¹⁸³ Department of Physics, Yale University, New Haven, CT, USA
- ¹⁸⁴ Yerevan Physics Institute, Yerevan, Armenia
- ^a Also at Borough of Manhattan Community College, City University of New York, New York, NY, USA
- ^b Also at Centre for High Performance Computing, CSIR Campus, Rosebank, Cape Town, South Africa
- ^c Also at CERN, Geneva, Switzerland
- ^d Also at CPPM, Aix-Marseille Université, CNRS/IN2P3, Marseille, France
- ^e Also at Département de Physique Nucléaire et Corpusculaire, Université de Genève, Geneva, Switzerland
- ^f Also at Departament de Física de la Universitat Autònoma de Barcelona, Barcelona, Spain
- ^g Also at Departamento de Física, Instituto Superior Técnico, Universidade de Lisboa, Lisbon, Portugal
- ^h Also at Department of Applied Physics and Astronomy, University of Sharjah, Sharjah, United Arab Emirates
- ⁱ Also at Department of Financial and Management Engineering, University of the Aegean, Chios, Greece
- ^j Also at Department of Physics and Astronomy, University of Louisville, Louisville, KY, USA
- ^k Also at Department of Physics and Astronomy, University of Sheffield, Sheffield, UK
- ^l Also at Department of Physics, Ben Gurion University of the Negev, Beer Sheva, Israel
- ^m Also at Department of Physics, California State University, East Bay, USA
- ⁿ Also at Department of Physics, California State University, Fresno, USA
- ^o Also at Department of Physics, California State University, Sacramento, USA
- ^p Also at Department of Physics, King's College London, London, UK
- ^q Also at Department of Physics, St. Petersburg State Polytechnical University, St. Petersburg, Russia
- ^r Also at Department of Physics, Stanford University, Stanford, CA, USA
- ^s Also at Department of Physics, University of Adelaide, Adelaide, Australia
- ^t Also at Department of Physics, University of Fribourg, Fribourg, Switzerland
- ^u Also at Department of Physics, University of Michigan, Ann Arbor, MI, USA
- ^v Also at Faculty of Physics, M.V. Lomonosov Moscow State University, Moscow, Russia
- ^w Also at Giresun University, Faculty of Engineering, Giresun, Turkey
- ^x Also at Graduate School of Science, Osaka University, Osaka, Japan
- ^y Also at Hellenic Open University, Patras, Greece
- ^z Also at Institutio Catalana de Recerca i Estudis Avancats, ICREA, Barcelona, Spain
- ^{aa} Also at Institut für Experimentalphysik, Universität Hamburg, Hamburg, Germany
- ^{ab} Also at Institute for Mathematics, Astrophysics and Particle Physics, Radboud University Nijmegen/Nikhef, Nijmegen, The Netherlands
- ^{ac} Also at Institute for Nuclear Research and Nuclear Energy (INRNE) of the Bulgarian Academy of Sciences, Sofia, Bulgaria
- ^{ad} Also at Institute for Particle and Nuclear Physics, Wigner Research Centre for Physics, Budapest, Hungary
- ^{ae} Also at Institute of High Energy Physics, Chinese Academy of Sciences, Beijing, China
- ^{af} Also at Institute of Particle Physics (IPP), Vancouver, Canada
- ^{ag} Also at Institute of Physics, Academia Sinica, Taipei, Taiwan
- ^{ah} Also at Institute of Physics, Azerbaijan Academy of Sciences, Baku, Azerbaijan

- ^{ai} Also at Institute of Theoretical Physics, Ilia State University, Tbilisi, Georgia
- ^{aj} Also at Instituto de Fisica Teorica, IFT-UAM/CSIC, Madrid, Spain
- ^{ak} Also at Department of Physics, Istanbul University, Istanbul, Turkey
- ^{al} Also at Joint Institute for Nuclear Research, Dubna, Russia
- ^{am} Also at LAL, Université Paris-Sud, CNRS/IN2P3, Université Paris-Saclay, Orsay, France
- ^{an} Also at Louisiana Tech University, Ruston, LA, USA
- ^{ao} Also at LPNHE, Sorbonne Université, Université de Paris, CNRS/IN2P3, Paris, France
- ^{ap} Also at Manhattan College, New York, NY, USA
- ^{aq} Also at Moscow Institute of Physics and Technology State University, Dolgoprudny, Russia
- ^{ar} Also at National Research Nuclear University MEPhI, Moscow, Russia
- ^{as} Also at Physics Department, An-Najah National University, Nablus, Palestine
- ^{at} Also at Physics Dept, University of South Africa, Pretoria, South Africa
- ^{au} Also at Physikalisches Institut, Albert-Ludwigs-Universität Freiburg, Freiburg, Germany
- ^{av} Also at School of Physics, Sun Yat-sen University, Guangzhou, China
- ^{aw} Also at The City College of New York, New York, NY, USA
- ^{ax} Also at The Collaborative Innovation Center of Quantum Matter (CICQM), Beijing, China
- ^{ay} Also at Tomsk State University, Tomsk, and Moscow Institute of Physics and Technology State University, Dolgoprudny, Russia
- ^{az} Also at TRIUMF, Vancouver, BC, Canada
- ^{aaa} Also at Università di Napoli Parthenope, Naples, Italy
- * Deceased